EFFECT OF CATALYST PORE SIZE ON HYDRODESULFURIZATION OF COAL DERIVED LIQUIDS

By

MATTHEW COLVIN SOOTER II

Bachelor of Science
Oklahoma State University
Stillwater, Oklahoma
1969

Master of Science
Oklahoma State University
Stillwater, Oklahoma
1971

Submitted to the Faculty of the Graduate College
of the Oklahoma State University
in partial fulfillment of the requirements
for the Degree of
DOCTOR OF PHILOSOPHY
May, 1974

EFFECT OF CATALYST PORE SIZE

ON HYDRODESULFURIZATION OF

COAL DERIVED LIQUIDS

Thesis Approved:

Billy L. Crynes
Thesis Adviser

Robert L. Robinson, Jr.

J. K. Jordan

R. N. Maddox

N. N. Durham
Dean of the Graduate College

PREFACE

An experimental apparatus was constructed to perform hydrodesulfurization studies over a temperature range of 77 to 950°F and a pressure range of 0 psig to 1800 psig. Experiments were carried out at 600, 650 and 700°F and space times of .375, .75 and 1.5 hours. Pressures of 500, 1000 and 1500 psig were investigated although nominally 1000 psig was used. Effect of catalyst particle size and catalyst bed height were also investigated. Hydrogen flow rate effects were determined and various kinetic models were compared for their ability to fit the data. Finally, the effect of a shift in most frequent catalyst pore diameter from 33 Å to 25 Å was determined.

I am deeply indebted to my thesis adviser, Dr. B. L. Crynes, for his patient and intelligent guidance, his willing helpfulness, and his excellent ability to keep graduate student time in the proper perspective. Discussions with other faculty members and my fellow graduate students were also of considerable help and a special note of thanks is due Dr. R. N. Maddox for his patience with the project.

Particular thanks is due Messors Mohamed Ghaly, D. C. Mehta, and Richard Cavett for their long hours of patient operation of the equipment.

Equipment funds and financial support for the project were gratefully received from the Office of Coal Research and Pittsburg and Midway Coal Mining Company.

I would like to thank fellow graduate student, Mr. Donald P. Satchell, Jr., for his fortitude throughout the entire project.

Finally, I cannot fully express the debt that I owe to my wife, Jean.

TABLE OF CONTENTS

Chapter Page

Chapter Page

LIST OF TABLES

LIST OF FIGURES

NOMENCLATURE

A	surface area of catalyst
B_o	Bodenstein Number
B_i	adsorption equilibrium constant of specie i
C_o, C_{in}	initial concentration of reacting specie
C^*	saturation concentration of gas in the liquid
C_f, C_{out}	final concentration of reacting specie
C_s	concentration of sulfur in oil
C_{si}	fraction of sulfur compounds of type i remaining
c	fraction sulfur removed
D	reactor diameter
D_T	tube diameter
D_p	particle diameter
D_a	eddy diffusivity
D_L	diffusion coefficient of sulfur compounds inside catalyst pores
D_f	most frequent catalyst pore diameter
D_{eff}	effective diffusion coefficient
ΔD_r	range of more frequent pore diameters
d_p	particle diameter
d_s	spherical diameter catalyst particle
E	dispersion coefficient
E	activation energy

f	fraction of feed sulfur compounds converted
ff	furnace factor
H	height of packing
h	constant defined on page 23
K	a constant depending on reaction conditions
K_i	first order rate constant which describes the kinetics of the i^{th} portion of the molecules
K_v	intrinsic reaction rate constant per unit of gross volume catalyst pellets
K	intrinsic reaction rate constant
k	rate constant
k	reaction rate constant per unit surface area, page 23
k	number of data points
k_i	rate constant for catalytic reaction
k_o	frequency factor
k_t	rate constant for thermal reaction
k_{LS}	mass transfer coefficient across liquid film
L	reactor length
L	particle length
m	constant that depends on reaction mechanism
m	reaction order
n	reaction order
P	system pressure
P_s	partial pressure of sulfur species
P_H	partial pressure of hydrogen
P_i	partial pressure of specie i
PD	pore distribution factor defined on page 25

R	pore radius of catalyst pore
R	average pellet radius
r	average pore radius
R	gas constant
S	standard deviation
S	specific surface area of catalyst
S_v	liquid volume hourly space velocity
SV	liquid volume hourly space velocity
t	time
T	temperature
u	linear liquid velocity in particle interstices
u	superficial liquid velocity
V	pore volume of catalyst pore
V_c	molar volume of reacting specie
X	determined sulfur value
$\overline{X}$	constant defined in Appendix G

Greek Symbols

α	fraction of sulfur molecules reacting at a "fast" rate
Φ	Thiele Modulus
ρ	density
μ	viscosity
η	effectiveness factor

CHAPTER I

INTRODUCTION

The late 60's and early 70's have brought to light our nation's dependence on an ample supply of energy. Electricity, natural gas, and possible fuel oil shortages have raised questions as to where we can obtain new and needed sources of energy.

Traditional sources of energy such as oil and gas wells have not proven sufficient to meet our demands. Present domestic discoveries of oil and gas are falling far short of previous yearly discoveries and are thus increasing our dependence on foreign sources for those fuels.

The one supply of energy which is available in abundant quantity is coal. Coal however, contains high levels of sulfur which can and will cause pollution problems on burning, and coal is not convenient for use in most modern day applications. Conversion of coal to alternate forms of energy such as gas and liquid fuels offers a solution to the energy crisis and the pollution problem. Conventional applications of energy would find gas or liquid fuels very tractable.

Gasification and liquefaction of coal are two different processes although there may be some overlap in later processing steps. The process of major concern in this study is the liquefaction of coal. Liquefaction processes of concern to this study rely on a solvent to carry the coal in solution through the liquefaction process. From the hydrogenation of the coal, additional solvent is produced. Some

solvent is recycled through the process to solvate more coal but the solvent also becomes a product of the process. The product solvent from the liquefaction process has promise as a substitute for crude oils. Possibly the first step to refining the product solvent as a synthetic crude would be a hydrodesulfurization process to upgrade the synthetic crude and reduce sulfur and other heteroatoms to acceptable levels.

Conventional hydrodesulfurization processes are performed over reactor beds of catalyst. The hydrodesulfurization catalysts now available have been developed with and for petroleum crudes which are primarily composed of straight chain alkanes and alkenes. The proposed synthetic crude from coal would be composed primarily of polyaromatics. Relatively little work has been done on development of a catalyst for desulfurization of aromatic oils, particularly a highly aromatic blend representative of a synthetic crude from a liquefaction process.

For a thorough economic analysis of coal liquefaction, the success of desulfurization and upgrading of the synthetic crude is an important step. A good byproduct credit for the synthetic crude could strongly affect the total economic analysis of a liquefaction facility. A $6.00/Bbl credit for excess solvent could mean a sufficient boost to process economics to proceed with multi-million dollar plant constructions.

Therefore the specific goals of this work were:

1) In the long run, to provide information to specifically tailor catalysts for up-grading coal derived liquids,
2) More specifically, to determine the effect of a shift in catalyst support pore size on desulfurization of a particular coal derived liquid,

3) To verify the effects of temperature, pressure, and space time on the desulfurization of a highly aromatic blend approximating a coal derived synthetic crude,

4) To establish the effects of liquid velocity on desulfurization, and

5) To establish the effect of catalyst size on desulfurization.

CHAPTER II

LITERATURE REVIEW

Hydrogenation of coal and coal liquids is a process which dates back to the 1920's and before. As one might suspect some criterion must be established to limit the literature review yet include the articles which would be most informative and applicable. Since this study was carried out in a trickle flow reactor, the petroleum desulfurization data were basically limited to articles on trickle flow equipment. Certainly liquid distribution would be limited to the trickle flow system. Desulfurization of coal tars and residuum are also included since these liquids would more closely approximate the aromatic structure of the liquid used in this study. Literature on aromatic liquids with respect to mass transfer effects, catalyst particle size effects and liquid distribution is severely limited and some additional petroleum articles must be included in the discussion of these topics. Some patent literature concerning catalyst support physical properties and their effects on petroleum desulfurizations is also included.

The literature review will begin with those articles concerned with the trickle flow reactor as they relate to liquid distribution and mass transfer. Hydrogen rate, temperature, pressure, and space time effects will follow next and last will be the effect of catalyst pore size. Factors pertaining to the reactor operational characteristics

and reaction kinetics are presented prior to the main emphasis on pore size effects to give the reader a better understanding of the many effects which often cloud the work done on pore size distribution.

To fully understand the kinetics of a reaction, the physical limitations of a system must be recognized and dealt with. Although many people recognize backmixing and radial liquid distribution problems in trickle flow systems, few, if any, have attempted to determine them for high pressure and temperature operations using hydrocarbon liquids.

Radial and Axial Liquid Dispersion in Packed Beds

Many have attempted to establish criteria for absence of liquid distribution problems in packed towers although a summary of much of the works yields an inconclusive result as will be seen. As early as 1919 Partington and Parker (40) suggested that the height of a packed column to the column diameter should not exceed a ratio of 5 to 1 for good axial liquid distribution. As might be suspected, problems with liquid dispersion at column entrances invalidated most early results; however, these results should be noted as the precursors of better work. Axial liquid distribution was investigated in 1935 by Scott (57) who set out to confirm the results of Weimann that a height to column diameter ratio (H/D) of 25 to 1 was necessary to avoid problems. Scott's work was done with water trickling over packing. Instead of confirming the results of Wiemann, Scott discovered that the critical H/D ratio was between 10 to 1 and 20 to 1 depending on the size packing used. Also about 1935 Baker, Chilton, and Vernon (4) reported on their

findings of liquid distribution using air and water in a packed column. Their conclusions were that, "A uniform distribution when obtained will persist down to any reasonable depth of packing," and "vapor velocity is without substantial effects." They also established a column diameter to packing diameter of 10 to 1 as the minimum to obtain good liquid distribution. Schwartz and Smith (54) reported on their work with a gas phase in packed beds in 1953. Their conclusion was that a tube diameter to particle diameter ratio (D_T/D_P) of 30 to 1 was necessary to avoid significant backmixing. Using a water system Schiesser and Lapidus (52) attempted to confirm the work of Baker et al. but, found that significant liquid distribution problems persisted to a D_T/D_P of at least 16 to 1. In 1963 Glaser and Lichtenstein (20) reported work with brine-air and kerosene-hydrogen systems. They showed no effect of D_T/D_P although all ratios were greater than 16 to 1. Another significant observation was that no gas phase effects were detected. As can be seen most of the above works have been somewhat sketchy and often contradictory and all are based on experimental efforts.

Other methods of establishing the absence of distribution problems have been based on parameters which include fluid physical properties. Satterfield (50) states that liquid and gas radial dispersion reaches a constant value above a particle Reynolds Number (defined below) of about 100 and axial dispersion reaches a constant value above a Reynolds Number of about 10. Satterfield seems to base these observations on some work done by Wilhelm (64). A close examination of Wilhelm's work is therefore merited. First one must recognize that Wilhelm's work represents the summary of many works by different

investigators on water and air systems and is therefore reasonably comprehensive. One must also recognize that these works were conducted with a fixed bed and single phase flow. A summary of the work is presented in a figure with a Peclet number (D_P u/E) as the ordinate and a Reynolds Number (D_P uρ/μ) as the abcissa. Here D_P is the partical diameter, u the linear liquid velocity in interstices, E the dispersion coefficient, ρ the density, and μ the viscosity. When viewed from the standpoint that all other things are held constant while liquid velocity is increased, one might expect that a velocity would be reached where radial and liquid distribution profiles become unimportant, the case indicated by Wilhelm. Wilhelm also notes that small scale laboratory experiments normally fall well below the critical Reynolds Number of 100 for radial dispersion unless special provisions are taken to assure that they do not. Schwartz and Roberts (55) indicate that radial distribution problems may exist in trickle flow reactors although they define the concept as "contacting efficiency." They do not present a method for a priori prediction of their contacting efficiency but suggest an experimental program to determine the efficiency and develop a correlation.

Backmixing in Packed Beds

Perhaps the best criterion for absence of backmixing was established by Mears (38). He suggests that a reactor length to reactor diameter (L/D_P) ratio, for first order reactions, greater than $(20/B_o)\ln(C_o/C_f)$ need be maintained. Symbols are: B_o equals Bodenstein number (d_s u/D_a); d_s equals spherical diameter catalyst particle, u equals superficial velocity, D_a equals axial eddy diffusivity; C_o and C_f equal

inlet and final reactant concentration, respectively. One of the most significant parts of Mears work is that he applies it to a bench scale hydrotreating unit. The work was on a straight run, gas oil feed and operating conditions were 700°F, 1500 psia and a liquid hourly space velocity of 2.0 hours. A minimum L/D_P of 350 was calculated.

In summary of the literature on liquid distribution, Mears presents a good method for estimating the absence of backmixing effects although prediction of the necessary parameters may prove to be an impossible task. Wilhelm (64) seems to present the easiest technique for prediction of radial and axial dispersion problems by virture of his graph and the method is related to that of Mears through a Peclet number. The recent paper by Schwartz and Roberts (55) confirms that the methods of Wilhelm and Mears for prediction of backmixing are adequate and presently the best, and the paper further states backmixing is often not important in trickle bed reactors.

All of this careful allowance for liquid distribution effects could be for naught if care is not taken in design of commercial reactors to distribute the liquid evenly over the packing. Evidence of poor commercial design is pointed out by Ross (48). Improper liquid distribution at the top of commercial size towers, or even pilot units, could cause erroneous interpretations of data obtained. If a column has poor liquid distributors, a reduction in particle size could give a higher reaction rate. The results however, instead of being interpreted as a mass transfer limited case with low effectiveness factor, should be recognized as at least partly caused by better liquid distribution due to an increase in the ratio D_T/D_P.

Particle Size and Mass Transfer Effects

Mass transfer, as seen above, can be intimately tied to liquid distribution effects and much care must be taken to separate the two. The problem is complicated by the fact that very little information is available regarding mass transfer limitations in trickle beds. There are several ways mass transfer can affect a reaction; (1) mass transfer across the film surrounding the catalyst pellet, (2) mass transfer within the pores, and (3) mass transfer of products back through the pores and into the bulk phase. Therefore, the sorting of mass transfer effects becomes quite complex. Some of the techniques for determining mass transfer limitations are listed below and a brief discussion of some experimental works is undertaken to show the various system for which mass transfer limitations have been determined. Satterfield (50) presents a good review of some of the work done with regard to mass transfer limitations in trickle reactors. He also presents a method for determining whether or not mass transport through a film surrounding the catalyst pellet is significant. If

$$\frac{10\ d_p}{3\ C^*}\left(\frac{-1}{V_c}\ \frac{d_n}{d_t}\right) > k_{LS}$$

Satterfield maintains mass transfer through the film is important. The symbols are d_p = particle diameter, C^* = saturation concentration of the gas in the liquid, $\left(\frac{-1}{V_c}\frac{d_n}{d_t}\right)$ = reaction rate, and k_{LS} = mass transfer coefficient across the film. With undefined or partially characterized feedstock oils, the problem becomes not whether Satterfield's method is correct, but first how to predict the needed

parameters in the above equation. Mass transfer coefficients and saturation concentrations are very difficult to predict. The final word is, of course, experimental evidence. Levenspiel (34) suggests varying catalyst bed height for a constant space velocity as one method for detecting gas film resistance. By keeping a constant space velocity or time, the gas velocity is increased through the bed and film turbulance increased. When turbulance has increased to the point that gas film resistance is unimportant, conversion will be constant for successive increases in gas velocity.

Diffusion of the reacting specie through catalyst pores was mentioned as another possible form of diffusion. Determining whether or not mass transfer through catalyst pores to inner surface area is limiting is also usually based on experimental evidence. The most common technique is a reduction of catalyst particle size other things constant, and thereby, a reduction in necessary diffusion distance. From the different rates with different catalyst particle sizes a parameter known as an effectiveness factor can be predicted. The effectiveness factor, η, is defined in one way as the average reaction rate within a pore divided by the maximum reaction rate if pore diffusion resistance were absent. Satterfield (50) has an excellent chapter on prediction of effectiveness factors for various type reactions. Levenspiel (34) and Smith (58) also present information on prediction of effectiveness factors although they are not quite as comprehensive. Most methods revolve about prediction of a parameter, Φ, known as a Thiele modulus. From this modulus, effectiveness factors can be predicted via prepared graphs or from theory. The trouble with this procedure is again one's ability to predict the parameters which

make up the Thiele modulus. For a first order reaction the modulus is $\Phi = L\sqrt{K/D_{eff}}$; where L is a particle length, K an intrinsic reaction rate constant, and D_{eff} an effective diffusion coefficient. Φ is related to the effectiveness factor, η, by performing a mass balance on a slice of catalyst pore and applying the appropriate boundary conditions. Then, coupled with the definition of η, an expression of the form $\eta = (\tanh L\sqrt{K/D_{eff}}) / (L\sqrt{K/D_{eff}})$ can be obtained. Smith (58) presents a method for determining the effectiveness factor from experimental data on two different sizes of catalyst pellets. An effectiveness factor of one or quite near one would indicate the absence of diffusion resistance effects as can be seen from the definition of η.

Several people have experimentally determined if catalyst pore mass transfer was important in desulfurization of petroleum feed stocks. Le Noble and Choufoer (33) did some excellent work in determining the presence of mass transfer limitations with a trickle flow reactor. By diluting their system with a liquid of higher diffusion coefficient their data definitely indicated diffusion effects were present in their system. Their work illustrates another method for conclusively proving diffusion limitation. Frost and Cottingham (17) show an increase in desulfurization of a topped crude oil with decreasing catalyst particle size however, no comment or evidence was shown to dispel the possible effects of liquid distribution. Mussagutov et al. (37) also show a particle size effect on a vacuum distillate from a crude oil. The smaller the particle, the higher the desulfurization. The important point is that the above researchers were able to demonstrate a pore mass transfer limitation in the desulfurization of various petroleum stocks. One research effort was conducted on a coal derived liquid and therefore

merits a detailed discussion. Jones and Friedman (32) indicated that supposed more active catalysts did not give better reaction rates and a conclusion was drawn that the no change in conversion indicated possible diffusion resistance. This lack of activity however, could easily have been caused by pore blocking from ash in the oil (.15%) or from improper activation of the respective catalysts. The actual sulfur results are inconclusive and their conclusion appears to be drawn on the basis of the oxygen and nitrogen data. Data are also reported on the effect of a reduction in catalyst particle size from 1/16" to 20-35 mesh. Desulfurization was stated to have doubled for the smaller size catalyst although by their own admission, the smaller catalyst had only been on stream a short number of hours and was probably more active than the 1/16" catalyst. Their data seem to contradict their conclusion since desulfurization appears to have worsened with the smaller particle size. Also, the average bed temperature was 25°F higher for the small catalyst runs. Let it suffice to say that their experimental results do not bear out their conclusions.

In summary, pore mass transfer limitations in trickle flow reactors are difficult to predict due to the present state of ability to predict other properties such as diffusion coefficients and effectiveness factors. Experimentation is the most reliable technique for detection of mass transfer limitations, but even so, one must guard carefully against liquid distribution problems. Several investigators have shown increases in sulfur removal on particle size reduction (indicating a low effectiveness factor and thus pore transfer limitations) for petroleum feed stocks.

Hydrogen Rate

Little literature on hydrogen rate effects exists. Most researchers (28,29,37,41,52,58,60) report hydrogen rate when experimenting with trickle flow reactors but few have studied the effects. Jones and Friedman (32) did some work in trickle flow reactors at hydrogen throughput rates of 13,500 standard cubic feet (SCF) H_2/barrel of feed (Bbl) and 5,700 SCF/Bbl. No effects on desulfurization were reported and after reconciling the differences in operating conditions they concluded only a 2.6% difference in oxygen removal was obtained. In view of the discrepancy in their data on desulfurization as mentioned in the section on liquid velocity effects, one must question whether there was actually any hydrogen effect as all. Hoog (28) demonstrated a slight effect of hydrogen rate from 250 SCF H_2/Bbl feed to 1500 SCF H_2/Bbl feed on desulfurization of petroleum oils although no effect was demonstrated beyond 1500 SCF/Bbl feed. Frost and Cottingham (18) used a H_2 feed rate of 6,000 SCF H_2/Bbl feed, Gwin (22) used from 1500 to 4500 SCF H_2/Bbl feed in hydrogenation of asphalt, Stevenson and Heinemann (59) used 2300 SCF of recycle gas of which only some 90% may have been H_2, Byrns (10) used 1260 SCF H_2Bbl feed for desulfurization of gasoline, and Berg (6) used 3000 SCF H_2/Bbl in desulfurization of gas oils.

Hydrogen consumptions reported by Frost and Cottingham (18) were from 200-700 SCF H_2/Bbl residuum with the high consumption being at the most severe conditions of 600°F, 800 psig. Schmid (56) reported consumptions from 290 to 730 SCF H_2/Bbl feed again with the most H_2 being consumed at the most severe conditions. In a separate work,

Hoog (29) reported consumption of 176-440 SCF/Bbl feed. The most applicable work was that of Hoog which indicated no effect of H_2 rate beyond 1500 SCF H_2/Bbl feed. Wan (61) investigated hydrogen rates of 3980 SCF/Bbl and 39,800 SCF/Bbl with no effect of either rate or concentration on desulfurization. Other researchers have used hydrogen rates from as low as 1260 SCF H_2/Bbl to as high as 6000 SCF H_2/Bbl. In summary, the literature suggests that hydrogen consumptions generally range from 176-730 SCF H_2/Bbl with higher temperatures and longer residence times being related to the high consumption. A feed hydrogen rate greater than 1500 SCF H_2/Bbl would be safe for operation although a check at higher rates should be made.

Temperature Effects

Temperature effects are reported consistently by almost everyone who has worked on desulfurization (37,41,42,56,61). Increasing temperature increases the rate of sulfur removal for all investigators reviewed here. Several investigators have reported activation energies for desulfurization reactions and there is a considerable range from 3.8 kcal/mole to 56.2 kcal/mole (6,66). The majority of the investigators (17,18,19,56) however, report an activation energy in the range of 24 to 34 kcal/mole. Activation energies of this magnitude are associated with chemical rate since the energy necessary to break the chemical bonds involved in the reaction are considered to be from 20 kcal/mole on up (6). One must also point out that these activation energies come from experiments on a wide variety of feed stocks and catalysts, under different experimental conditions, and with desulfurization kinetic models ranging from 1st order to 3rd order. An observation

can be made that in-spite-of-the-fact that so many conditions were investigated, most researchers found activation energies outside the range (2-8 kcal/mole) that is generally associated with diffusion controlled kinetics for desulfurization of petroleum stock. Two investigators (37,57) desulfurizing petroleum based stocks report changing activation energies with increasing temperature, thus indicating a possible change in mechanism from chemical control to diffusion control. A summary of temperature effects must say that increasing temperature increases sulfur removal and for the majority of cases activation energies were found to be larger than those associated with diffusion controlled kinetics. Temperature effects will be further discussed as they relate to kinetic modeling.

Pressure Effects

Hydrogen pressure effects on desulfurization are almost as varied as temperature effects. Distinguishing a definite pattern is much more difficult however. Hoog (28), Schmid (56), Frye and Mosby (19), Quader and Hill (42) and Berg et al. (6), and others report an increase in desulfurization on increasing pressure for a variety of feed stocks and conditions. Jones and Friedman (32), however, showed no noticeable pressure effect. Closer examination of some of the above mentioned works is necessary to yield some interesting conclusions. Schmid (56) shows a dramatic increase in sulfur reaction rate with increasing pressure up to approximately 1000 psia using a trickle flow reactor on a vacuum residuum. The rate then levels off at an almost constant value above 1000 psia. Hoog (28) shows that only a slight increase in sulfur removal is affected with a pressure increase from 735 psia

to 2200 psia on a shale oil at 750°F. Jones and Friedman (32) were unable to show a significant increase in sulfur removal with a pressure increase from 2000 psia to 3000 psia on a coal derived liquid (COED oil) at 725°F. Quader and Hill (42) also show a decreasing effectiveness of pressure on sulfur removal from a low temperature coal tar, although they show a leveling off at approximately 1500 psia, slightly higher than Schmid's work. The work of Wan (61) on the same feed stock as used in this thesis work also shows no significant increase in sulfur removal upon a pressure increase from 1000 to 2500 psia. Most workers such as Wilson et al. (66) and Berg et al. (6), who showed a dramatic increase in sulfur removal on petroleum feed stocks with an increase in pressure, were conducting experimental work below a pressure of 735 psia. At least one conclusion is beginning to emerge from the maze of data. Dramatic increases in sulfur removal are obtained for pressure increases in the range of 100 psia to 1000 psia and the effectiveness of pressure on sulfur removal is severely decreased beyond 1000 psia. Higher pressure operations from 3000 to 6000 psia were not considered here due to the poor commercial economics of such an operation.

As with temperature effects, one of the most striking or interesting points is that the work on pressure effects was on a variety of feed stocks ranging from light catalytic cycle oil (26) to low temperature coal tar (43) and resid (18). From such a diversity of works one would tend to generalize the results to say that for sulfur removal one can expect a significant increase as pressure is varied up to about 1000 psia with little gain beyond that point.

Space Time and Kinetics

The effects of space time must include a discussion of the kinetic models for completeness. All investigators reviewed by this author showed increases in desulfurization with increases in space time or, alternatively, with decreases in space velocity. The degree of increase and thus the corresponding model for the description of desulfurization had a considerable variation though. Desulfurization on both coal liquids and petroleum stocks has been described by first order kinetic models (17), second order kinetic models (56) and even the suggestion that some data best fit a third order kinetic model (18). Fry and Mosby (19) and Hammar (23) fit Hougan and Watson type models to their desulfurization data from gas oils. A closer examination of some of the above articles will begin to shed some light on this seemingly bewildering situation.

Hoog (26) is responsible for much pioneering work in the area of understanding desulfurization in a trickle flow reactor. Hoog formulated a first order kinetic model to describe the desulfurization of a Middle East gas oil and proceeded to take data to fit the model. To his surprise the data did not fit the model and when plotted on a semi-log basis the data were shown to curve. Fortunately, Hoog also took data on some narrow boiling fractionations of the same gas oil. He found that the narrow fractions did follow a first order relationship with the lighter fraction having a larger reaction rate constant than the heavier fraction. At this juncture Hoog speculated that "the higher the molecular weight of the sulfur compound, the more the sulfur atom may be shielded from the hydrogen atoms by hydrocarbon

groups." A colleague of Hoogs, Dr. Schuit (26), offered the alternative explanation that the phenomenon might be due to an increase in specific absorbability with increasing molecular weight, the inherent reactivity of the sulfur-bearing molecules being probably independent of molecular weight. Hoog's contributions still stand out as possibly the best to date and the explanations of the data are certainly as palatable as some later ones.

Frost and Cottingham (18) have conducted some meaningful research on a residual fuel. They found that their results obtained at 600°F more nearly exhibited psuedo-third order kinetics, those at 740°F, psuedo-second order kinetics and those obtained at 800°F, nearly first order kinetics. They finally concluded that the data best fit, over the entire temperature range, a psuedo-second order model if pressure corrected. That is, a plot of $c/(1 - c)$ vs. $P/\sqrt{SV}$ gave straight lines. Here c = fraction sulfur removed, P = pressure, and SV = liquid volume hourly space velocity. They also noticed a decrease in activation energy as space velocity was increased and concluded that diffusion must be important. No independent checks for diffusion effects were made, therefore, Hoog's explanations also explain the data.

Massagutov et al. (37) show that their data are best fit by a second order model. They also report that the activation energy changes from 33 kcal/mole to 5.3 kcal/mole with an increase in temperature from 662 to 806°F, and they concluded that diffusion must play an important role at high temperatures. To support the conclusion that diffusion is important they show an increase in rate by a factor of 4.3 with a decrease in particle size by a factor of six, from 0.3 cm to 0.05 cm. Massagutov's work was done on a vacuum distillate from a crude oil.

Hammar (23) conducted desulfurization studies on gasolines that were primarily focused on thiophene compounds in the gasoline (Using experimental conditions of 647°F, 300 psia). Hammar was unable to reconsile the data with a first order model and a Hougen and Watson approach to fitting the data was taken. Fourteen models were tested and of the fourteen tried, only one successfully fit the data. The model which best fit the data was based on a reaction between one absorbed component and one in the bulk phase. It is interesting to note that the model proposed can be condensed into a second order model by combination of constants and considering the concentration of H_2S in the vapor phase negligible compared to that of hydrogen.

In a later work, Frost and Cottingham (18) desulfurized two resids from Venezuelan crude. The work was carried out at approximately 750 to 805°F and 800 to 1600 psia. They found that the desulfurization fit a first order model quite well. In this work they also conducted catalyst size studies over a range of 6-8 mesh to 16-20 mesh and found substantial increase in sulfur removal indicating diffusion plays an important role. This also seems to confirm Massagutov's effect of particle size at high temperatures. Fry and Mosby (19) have conducted some of the most significant recent research. They found the desulfurization of a light catalytic cycle oil at 500° - 700°F did not follow first order kinetics. They next developed a model based on a Hougen and Watson approach. On the assumption that surface reaction was the rate controlling step, the equation

$$\frac{ds}{dt} = k\, P_S\, P_H\, (1 + B_i\, P_i)^m$$

was developed, P_S, P_H, and P_i represent the partial pressure of sulfur, hydrogen, and specie i respectively, k is a rate constant, t is time, m is a constant that depends on reaction mechanism, and B_i is the adsorption equilibrium constant of specie i. Using this model they were able to fit their data, as well as account for the partial vaporization of the liquid. Their data also includes the results of studies of single specie, trimethylbenzothiophene and dibenzothiophene, desulfurization rates. The single specie desulfurization data confirmed that the low boiling sulfur compounds are significantly easier to desulfurize than the higher boiling compounds. First order plots for the single specie sulfur removal followed the straight lines. Fry and Mosby also showed that sulfur compounds with about the same boiling point can vary in desulfurization rate by a factor of five. Thus, structural effects in desulfurization were concluded to be large. These results of Fry and Mosby serve to confirm the findings of Hoog some 17 years after Hoog's first reports.

The last work to be reviewed here with respect to kinetics is that of Schmid and Beuther (56). For hydrodesulfurization of an atmospheric resid at 675° to 790°F and 1000 psia, Schmid and Beuther found that the data best fit a second order rate expression. They too suggested that the second order fit is the result of many different species of sulfur reacting at different rates. Schmid also discovered that asphaltenes play a significant role in the rate of desulfurization. A 20% removal of asphaltenes increased the rate of desulfurization by a factor of four due to removal of the particles with a coking tendency. A model presented for the structure of asphaltenes indicates there could be significant difficulty in adsorbing a given asphaltene sulfur molecule

on an active catalyst site. Schmid and Beuther also investigated the effect of catalyst surface area, pore radius and pore volume. The empirical equation: % desulfurization = K + .0589 A + 13.2 V + .012 R summarizes the effects of catalyst parameters. K = a constant depending on reaction conditions, A = surface area of catalyst, R = pore radius, and V = pore volume. Schmid and Beuther recognize that the variables are not independent and that a compromise will be necessary to maximize desulfurization. Several more articles on desulfurization could be presented (11,12,27,53,63) but the results would not be significantly different from those above. In the above presentation, temperatures as well as other influencing factors are often included not to add to the confusion but to try to provide a small thread of hope for reaching a conclusion or at least tying the results together.

Summarizing all of these reports begins to show some general trends for petroleum stocks. Investigations carried out at lower temperatures ($600^{\circ}F$) tend to show second order reaction rates as the best describing rate equation. Those studies carried out at higher temperatures (around $800^{\circ}F$) indicate a first order reaction. Particle size effects as well as low activation energies point to a diffusion limitation at higher temperatures. A general conclusion would then be that at lower temperatures reaction proceeds at slow enough rate that reaction is controlling. The higher temperature and thus higher rate could in turn cause a diffusion limitation. Therefore, to understand the reaction and its mechanism, low temperature studies are necessary.

Catalyst Pore Size Effects

The next question of some interest, pore size effect, ties in with the work of Schmid and Beuther as indicated above. Also immediately

recognizable is that the effect of changing pore size is not a simple matter to discern. The unfortunate part of making changes in catalyst pore structure is that the effects must be sifted through a maze of other influencing factors before the results are known. Film diffusion, liquid distribution, liquid backmixing, pressure effects and the reaction kinetics need to all be accounted for before a meaningful pore size or distribution data can be properly interpreted. Theory provides guidelines for changing catalyst physical properties and it definitely must be relied upon when doing experimental work. Perhaps the best paper on the subject of changing catalyst support parameters is one by Van Zoonen and Douwes (60). As they indicate, one must understand the relationship between the physical properties of a catalyst and its apparent activity. The theory of Thiele and Wheeler (50) provides the necessary link between physical properties and activity. As an example, Van Zoonen and Douwes consider a continuous-flow tubular reactor with a catalyst bed and plug flow conditions. For a first order reaction the following equations are presented:

$$\ln\left(\frac{C_{in}}{C_{out}}\right) = \ln\left(\frac{1}{1-f}\right) = \frac{k}{S_v}\,S\eta$$

$$\text{with:}\quad \eta = \frac{1}{h}\left(\frac{1}{\tanh 3h} - \frac{1}{3h}\right)$$

$$\text{and } h = \frac{R}{3}\sqrt{\frac{2k}{rD_L}}$$

The symbols are defined as follows:

C_{in} and C_{out} concentrations of total sulfur in feed and product respectively

f	fraction of feed sulfur compounds converted
k	reaction rate constant per unit surface area
S_v	liquid volume space velocity of the oil
S	specific surface area of catalyst
η	fraction of catalyst surface effectively used during the reaction (effectiveness factor)
$2R$	average pellet diameter
r	average pore radius
D_L	diffusion coefficient of the sulfur compounds inside the pores

Wakao and Smith (62) present more elaborate developments for diffusion and reaction in porous catalysts but their treatments will be left to the reader for more detailed reading.

As may be recalled, h is the Thiele modulus previously defined as Φ under the section on diffusion effects. Derivation of the above equations also follows the explanation under diffusion effects. One might suspect, and rightly so, catalyst activity is strongly influenced by many of the parameters considered in the section on liquid distribution and diffusion effects. The purpose of the theory here is to show how the physical properties such as pore radius relate to activity. From a set of carefully designed experiments Van Zoonen and Douwes were able to show first that the desulfurization of a gas oil was diffusion limited at 700°F. Diffusion limitation was established by obtaining higher rates with smaller pellets. Next they were able to show that by eliminating the large pores of a catalyst, while keeping the surface area constant, a significant reduction in desulfurization was affected. Their conclusion was that a catalyst should have a set of narrow pores

to create sufficient internal surface area and a set of wide pores to make this surface accessible. They were also able to demonstrate that a loss of internal surface area causes a reduction in rate, as one would expect. Although much commercial data on hydro-desulfurization catalysts is available, little information is published about the pore size. Also as Van Zoonen and Douwes point out, unless the specific pore size vs. pore volume data are given it is almost impossible to compare average pore radii as there are many enigmas associated with the correct determination. Van Zoonen and Douwes do not stand alone in their prediction of the effect of large pores on the rate of desulfurization. The formula of Schmid and Beuther (56) also predicts that for a reduced pore radius, with constant surface area and volume, a decrease in desulfurization is expected.

Additional information concerning the effects of pore size and pore size distribution can be obtained from patents. Likins (35) has prepared a review of pertinent patent literature and some interesting concepts are pointed out. One of the first points mentioned is that hydrocarbon molecules are frequently rod like in conformation. A C_{45} molecule should have a cross sectional diameter of 4 Å and a length of 50 Å. A molecule with average pore diameter less than 50 Å could likely enter the pores based on cross sectional area but not on its linear dimension. The significance of increasing average pore size can easily be seen when dealing with large molecules. One patent (U.S. 2,890,162) presents new methods for characterizing pore size and distribution based on results obtained by hydrodesulfurization of gas oil feed stocks. Briefly, the patent recommends a catalyst having a most frequent pore diameter (D_f) of above 60 Å and a spread of the

range of the more frequent pore diameters (ΔD_r) of at least 10 Å. Also a pore distribution factor (PD) of at least 5.0 is preferred.

$$PD = \frac{(D_f)^2 \times \Delta D_r}{10^4}$$

The parameters as determined from mercury penetration procedures are obtained as follows:

1) Draw a base line from the lower extremities of the pore distribution curve.
2) Draw a vertical line from this base line to the apex of the pore distribution curve.
3) Draw a horizaontal line half way up the vertical line parallel to the base line.
4) The points at which the parallel line crosses the two branches of the distribution curve defines the range of more frequent pores.
5) The pore diameter corresponding to the apex of the distribution curve is the most frequent pore diameter.

The method provides a valuable guide in that it quantizes however arbitrairly a discussion of pore sizes and distributions. Experimental evidence that substantiates the limiting values of D_f, ΔD_r and PD is presented in the patent. The experimental catalysts were of the cobalt molybdate type supported on low silica gamma alumina. Likins generally proceeds to substantiate the claims of patent (U.S. 2,890,162) by reviewing further patents and experimental work based in the same general area. Patent (U.S. 2,924,568) by the same authors as patent (U.S. 2,890,162) substantiates the PD factor. Patent (U.S. 3,245,919)

describes results of desulfurization of hydrocarbon oil stocks at 580 to 780°F and pressures of 200-800 psi. Catalysts whose average pore diameter were greater than 80 Å exhibited better diffusion characteristics. Patent (U.S. 3,383,301) issued to Gulf Research and Development Co. discusses the effect of pore structure on residue desulfurization. The Gulf patent recommends a catalyst with pores from 0 to 300 Å radius with the majority of pores evenly distributed from 0 to 120 Å. Evidence to the superiority of their catalyst is presented for desulfurization of a Kuwait crude. Most patents are fairly consistent and recommend large pores but with a uniform distribution of pores. Some patents are reviewed by Likins which seem to contradict the trend but which on closer scrutiny seem to yield to the large pore concept. Patent literature therefore seems to substantiate the concept advanced by Van Zoonen and Douwes.

A summary of the section of the effect of pore structure must contain some obvious points. First, theory predicts that for a diffusion limited case the smaller the pore radius the slower the rate of reaction provided total surface area is about constant. The second point brought to light is that large pores are necessary to make the internal surface area of the smaller pores completely accessible. Patent literature seems to substantiate the need for larger pores and a method for determining if a catalyst meets the proper requirements for good desulfurization is presented.

Sulfur Compound Identification

As previously indicated, the literature for the above survey contains information on many different feed stocks. One could therefore

wonder at the validity of comparing the works. Several people have done much work on determining the types of sulfur compounds in the various feed oils. On petroleum, the U.S. Bureau of Mines (45) has developed the most complete and available knowledge of sulfur compounds present in oils, having identified some 200 species. Contained in the Bureau of Mines report is an interesting account of the origin of sulfur compounds in oil from living matter. From the beginning, coal and petroleum oil must contain the same building blocks. The compounds

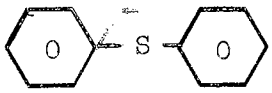

and

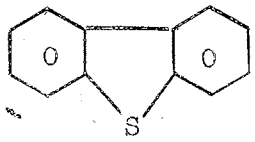

are the largest cyclic sulfur structures identified in petroleum oil, with most sulfur compounds being either mercaptains or sulfides and and some alkylated thiophenes. Huntington (31) in his postulation of the structure of coal indicated that most sulfur molecules are present as sulfide linkages or pendant to aromatic rings in a manner that would yield mostly mercaptains and sulfides and some thiophenes. Quader and Hill (43) indicate that the largest of the fundamental structures of sulfur compounds in a coal tar is dibenzothiophene, a compound located by the Bureau of Mines in petroleum. Fry and Mosby (19) indicated the largest sulfur molecules of concern in a catalytic cycle oil are again dibenzothiophenes. Hammar (23) indicates that thiophenes are the compounds of major concern in a shale oil gasoline. Wilson et al. (66) conducted their work on a naphtha doped with dibenzothiophene. Lowry (36) lists several sulfur compounds located in coal tar that Quader and Hill had not isolated. The compounds located, mercaptains, thiophenes, etc., provide more evidence that there is a

strong relationship between petroleums and coal derived oils. Some of the coal tar sulfur compounds were however much heavier than those identified in petroleum feeds. More work can be cited (27,30) to lend evidence that most of the sulfur compounds present in petroleum oils, shale oils, resids, and coal tars are similar. The reactions would therefore be expected to be similar and the works therefore have a very sound basis for comparison.

Literature Summary

From each of the above detailed literature reviews of various subjects, a massive condensation must be made to prepare a brief guideline document for this research project. The summary is as follows: (1) Pressure effects are expected to be insignificant above 1000 psig although below that pressure there is a significant effect; (2) Temperature has a very significant effect on desulfurization and appears to slow the reaction enough at temperatures from 700°F and below to cause the chemical reaction to be rate controlling. At temperatures higher than 700°F, the chemical reaction rate is fast enough that diffusion becomes the rate limiting mechanism; (3) Liquid distribution is very important in research equipment although radial profiles may be constant above a Reynold's Number of 100 and axial profiles or backmixing is unimportant above a Reynold's Number of 10. Liquid distribution effects should be experimentally verified; (4) Diffusion plays an important role as indicated by temperature effects. Absence or presence of diffusion control can be verified by changing catalyst particle size by a factor of at least four and would not be expected to have an effect below a temperature of 700°F.

Catalyst pore size changes will influence the desulfurization rate the smaller the size the slower the rate for constant surface areas. Large pores are necessary to provide accessibility to the catalyst surface area available in the smaller pores. Similar sulfur compounds have been isolated in both petroleum feed stocks and coal tars and there is reasonable evidence to expect coal liquids to behave similarly to petroleum stocks. Armed with the above information a sound experimental program can be embarked upon.

CHAPTER III

EXPERIMENTAL APPARATUS

The initial experimental apparatus, a backmix or mixed flow reactor and supporting equipment, was built by Skinner and theoretically, had some advantages in determining correct kinetic models. This reactor was seen as giving good liquid-solid contact and sufficient gas-liquid contact to eliminate any discrepancies which could be caused by poor phase contacting. Unfortunately, the problems encountered led to abandonment of the reactor. A brief description of the mixed flow reactor system is included in Appendix A. Some of the difficulties are discussed to benefit persons interested in a similar system.

The success of Wan (61) in using a trickle flow reactor to process the same feed stock as that used in this work promoted construction of a trickle flow reactor system, Figure 1. The success of Frost and Cottingham (17) and Jones et al. (32) with trickle flow reactors was also encouraging. This system was carefully designed to fulfill the following requirements:

1) The reactor should be capable of operating at temperatures to 800°F, the upper limit was established at 800°F since large amounts of cracking and increased coke deposition occur above this temperature. The reactor must be capable of isothermal operation along the length of the reactor.

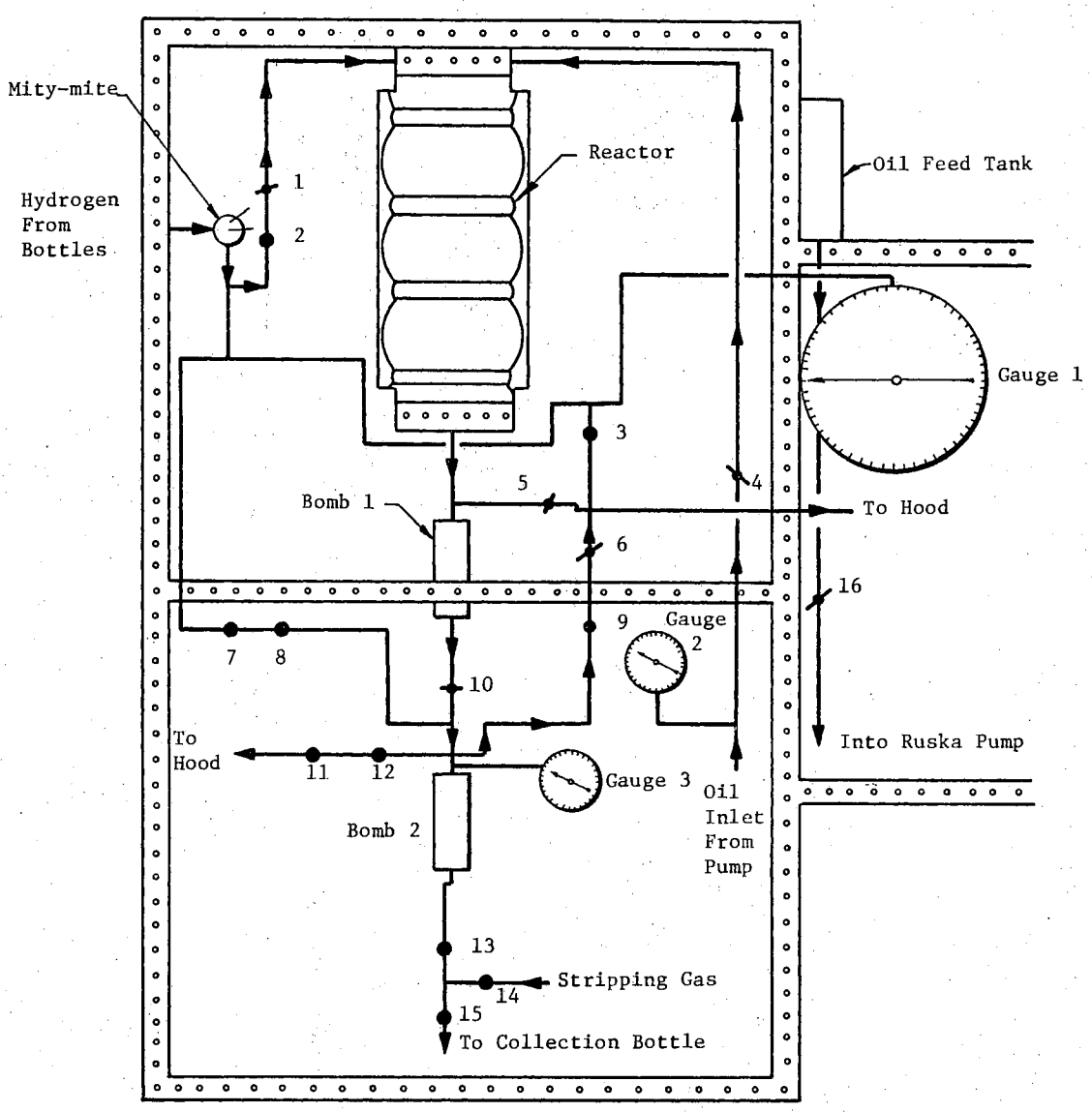

Figure 1. Sketch of Equipment Board Approximately to Scale

2) The pressure range should be from atmospheric to 2000 psig. The 0-2000 psig pressure range represents the range of variables indicated in the literature as suitable. Furthermore, 2000 psig is the maximum pressure rating for most readily available bombs, tubing, etc.

3) The system should allow no voids for oil accumulation which could invalidate the results.

4) Continuous 24 hour operation should be possible, therefore, continuous oil feeding and withdrawal must be possible. An ample hydrogen supply must also be available.

5) Change of bed height sould be possible to allow variation of operating conditions.

6) Reactor replacement should also be made as easy a task as possible.

Figure 1 shows that hydrogen enters in the upper left portion of the equipment and oil enters the right side of the equipment. Following the arrows, the hydrogen and oil flows respectively can be traced to the top of the reactor where they meet and flow concurrently down through the catalyst packed reactor. The liquid and vapor from the bottom of the reactor are then separated in one of two bombs which follow the reactor. The vapor and excess hydrogen gas are vented and the liquid is collected from the bottom of Bomb 2. Provisions were made for pressure, temperature, and flow control and monitoring throughout the system. Also rupture release lines and hydrogen gas detectors were installed for safety. A detailed description of each section of equipment follows.

Reactor

The reactor was a 33 inch long, 1/2 inch o.d., 316 stainless-steel tube. Figure 2 is a drawing of the reactor. The connections at the top and bottom of the reactor were a one-half inch Swagelok cross and straight union respectively. As can be seen from Figure 2 a one-eight inch stainless tube was used as a thermowell down the center of the reactor. The thermowell was welded shut on the bottom end and was secured at the top of the reactor by another Swagelok fitting. The 1/4" to 1/8" reducer through which the thermowell passes was drilled out to allow the tube to slip completely through. A 36" iron-constantan thermocouple was moved along the length of the well to take temperature profiles. As can be seen from Figure 2, 1/2" to 1/4" reducers were used to connect the reactor to the other parts of the system. Small fifty mesh stainless steel screens were placed at both ends of the reactor to hold the catalyst in the reactor. The screens were wedged between the 1/2" tube and the fittings at each end. See Figure 2 for placement.

Reactor Heaters

Specially designed aluminum blocks wrapped with heating elements provided heat to the reactor. There were five of the blocks arranged similar to that shown in Figure 4. As can be seen, the blocks were of different lengths to provide better heat distribution and temperature control. A more detailed drawing of one of the blocks is shown in Figure 3. Figure 3 shows that the blocks were solid aluminum with a 1/2" diameter hole for the reactor. The blocks were grooved with 3/8"

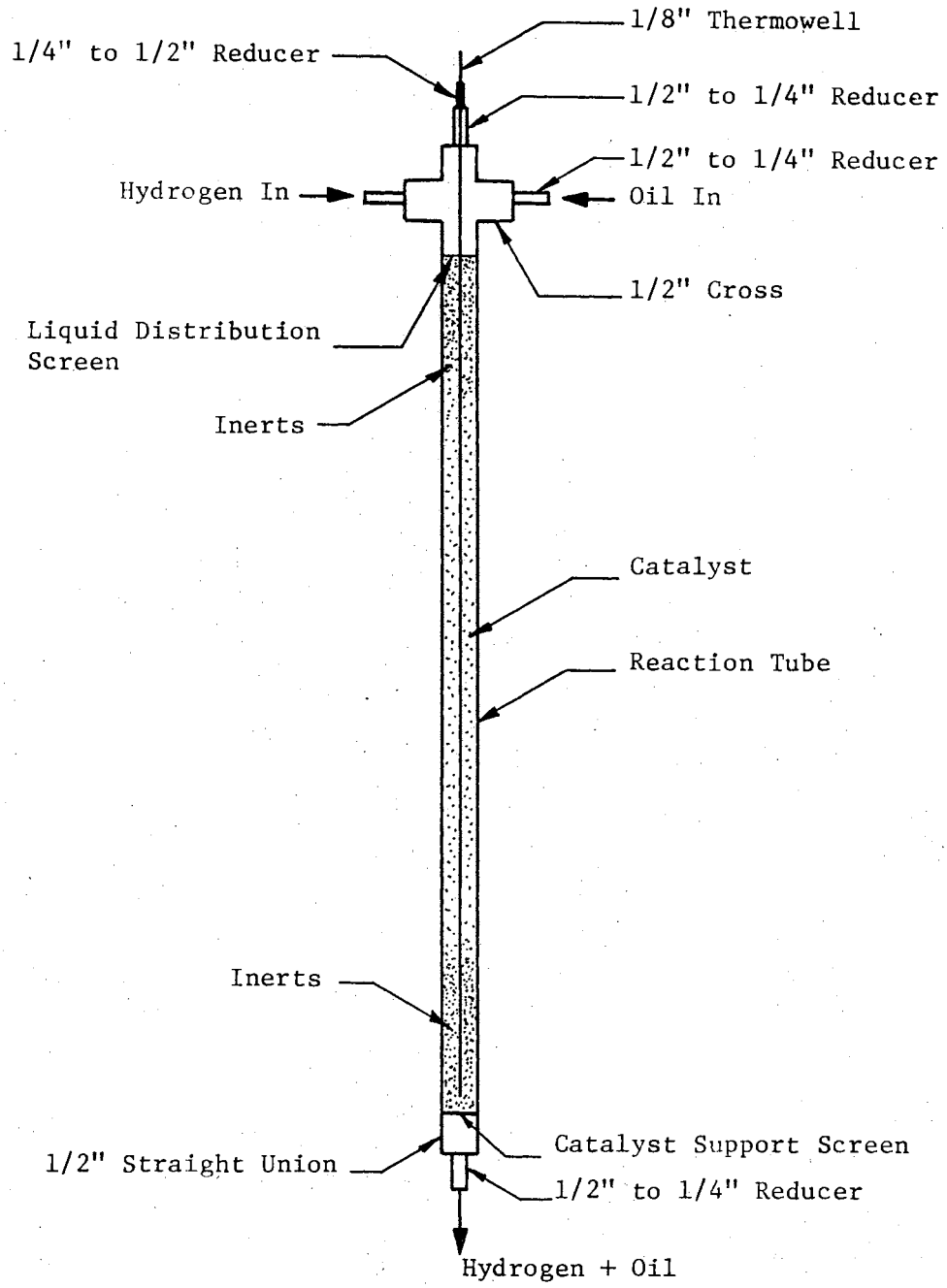

Figure 2. Reactor and Connections

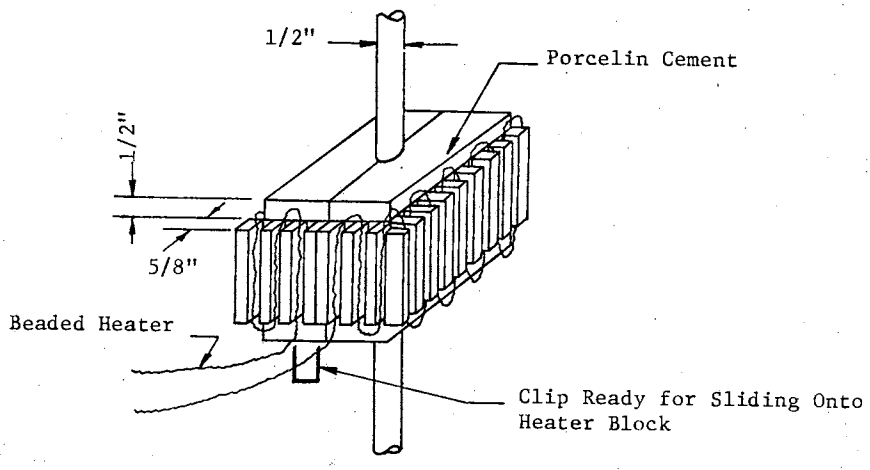

Figure 3. Heater Block Showing Tube and Beaded Heater

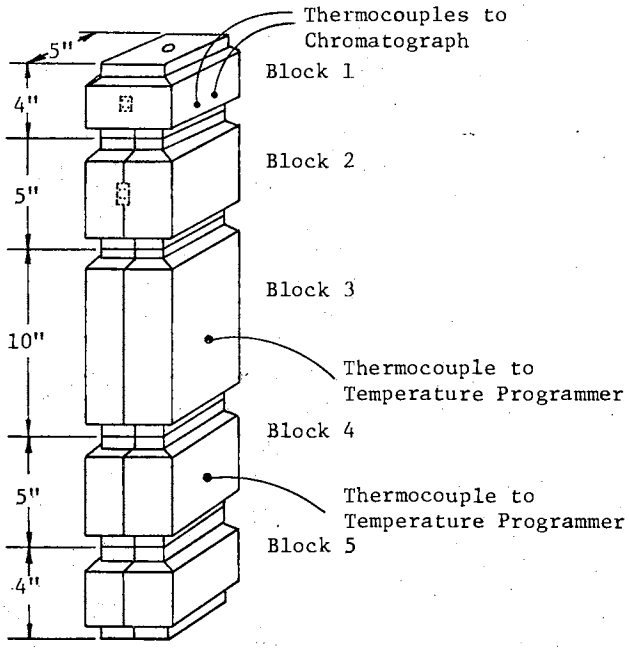

Figure 4. All Heater Blocks Showing Sizes and Suggested Arrangement

wide by 5/8" deep slots. In the grooves beaded heaters were wound according to Figure 3. Occasionally some porcelin cement was used to hold the heater in its groove. The blocks were split in the middle and hinged on one side to provide for easy reactor removal. When around the reactor, the blocks were held shut with small metal clips placed according to Figure 3. Control of the heaters was maintained by either Hewlett-Packard Model 240 controllers or powerstats. Control thermocouples for the controllers were placed in small holes adjacent to the beaded heater, see Figure 4. Best control was affected by placement close to the heating element. Control with the powerstats was maintained by balancing heat input with loss by trial and error to achieve the desired temperature profile. Final placement of controllers and rheostats was as follows: block 1 - Hewlett-Packard model 240 controller; block 2 - powerstat; block 3 - Hewlett-Packard model 240 controller; block 4 - Hewlett-Packard model 240 controller; and block 5 - powerstat. Operation of controllers is described in Hewlett-Packard model 240 operations manual.

Reactor Insulation

The heating blocks were wrapped first with a one-inch layer of felt insulation fabric. The felt insulation was held in place by strips of asbestos tape. Next, a two-inch layer of fiberglass insulation was added to the reactor, see Figure 5. The fiberglass insulation was also held in place by strips of asbestos tape. See Figure 1 for view of insulated reactor in the system. The breaks in the insulation, i.e. where the pieces fit together, were placed in the back of the equipment;

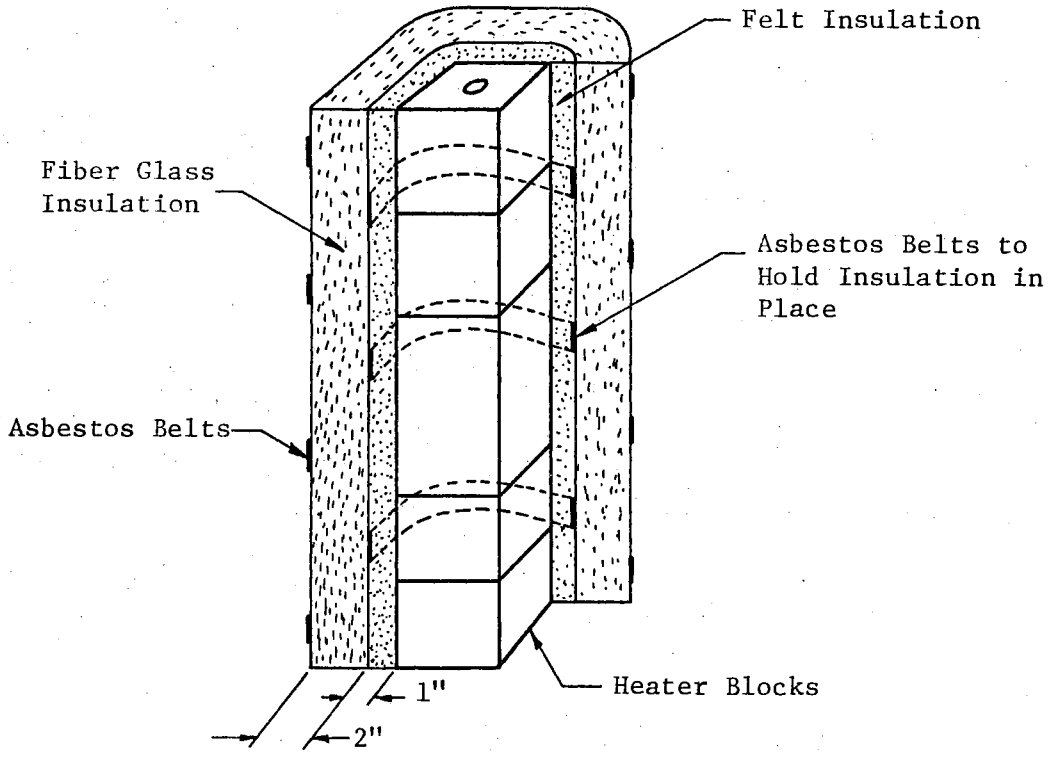

Figure 5. Heater Blocks Showing Insulation

and, electrical connections for the heaters were made in these breaks. The breaks were then carefully packed with small bits of insulation to avoid unnecessary heat loss.

Sampling System

The sampling system was designed to provide continuous operation with no dead space to entrap liquid. The bottom of the reactor was attached to the 1st sample bomb with a short piece of 1/4" stainless tubing. This sample bomb was a one liter stainless-steel bomb rated to 1800 psig. The 1800 psig established the maximum safe working pressure of the system. A detailed view of the bomb and the fluid flow into the bomb can be seen in Figure 6. The entry of the 1/4" stainless tube into the bomb was made possible by drilling out the 1/2" to 1/4" Swagelok reducer to allow the 1/4" tube to slip through. The seal on the tube was made by a Swagelok fitting on the 1/4" tube. Vapor and liquid disengagement occurred within the bomb, and the liquid then was allowed to collect in the bottom for sampling. Another sample bomb was placed directly below the first bomb, (Bomb 2 is exactly the same as Bomb 1). Adequate valving and bypass lines were provided between the bombs to insure smooth operation, see Figure 1 or 7 for valves. Liquid flow and sampling technique will be described in the section on experimental procedure.

Pressure and Flow Control

Pressure control was maintained with a Mitey-Mite pressure controller as seen in Figure 1. The system pressure was monitored on a 0-5000 psig Heis gauge. Best pressure control with a Mitey-Mite was obtained

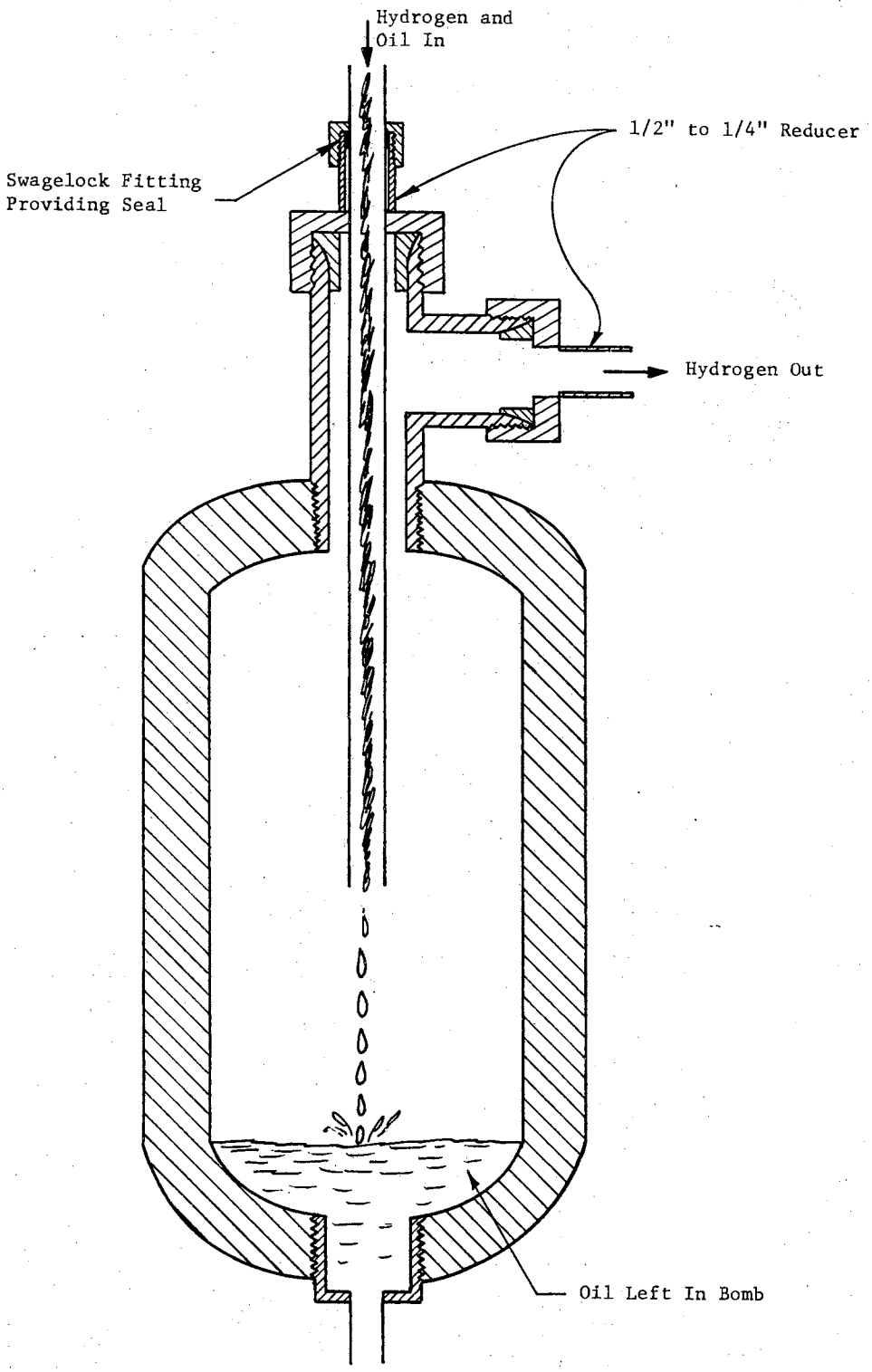

Figure 6. Exploded View of Bomb

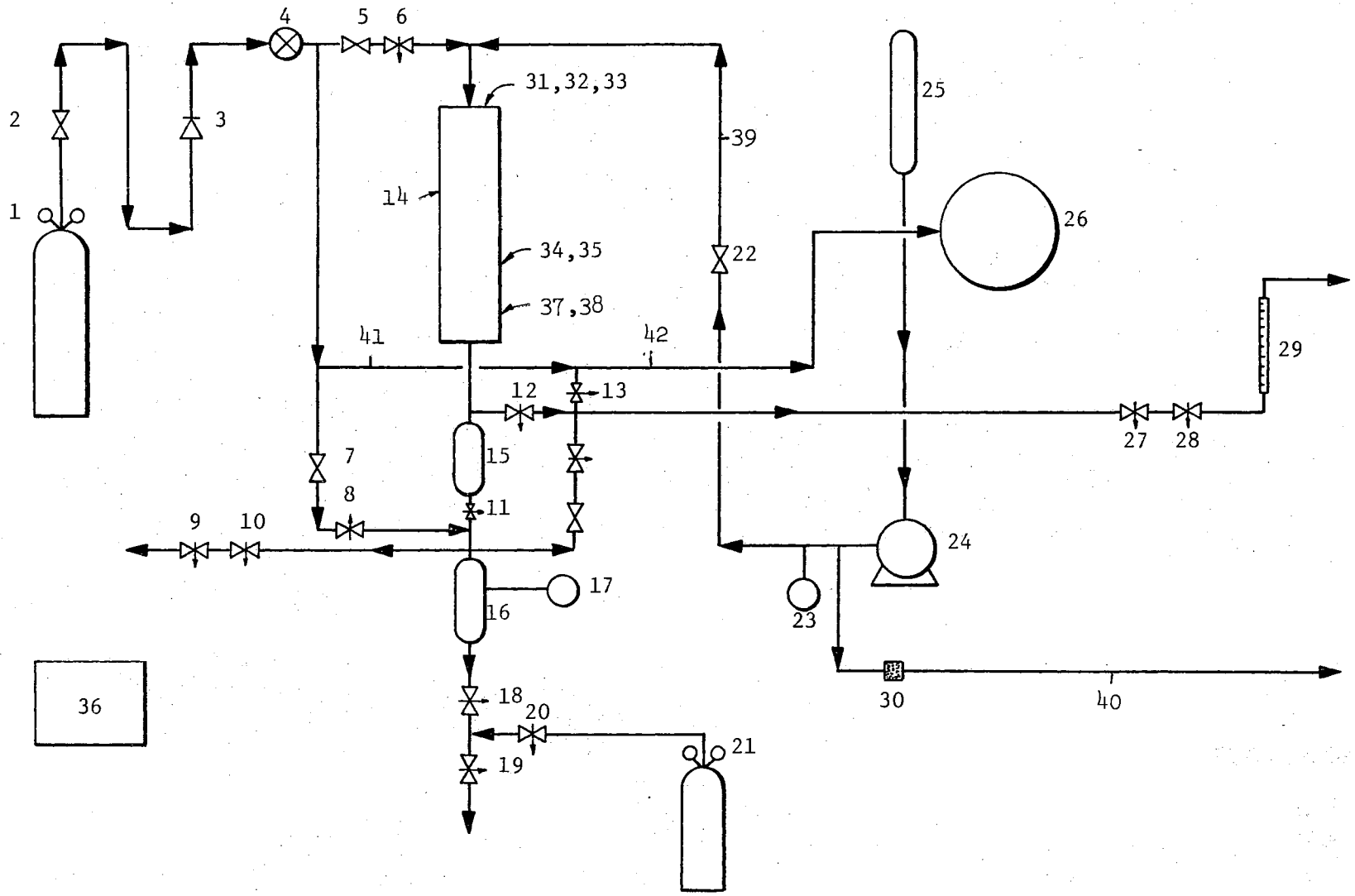

Figure 7. Schematic Flow Sheet of Reaction System

by having a small pressure differential across the controller. Pressure up stream from the controller was maintained by Matheson Model 8 regulators to approximately 200 psig above system pressure. With accurate pressure control, the system gaseous flow control could be maintained with two valves down stream from the reactor. See Figure 1 for location of valves. The first flow control valve was an Autoclave vee tip type valve (Model 10V-4071) designed to take a major portion of the pressure drop. The second valve was a Whitey needle valve (Model SS-22RS4) used for fine control of gas flow. Down stream from the control valves, the gas flow rate was monitored on a 0-25 ml bubble meter at low flow rates and on a Precision-Scientific wet test meter at extremely high gas flow rates.

Oil and Hydrogen Feed Systems

The oil feed system consisted of a Ruska positive displacement pump, and a 2250 cc feed storage tank. The feed storage was connected to the pump according to Figure 1. Hydrogen was fed to the reactor directly from bottles. A manifold was constructed to allow switching hydrogen bottles during a run. The only other special provision in the hydrogen system was an excess flow value which would shut the system down if a sudden drop in pressure occurred in the system. See Figure 8 for hydrogen manifold and valves.

Temperature Readout

Reactor temperature was monitored by moving a 36" thermocouple along the reactor thermowell and reading the temperature on a Leeds and Northrup digital readout. Temperature control for the first few inches

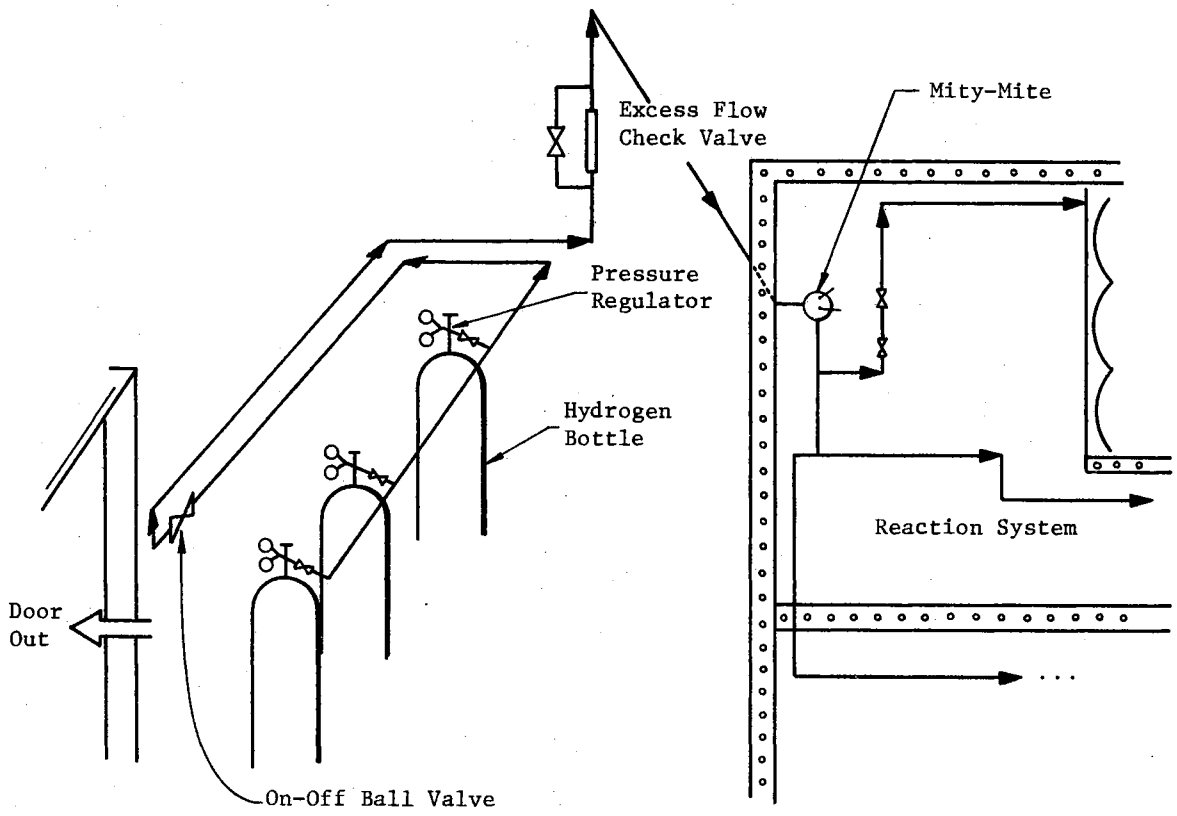

Figure 8. Sketch Showing Hydrogen Bottle Manifold

of catalyst bed became more difficult as temperature increased; however, the deviation was rarely more than 5°F from the average temperature. The thermocouples used to measure the temperature were Conax, J-SS4-G-T3-36", iron-constantan thermocouples. The thermocouples were calibrated against a platinum resistance thermometer or a platinum-rhodenium thermocouple according to Appendix B. Calibration of programmer thermocouples need not be done except for convenience. The digital readout was linearized according to the procedure set forth in Leeds and Northrup model 900 digital readout operations manual. The results of the linerization are presented in Table XXI of Appendix C.

System Materials

Figure 7 is a schematic of the system with numbers. The numbers correspond to Table I which lists all materials of construction and vendor. All instrumentation is also numbered and listed. Gases and chemicals are listed in Appendix D, as are catalysts and catalyst physical properties.

Safety Devices

Working with high pressure hydrogen is cause for considerable safety. Two types of precautions were taken, one to detect any leaks in the system and the other to provide for proper release of pressure or for system shut down in the event of a line rupture. Working in an enclosed room offers the possibility of hydrogen accumulation. To detect possible hydrogen accumulation, a MSA model 501 hydrogen detector was installed. The detector has two diffusion heads which were located near the ceiling of the room. The alarm was set to go off when the

TABLE I

LIST OF EXPERIMENTAL EQUIPMENT

1. Regulator - Matheson Model 8
2. Ball valve - Whittey No. SS-4152
3. Check valve - Autoclave No. SK-4402
4. Pressure Regulator - "Mitey-Mite" model, Grove Valve and Regulator Co.
5. Soft Seat valve - Whittey No. SS-3TS4
6. Vee Tip valve - Autoclave No. 10V-4071
7. Soft Seat valve - Whittey No. SS-3TS4
8. Vee Tip valve - Autoclave No. 10V-4071
9. Vee Tip valve - Whittey No. SS-1VS4
10. Needle valve - Autoclave No. 10V-4071
11. Vee Tip valve - Autoclave No. 10V-4071
12. Vee Tip valve - Autoclave No. 10V-4071
13. Vee Tip valve - Whittey No. SS-1VS4
14. Reactor - 1/2" O.D. 316 Stainless, .049" walls, 33" length
    a) Thermowell 1/8" O.D. 316 Stainless, 33" length
15. Receiving Bomb - 316 Stainless, 1000 cc, Matheson
16. Receiving Bomb - 316 Stainless, 1000 cc, Matheson
17. Pressure Gauge - 0-3000 psig, Autoclave No. p-480
18. Vee Tip Valve - Whittey No. SS-1VS4
19. Vee Tip Valve - Whittey No. SS-1VS4
20. Vee Tip Valve - Whittey No. SS-1VS4

TABLE I (Continued)

21. Regulator - Air Products No. E11-F-N115G
22. Vee Tip Valve - Autoclave No. 10V-4071
23. Pressure Gauge - 0-3000 psig, Autoclave No. P-480
24. Ruska Positive Displacement Pump - Variable Drive, 0-1200 psig
25. Feed Tank - 2250 cc, 316 Stainless, Matheson
26. Pressure Gauge - 0-5000 psig, Heise-Bourdon Tube
27. Vee Tip Valve - Autoclave No. 10V-4071
28. Needle Valve - Whittey No. SS-22RS4
29. Bubble Meter - 0.25 cc
30. Rupture Disk - 3000 psig, Autoclave
31. Connax Thermocouple - No. J-SS4-G-T3-36"
32. Bonded Heater - Precision Scientific
33. Leeds and Northrup Digital Read Out - Model 900-001-003-1
34. (Three) Hewlett-Packard Temperature Programmers - Model 240, 0-1500°C
35. (Two) Powerstat - Fisher No. 9-521
36. MSA-Hydrogen Detector - Model I-501 Wall Mount, dual diffusion head
37. Felt Insulation Fabric - McMaster-Carr No. 9326P5
38. Fiberglas Insulation - McMaster-Carr No. 9356M13
39. 1/4" O.D. x .083" I.D. 304 Stainless Tubing - Includes all tubing unless otherwise specified
40. 1/2" O.D. x 3/8" I.D. 304 Stainless Tubing
41. 1/8" O.D. x 1/16" I.D. 304 Stainless Tubing
42. 1/8" O.D. x 1/16" I.D. 304 Stainless Tubing

hydrogen concentration in the room reached 50% of the lower explosibility limit. Pumping the liquid with a constant displacement pump offers the possibility for tremendous pressure build up and possible pump damage if the liquid delivery lines become clogged. To avoid this possible pressure build up, rupture disks rated for 3000 psi were placed on the liquid delivery line close to the pump exit, see Figure 7. The rupture disks were vented with 1/2" stainless tubing to the hood. Line rupture within the system while operating is always a possibility. Such a rupture would allow hydrogen to pour into the room at hydrogen delivery pressure until the entire bottle was emptied if no check were provided. To prevent such an occurrence the excess flow valve, shown in Figure 8 was installed.

CHAPTER IV

EXPERIMENTAL PROCEDURE

Experimental procedure can be broken down into five basic categories: catalyst preparation and loading, normal operation, sampling, shutdown, and analysis. An additional section devoted to specific operating conditions, changing them and reaching steady state is also required to complete this section on experimental procedure.

Catalyst Preparation and Loading

The catalyst was crushed from the normal 1/8" extrudates, as received, to 8-10 mesh particles. The choice of size corresponds to a tube diameter to particle diameter (D_T/D_P) ratio of 4.7/1.0 and a tube length to particle diameter ratio (L/D_P) of 232 which should give good catalyst-liquid contacting as well as absence of backmixing effects. After crushing, the catalyst was loaded into the reactor tube. A catalyst bed depth of 20 inches was chosen to allow liquid volume hourly space times of 1.5, .75, and .375 hours for liquid feed rates of 25, 50, and 100 cc/hour respectively. The 20 inch catalyst bed was placed in the middle of the reactor to minimize end effects due to preheat and end heat loss. With the preceeding considerations in mind, the reactor, removed from the system, was packed according to the following procedure, pouring material in the bottom of the reactor and packing from the top down. The retaining screen was first inserted at the top of the reactor.

1) Pour in 6.5" of porcelin crushed berl saddles (inerts), 8-10 mesh, tapping reactor vigorously for proper settling.
2) Pour in 20" of catalyst, 8-10 mesh, tap reactor vigorously while pouring in catalyst.
3) Pour in 6.5" of inerts, 8-10 mesh, tap reactor vigorously while pouring.
4) Place small 50 mesh screen on bottom of inerts, place straight-union on tube and screen, tighten Swagelok fitting. Note: On all threads of 1/2" Swagelok fittings, a lubricant such as "silver goop" facilitates tightening and loosening and prevents seizing. Silver goop is particularly useful on connections which are frequently loosened.

The packed reactor was then secured in the system by the two feed lines at the top and one exit line at the bottom. Immediately after connecting the reactor to the rest of the system a nitrogen pressure test to 2000 psig was conducted at room temperature. Waiting to test until the heating blocks are on is a mistake, since there will not be enough room to make good visual observation of the fittings. Each fitting in the entire system should be checked at this time using soap solution or some other suitable detecting solution. The heating blocks can be put in place and secured after a satisfactory leak check of the system. Insulation goes on after the heating blocks. Care must be taken to keep all thermocouples in their proper positions while insulating the heating blocks. Access to the ends of the beaded heaters also needs to be maintained during the insulation process. Next, the temperature controllers need to be connected to the heating blocks and the thermocouple placed in the reactor thermowell.

Care should be taken in connecting the heaters to controllers and a check for short circuits with a volt-ohm meter must be made before applying current. The catalyst bed was then heated to 450°F and a low flow rate of prepurified nitrogen was allowed to flow over the bed for 12 hours to remove excess moisture.

The last step in catalyst preparation is the sulfiding. Before sulfiding the catalyst, the Mity-Mite regulator was capped such that no H_2S could reach it. The line to the Heis gauge was broken at a union and connected to a bottle of 5% (vol.) H_2S in hydrogen. The temperature of the catalyst bed was held constant at 450°F and the H_2S mixture was allowed to flow over the catalyst at a rate of 1/2 cc/sec. for 1.5 hours. The exit stream was passed into a caustic solution. The system was flushed with nitrogen before reconnecting the Mity-Mite and the Heis gauge.

Normal Operation

Immediately after the Mity-Mite and Heis are reconnected, the oil is turned onto the catalyst and the pressure raised to operating pressure. (A leak check with soap solution was made at this time.) The temperature controllers were set to operating temperature and the system was allowed to come to steady state. Approximately 48 hours of line-out operation on oil were made before experimental sampling was begun. The system was considered to be at normal running conditions when the reactor exit flow went to the second bomb.

To fully understand the flow scheme under the mentioned conditions refer to Figure 1. Figure 1 shows that during "normal running" hydrogen enters the system through Valves 1 and 2 and flows down through the

reactor through Bomb 1, through Valve 10 and into Bomb 2. From Bomb 2, the hydrogen and gases from the system go through Valve 9, Valve 6, then through the control valves and to the hood. Under the hood the hydrogen and gases were bubbled through a 50% sodium hydroxide solution to remove acid gases and then taken through a bubble meter. The oil enters through Valve 4, flows down through the reactor and collects in Bomb 2. A summary of valve position for "normal running" is shown in Table II.

TABLE II

VALVE POSITION SUMMARY FOR "NORMAL RUNNING"

Valve		Valve	
1	open	9	open
2	open	10	open
3	closed	11	closed
4	open	12	open
5	closed	13	closed
6	open	14	closed
7	closed	15	closed
8	open	16	closed

Note that there are two valves-back-to back in some positions with one of the valves serving no apparent function. In each case, the extra

valve is provided as a back up valve to the first. Past experience revealed the need of the extra valve to maintain continuous operation in the event of failure.

Sampling

Actually there is more than one situation which demands deviation from the "normal" settings. Most of the deviations from normal, however, can be convered by the "sampling" procedure. Assume for a moment that there is a sample in Bomb 2. The objective is to remove the sample and cause as little disturbance to the system as possible. The first step is to provide an alternate route for the gas to leave the system. The alternate route is obtained by opening Valve 5 (refer to Figure 1). Now close Valve 9 and the hydrogen still has a route through the reactor to the hood. Next, close Valve 10. Bomb 2 has now been completely isolated from the rest of the system and liquid will collect in Bomb 1. Valve 11 can be carefully cracked opened and the pressure on Bomb 2 bled off. When the pressure has reached atmospheric, Valve 12 and 14 can be opened and the sample can be stripped with nitrogen to remove NH_3 and H_2S. After stripping, Valve 11 is closed and a small positive pressure is left on Bomb 2.

Valve 14 is closed, Valve 15 opened and the sample can be collected from below Valve 15. Valves 13 and 15 are closed after sample collection and Bomb 2 is ready to repressure. Bomb 2 is repressured by carefully opening Valve 7. Before opening Valve 7, Valve 2 should be closed. Repressuring Bomb 2 takes only a short time (approximately 30 seconds) and the hydrogen flow is interrupted only for this short period of time. When the pressure on Gauge 3 reaches system pressure,

return all of the valves to the settings listed in Table II. The liquid collected in Bomb 1 will now quickly drain into Bomb 2 and can be collected if desired. Refilling the Ruska feed pump was sometimes necessary during a run although a certain amount of planning will allow most fillings to occur during transient periods of changing operating conditions. To fill the pump with the minimum amount of upset to the system, turn the pump off and close Valve 4. Slowly open Valve 16, watching the pressure decrease on Gauge 2. Make certain the oil feed tank has adequate oil and turn the pump to reverse. The pump will draw the oil into its barrel. Valve 16 is closed and valve 4 slowly opened again watching the pressure on Gauge 2. The pump filling operation can be minimized to from one to two minutes. A small amount of practice will make the sampling procedure much shorter than it now seems. The procedure may seem a bit confusing but following the above steps in sequence will help assure safe operation and a quick understanding.

Shutdown Procedure

Shutdown of the equipment is simple. The valves are left in the positions listed in Table II. The hydrogen is shut off at the tank and the electrical equipment (temperature controllers, pump, etc.) is turned off. The system pressure is bled down to 200 psig through Valve 11 and the system is allowed to cool to room temperature before the remainder of the pressure is released. A hydrogen atmosphere should remain in the system until cooling is complete to avoid coking reactions. A nitrogen purge is made after the system has reached atmospheric pressure and before any connections are loosened. Cooling can be expedited by removing the two layers of insulation.

Temperature Measurement

As was previously described a thermowell was incorporated in the reactor. The temperature of the reactor was recorded at one inch intervals beginning above the catalyst bed and continuing well below the catalyst bed. A typical temperature profile is shown in Figure 9 for each of the temperatures run (600°F, 650°F, and 700°F). All temperature measurements were taken by downward movement of the thermocouple. The digital temperature readout was allowed to stabilize before each reading was taken.

Temperature profiles for all runs were equal to those presented in Figure 9. Inspection of the temperature profiles shows that in no case did deviation from the operating temperature exceed $\pm$ 5°F and was closer to $\pm$ 1°F for the 650°F and 600°F profiles. Radial temperature profiles were also considered. Since the axial temperature measurements were made in the radial center of the catalyst bed, some knowledge must be obtained as to how representative the axial temperature is of the temperatures close to the outer reactor wall. Measurements of the catalyst radial center temperature were made in the axial center of the catalyst bed and at a corresponding point in the same horizontal plane on the external surface of the reactor tube wall via a hole drilled through the heating blocks. The same thermocouple was used for both measurements. Table III on the next page shows the results of the measurements. The maximum radial ΔT detected was 3.1°F. The measurements were made at maximum temperature of 750°F and must therefore be taken as a conservative measurement of radial temperature gradients at lower temperatures. Note also that the catalyst bed itself will be much

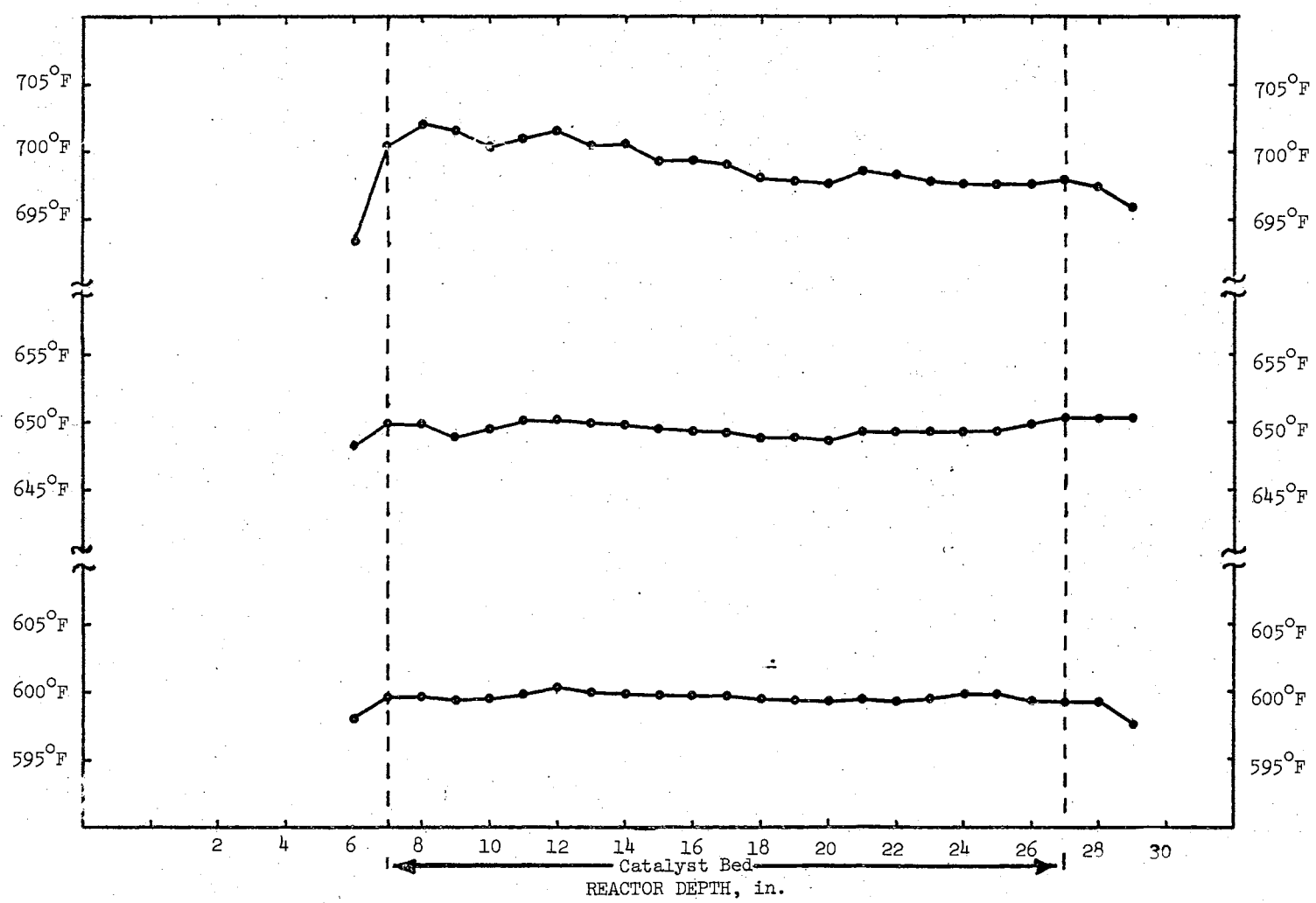

Figure 9. Axial Temperature Profiles

closer than this 3°F since the temperatures measured are really tube wall temperatures and there is a ΔT across the wall (admittedly small) and across the inside films (the larger ΔT).

TABLE III

RADIAL TEMPERATURE MEASUREMENTS IN REACTOR

Inside Temperature	Outside Temperature
763.4°F	760.7°F
761.3	758.0
758.2	756.2
754.2	757.1
756.1	753.2

Operating Conditions and Steady State

Bringing the equipment to steady state before each sample was taken was briefly mentioned in the section on "normal running" and bears further explanation here. When first starting the equipment up about two to three hours are required for the catalyst bed temperature to line out. Temperature profiles need to be taken at 15 minute intervals during transient periods of heating to minimize the amount of time for bringing the equipment to steady state. After the temperature profile

had stabilized on initial start-up, a minimum of 48 hours of oil contacting catalyst was used to assure the catalyst activity had stabilized before sampling began. Checks of samples taken during this start up period showed that the catalyst did not change activity after the first 10 or 12 hours.

A detailed description of the method used to take data for two isotherms will suffice as a guide for operating technique. After the catalyst had been "lined out" on a particular isotherm, say 600°F, the pump was set for a volume hourly space time of 1.5 hours. After two or three volumes of oil per volume of catalyst had passed through, the reactor was considered to be at steady state. A temperature profile was taken at steady state and a sample was also taken. For long space times, 50 cc samples were taken (time required was approximately two hours for the 50 cc). Before changing conditions another sample was also taken to assure the system had reached steady state. The samples were stripped with nitrogen for approximately 15 minutes before they were collected from the sample bomb. Temperature profiles were always taken at minimum of 1 hour intervals to detect any upsets the system might have incurred. Continuous temperature monitoring of a specified single point in the reactor was always made. Once the samples had been taken, the oil feed pump was moved to a new setting to give a space time of .75 hours. Again two or three volumes of oil were allowed to pass through the reactor before sampling (Frost and Cottingham (18) used the same criterion of two or three volumes of oil for steady state in their trickle flow reactor). Two 50 cc samples and a temperature profile were taken before conditions were changed again. Next, a space time of .375 hours was used. The 100 cc samples were

taken in an analogous fashion. After operation at .375 hour space time, the reactor was returned to 1.5 hour space time operation and samples were again taken. This return to the 1.5 hour space time setting was made as a check to insure that catalyst activity had not changed during operation. Temperature programmer settings were changed to yield a 650°F profile and temperature monitoring was increased to 15 minute intervals. After the temperature profile had stabilized at 650°F, the same procedure was followed as with the 600°F isotherm. Two samples were taken at each space time setting and the 1.5 hour space time setting was repeated at the end. After 700°F and 750°F isotherms were run, the reactor was returned to 600°F and additional samples were taken at 1.5 hour space time. Return to the first set of operational conditions run was another check to assess the extend of change in catalyst activity. Usually about 120 hours of operation had elapsed between the first and final runs at 600°F. The above description of experimental conditions and run sequencing should suffice as an adequate guide to reproducing the results on a similar experimental piece of equipment. Slight variations did exist from this described operating technique for the various catalyst loadings. However, the basic methods and concepts remained the same.

Sample Analysis

Sulfur analysis was previously described by Wan (61), however, the procedure will be reiterated here with more detail. The sulfur contents of the products as well as of the feed were analyzed by means of a Leco automatic sulfur determinator. The general procedure for analysis with the equipment is described in the Leco Bulletin.

The basic concept of the equipment operation is to burn the sulfur to SO_2 in the combustion furnace and then titrate the SO_2 by an iodate method.

The details of the procedure are as follows. First, a starch solution is prepared by adding 2 gm. of Arrow root starch to 50 ml. of distilled water. Pour the 50 ml. of water and starch into 150 ml. of boiling distilled water. Bring the mixture to a boil and allow to boil for 1 minute. Turn off heat and allow the solution to cool slowly to room temperature. When cool, stir in 6 gm. of KI making sure all the KI is well dissolved. This solution should be made new each day. Other solutions which are required, but may be kept for periods up to one month, are an HCl solution and a KIO_3 solution. The HCl solution is made by pouring 15 ml. HCl in a 1 liter flask and diluting to 1 liter with distilled water. The KIO_3 solution is made by adding .111 gm. to a one liter flask and diluting to one liter with distilled water. Care must be taken to dissolve the KIO_3 well. The Leco furnace and titrator are turned on approximately 30 minutes prior to use to allow the equipment to warm up. Rinsing the titrator with water is a recommended practice prior to running. A mark should be made on the titrant receiver before filling with HCl solution. The mark will assure a constant amount of HCl solution each time an analysis is run. The oxygen flow should be turned on and allowed to bubble through HCl solution in the titrant receiver for approximately 15 minutes prior to operation. The bubbling action helps clean the titrating equipment. Also 15 minutes prior to operation, the heating wire trace between induction furnace and titrant receiver should be turned on. A powerstat setting of 40 appears to be

optimum for the length of wire and conditions of this particular analytical equipment.

Sample preparation is the next step to the analysis. To a crucible, see equipment list, add .282 ± .005 gm. of magnesium oxide. Weigh the crucible and MgO then add .1 ± .002 gm. oil. Next add another .282 gm. MgO. Top with 1.5 ± .005 gm. iron chips and .77 gm. tin granuals. Cover with a crucible lid and the sample is ready to be analyzed. The above sequence is also important and must be followed as set forth.

The sample must next be combusted. A describtion of the process follows. Fill the titrant vessel up to the line (suggested earlier) with HCl solution. Add approximately 5 ml. starch solution to the HCl solution and bubble oxygen through the mixture. Turn the tritrator to "end point" and let the titrator reach a medium blue end point. Approximately 4 to 5 divisions on the titrator burette should suffice to make the medium blue solution. The reactions involved in this step are:

$$KIO_3 + 5KI + 6HCl \longrightarrow 3I_2 + 6KCl + H_2O$$

$$I_2 + \text{starch} \longrightarrow \text{blue complex.}$$

The titrator next is turned to its mid position and .7 gm. sodium azide is added to the titrant receiver. The azide complexes the NO formed during sample combustion and thereby prevents interference of NO with the analysis. The amount that should be added is variable and if the blue solution turns dark before SO_2 titration begins, (while sample combustion is occurring) more sodium azide should be added.

After the azide is added, the titrator burette is refilled and the crucible is inserted in the furnace for burning. Turn the titrator to "titrate." The sulfur is burned to SO_2 which reacts according to

$$SO_2 + I_2 + H_2O \longrightarrow H_2SO_4 + 2HI$$

which is no longer a blue color. To keep the solution blue, KIO_3 is tritrated to release more I_2. The burette reading can then be turned into a sulfur %. Sample calculations are given in Appendix E. Usually three analyses were run on each sample and the average value was reported. General calibration procedure and the results of calibration are given under the Results section of this thesis. Good sulfur analysis relys heavily on technique of the operator and no substitute can be had for many hours of equipment operation to gain the skill and finesse necessary.

In this section of the thesis, a description was first given of the catalyst loading and preparation. Pressure testing and normal operation were described, followed by a description of the sampling procedure. Shut down procedure was covered after the sampling procedure. A detailed description of operating conditions and reaching steady state was included to provide a readable account of changing operating conditions. Last was a brief description of the sulfur analyzing procedure. The results of operating according to the procedure presented in this section, follow in the next section on Experimental Results.

CHAPTER V

EXPERIMENTAL RESULTS

Experiments were designed to determine the effect of (1) homogeneous or noncatalyzed reaction, (2) liquid distribution, (3) particle size, (4) temperature, (5) pressure, (6) space time, (7) hydrogen rate, (8) catalyst life, and (9) catalyst pore size. Also analytical and experimental precision were determined. Finally both feed and product were separated into eight distillation fractions and a determination was made about the sulfur present within each fraction. The results of fitting these data to various rate equations are also presented.

The data from each experimental run will be presented with an explanation of the reason for making the experiment. A brief summary of the results then follows. All results are presented as wt % of sulfur remaining in the product oil, i.e.

$$\text{wt } \% \text{ S} = \frac{\text{wt. sulfur}}{\text{total wt. sample}} \times 100$$

All curves presented in the following figures were drawn without least square techniques. However, fitting of the curves to a rate model was accomplished by least squares curve fit routines. Space times are reported as liquid volume hourly space times (LVHST) (volume catalyst per volume feed oil per hour). The catalyst weight for each reactor

loading is presented with each table of results for conversion to weight hourly space time (weight of catalyst per weight feed oil per hour) if desired. Nominal temperatures and pressures are presented in lieu of the actual temperature and pressure. Actual temperature never varied more than $\pm$ 5°F from the nominal temperature and then only for a short portion of the reactor length. Average temperature was within $\pm$ 2.0°F of nominal temperature as was shown in the previous section. Actual pressure was within $\pm$ 20 psia of nominal.

Analytical Precision

The first set of results to be presented is the precision of the analytical equipment. The lowest sulfur level which could be analyzed on a typical sample was 0.02 wt. %. Seven prepared known samples were analyzed on the Leco unit for their sulfur content five times each on a different day and in a random order each day to determine the precision of the analytical equipment. A standard deviation was calculated for each level of sulfur analyzed and is presented in Table IV. Sulfur analysis results and calculation of standard deviation are presented in Appendix F. As can be seen from Table IV the ability to accurately determine the amount of sulfur by the technique used at a concentration of 200 parts per million (0.02%) was badly deteriorated. The precision, however, fell quite sharply between 400 parts per million (ppm) and 200 ppm, but satisfactory results were obtained down to 400 ppm. Additional experimental results confirm the results of Table IV and show that the determinations are independent of sulfur type. These additional results, Table V, were obtained on samples made by diluting p-toluenethiol with toluene to the desired sulfur concentration. The difference between the

knowns prepared and analyzed in Table IV and those prepared for Table V were the sulfur compounds used. Table V knowns were prepared using p-toluenethiol as the sulfur compound and Table IV knowns were prepared using anthracene oil (feed material) of known sulfur concentration .43%.

TABLE IV

COMPARISON OF KNOWN SAMPLE CONCENTRATION OF ANTHRACENE OIL SULFUR IN TOLUENE WITH EXPERIMENTAL DETERMINATION OF SULFUR CONCENTRATION

% Sulfur	Std. Dvn.		% of Sulfur Level
.2	± .00838	or	± 4%
.15	± .00525	or	± 3.5%
.1	± .00581	or	± 5.8%
.08	± .00692	or	± 8.6%
.06	± .00491	or	± 8.2%
.04	± .00379	or	± 9.5%
.02	± .00400	or	± 20%

As a check of precision at high sulfur concentration two samples of p-toleuene-thiol in toluene were prepared, .43% S and .516% S. Experimental determinations were then made on the known samples. Comparison of the known sulfur concentrations with the experimentally determined concentrations, Table VI shows a deviation of some 4%. The

experimental precision was therefore established at ± 4% from .2% S to .516% S.

TABLE V

COMPARISON OF KNOWN SAMPLE CONCENTRATIONS OF P-TOLUENE-THIOL IN TOLUENE WITH EXPERIMENTAL DETERMINATION OF CONCENTRATION

% S	Determination	Dvn.	% S	Determination	Dvn.
.1	.096	.004	.2	.203	.003
.08	.0785	.0015	.08	.082	.002
.06	.0552	.0048	.06	.061	.001
.04	.032	.008	.04	.038	.002
.02	.026	.006	.02	.0147	.0053

TABLE VI

EXPERIMENTAL DETERMINATION OF KNOWN SULFUR CONCENTRATION IN HIGH RANGE

% S Known	Experimental Determination	Dvn.
.43	.447	+.017
.43	.456	+.026
.516	.499	-.017
.516	.497	-.019

Start Up Effects

During earlier stages of the program when equipment and procedures were under development some runs were made on Nalco Catalyst 474 to determine the effects of cooling the equipment and catalyst bed down and then starting up on the same catalyst loading on another day. Samples were taken after the temperature profile had stabalized, usually about 2 hours after start up. The results are presented in Figure 10, and indicate several valuable facts. First, about six hours of operation are necessary to line out again each time the equipment is started up. From these data the rather obvious conclusion was reached that the best way to take data would be to run the equipment on a continuous basis. Not only would continuous running save a half a day for each day of data taking, but the possibility of start up and shut down effects would be eliminated.

Equipment Precision

The first series of experiments run on the equipment were in part to determine the reproducibility of the equipment for operation at the temperatures, pressures, and space times of concern. These first series of runs were conducted with Nalco Catalyst 474. Catalyst pre-conditioning and run conditions were identical for each of three separate runs.

For each space time and temperature a standard deviation was calculated, and the results are presented in Table VII. The largest standard deviations are associated with the shortest space time as expected. The fast rate of desulfurization at short space times

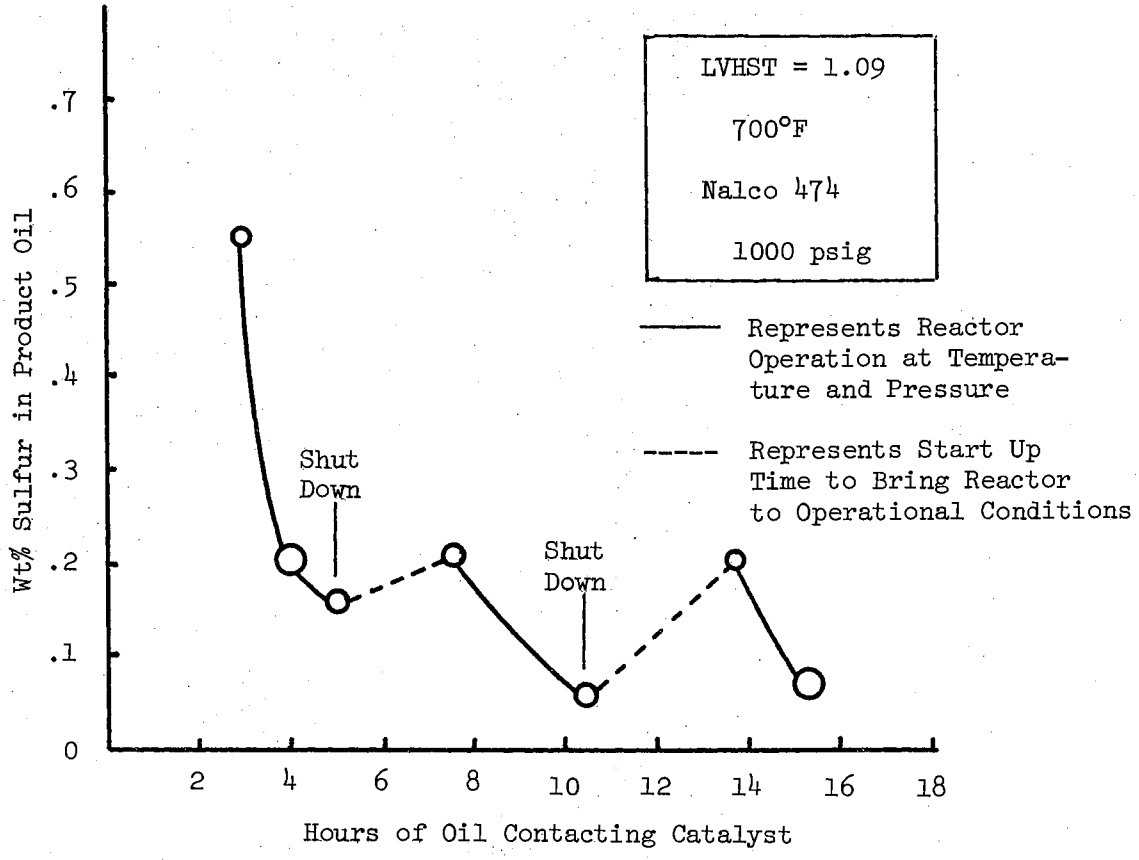

Figure 10. Effects of Daily Start Up and Shut Down on Sulfur Removal

causes larger errors in measurement of the sulfur removal. Also the trend towards larger error with decreasing sulfur content is followed by all cases except 600°F and .75 hr.

TABLE VII

STANDARD DEVIATIONS FOR EXPERIMENTAL POINTS
CATALYST NALCO 474
PRESSURE 1000 Psig

	LVHST		
Temp.	.375 hr.	.75 hr.	1.5 hr.
600°F	.179 ± .00903 %S	.129 ± .0136 %S	.091 ± .00858 %S
650°F	.102 ± .012	.079 ± .0033	.047 ± .00648
700°F	.062 ± .0139	.031 ± .0102	

Tables VIII, IX, and X show the experimental results of the runs made to establish equipment precision. Runs 2 and 3 were conducted at the beginning of the project to establish routine and early precision. Run 10 was the last run made at the end of the project to confirm that operational procedures had not changed. All three runs were made on fresh Nalcomo 474 catalyst, 8-10 mesh. Presulfiding and start up conditions were as described under experimental procedure. A compilation of all runs and actual conditions are presented in Appendix H. Summaries and tables are presented in this section and Appendix H should be consulted for actual results.

TABLE VIII

EXPERIMENTAL RUN #2, NALCOMO 474
8-10 MESH

Sample No.	Nominal Temperature	Nominal Pressure	LVHST	Wt. % S Oil Product
44	700	1000	.75	.026
45	700	1000	.375	.044
46	700	1000	.375	.047
65	650	1000	1.5	.050
66	650	1000	1.5	.048
67	650	1000	.75	.075
68	650	1000	.75	.079
69	650	1000	.375	.087
70	650	1000	.375	.112
71	650	1000	1.5	.050
72	650	1000	1.5	.050
73	650	1000	1.5 20,000 SCF	.043*
74	650	1000	1.5 20,000 SCF	.042*
75	600	1000	1.5	.094
76	600	1000	1.5	.088
77	600	1000	.75	.133
78	600	1000	.75	.129
79	600	1000	.375	.186
80	600	1000	.375	.177

* Normal operation was with approximately 1500 SCF of H_2 per Bbl OIL FEED. These two runs were conducted at 20,000 SCF of H_2 per Bbl OIL FEED. to determine the effect of increased hydrogen rate if any.

TABLE IX

EXPERIMENTAL RUN #3, NALCOMO 474
8-10 MESH

Sample No.	Nominal Temperature	Nominal Pressure	LVHST	Wt. % S Oil Product
PF 91	700	1000	.75	.024
PF 92	700	1000	.75	.021
PF 93	700	1000	.375	.079
PF 94	700	1000	.375	.063
PF 107	700	500	1.5	.024
PF 108	700	500	1.5	.029
PF 110	700	500	.75	.043
PF 111	700	500	.375	.086
PF 112	700	500	.375	.083
PF 113	650	1000	1.5	.043
PF 114	650	1000	1.5	.041
PF 115	650	1000	.75	.076
PF 116	650	1000	.75	.080
PF 118	650	1000	.375	.093
PF 119	650	1000	1.5	.034
PF 120	650	1000	1.5	.038
PF 121	650	1500	1.5	.039
PF 122	650	1500	1.5	.040
PF 123	650	1500	.75	.052
PF 125	650	1500	.375	.097
PF 126	650	1500	.375	.110
PF 128	650	1500	1.5	.034
PF 129	650	500	1.5	.069
PF 130	650	500	1.5	.055
PF 131	650	500	.75	.096
PF 132	650	500	.75	.093
PF 133	650	500	.375	.128
PF 134	650	500	.375	.140
PF 135	650	500	1.5	.064
PF 136	650	500	1.5	.060
PF 137	600	1000	1.5	.086
PF 138	600	1000	1.5	.077
PF 139	600	1000	.75	.120
PF 140	600	1000	.75	.107
PF 141	600	1000	.375	.170
PF 142	600	1000	.375	.162
PF 144	600	1000	1.5	.091
PF 146	600	1500	1.5	.074

TABLE X

EXPERIMENTAL RUN #10, NALCOMO 474
8-10 MESH

Sample No.	Nominal Temperature	Nominal Pressure	LVHST	Wt. % S Oil Product
PF 310	600	1000	1.5	.090
PF 311	600	1000	1.5	.091
PF 312	600	1000	.75	.142
PF 313	600	1000	.75	.141
PF 314	600	1000	.375	.187
PF 315	600	1000	.375	.190
PF 316	600	1000	1.5	.092
PF 317	600	1000	1.5	.111
PF 318	650	1000	1.5	.052
PF 319	650	1000	1.5	.054
PF 320	650	1000	.75	.084
PF 321	650	1000	.75	.081
PF 322	650	1000	.375	.102
PF 323	650	1000	.375	.115
PF 324	650	1000	1.5	.054
PF 325	650	1000	1.5	.051
PF 328	700	1000	.75	.043
PF 329	700	1000	.75	.041
PF 330	700	1000	.375	.070
PF 331	700	1000	.375	.070

Blank Runs

The amount of non-catalysed reaction that occurs was another variable in need of clarification. For this series of experiments the catalyst bed was replaced with an inert bed of porcelain berl saddles crushed to the same size as the catalyst, 8-10 mesh. Table XI shows the conditions and results of these runs. At 600°F no sulfur removal was detected. However, at 800°F and a space time of 1.5 hours (the maximum time - temperature stress) the sulfur remaining dropped to .105%. The sulfur retention at 700°F and .75 hr. was .272%. For less severe conditions of time and temperature (650°F and 1.5 hr) sulfur in product oil dropped to only .38 wt %. Figure 11 is a semi-logarithm plot of the wt. % S in the product oils vs. LVHST for the various temperatures.

Liquid Velocity Effects

To determine the effect of changing liquid velocity through the catalyst bed, a series of experiments were conducted on a bed of catalyst ½ the volume of the normal bed. Space time and hydrogen flow rate were held the same as for a full bed of catalyst. Thus, for identical space times for each catalyst bed height, liquid velocity through the beds must differ by a factor of two. Runs were made at 650°F and 700°F and a total reactor pressure of 1000 psig. The results are presented in Table XII. When compared to the results of a full bed, the ½ bed data shows a decrease in sulfur removal. Possible reasons for the decrease in sulfur removal will be discussed in the following chapter.

TABLE XI

EXPERIMENTAL RUNS #1 AND #9, INERTS
8-10 MESH

Sample No.	Nominal Temperature	Nominal Pressure	LVHST	Wt. % S Oil Product
PF 289	600	1000	1.5	.465
PF 290	600	1000	1.5	.460
PF 295	650	1000	1.5	.39
PF 296	650	1000	1.5	.38
PF 297	650	1000	.75	.41
PF 298	650	1000	.75	.41
PF 299	650	1000	.375	.46
PF 300	650	1000	.375	.47
PF 25	700	1000	1.5	.272
PF 26	700	1000	1.5	.298
PF 27	700	1000	.75	.337
PF 28	700	1000	.375	.383
PF 29	700	1000	.375	.408
PF 30	750	1000	1.5	.225
PF 31	750	1000	.75	.298
PF 32	750	1000	.75	.285
PF 33	750	1000	.375	.351
PF 34	750	1000	.375	.363
PF 18	800	1000	1.5	.105
PF 19	800	1000	1.5	.110
PF 20	800	1000	.75	.188
PF 21	800	1000	.75	.200
PF 22	800	1000	.375	.287
PF 23	800	1000	.375	.288

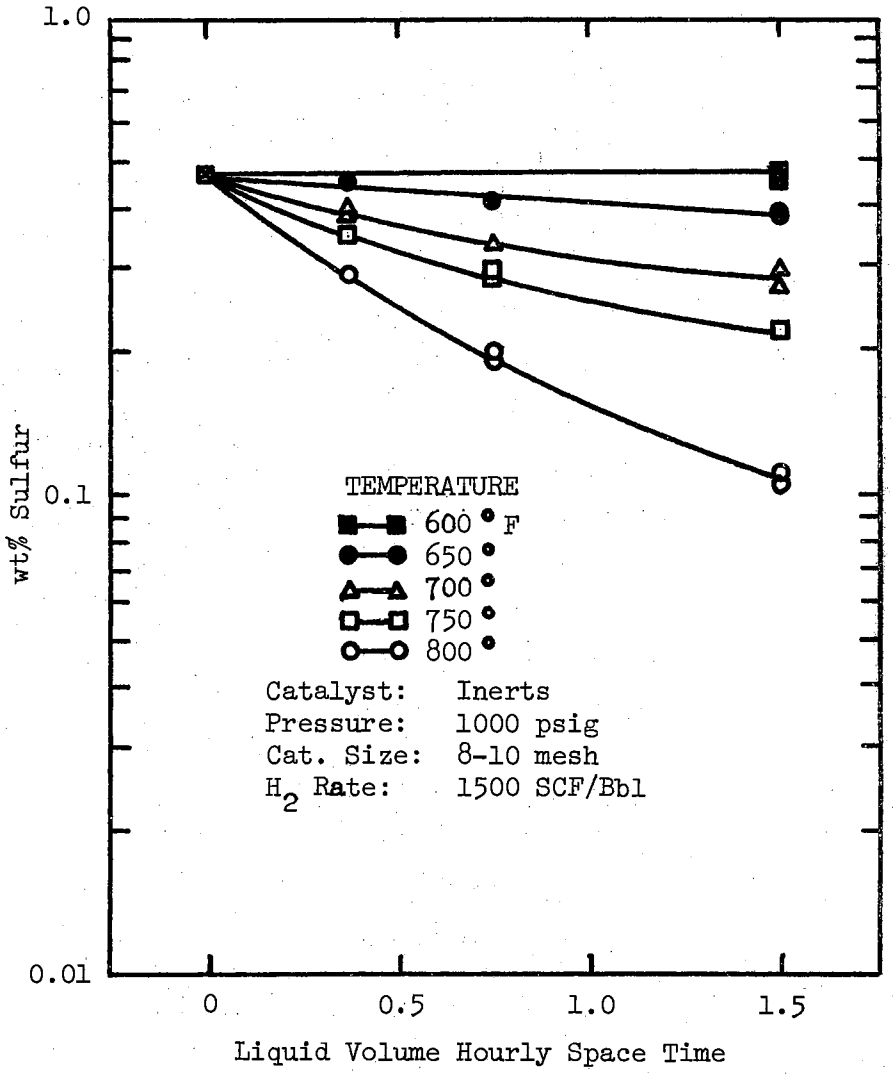

Figure 11. First Order Plot of Non-Catalyzed Data

TABLE XII

EXPERIMENTAL RUN #4, NALCOMO 474, ½ BED
8-10 MESH

Sample No.	Nominal Temperature	Nominal Pressure	LVHST	Wt. % S Oil Product
PF 187	650	1000	.75	.098
PF 188	650	1000	.75	.094
PF 189	650	1000	.75	.107
PF 190	650	1000	.75	.097
PF 191	650	1000	.75	.096
PF 192	650	1000	.75	.107
PF 193	650	1000	.75	.097
PF 194	650	1000	1.5	.064
PF 195	650	1000	1.5	.126
PF 196	650	1000	.75	.104
PF 197	650	1000	.75	.093
PF 198	650	1000	.375	.160
PF 199	650	1000	.375	.153
PF 200	650	1000	1.5	.065
PF 201	650	1000	1.5	.074
PF 204	700	1000	.75	.051
PF 205	700	1000	.75	.075
PF 206	700	1000	.375	.098
PF 207	700	1000	.375	.103

Particle Size Effects

To ultimately determine the effect of pore size distribution, a firm knowledge of all possible influencing factors must be had. Particle size effects will shed some light on both liquid distribution and diffusion effects. Runs were conducted at 1000 psig and 600°, 650°, and 700°F. Particle size was reduced from the usual size of 8-10 mesh to 40-48 mesh. Table XIII shows the results of the particle size runs. Comparison with a run on 8-10 mesh catalyst at identical conditions, shows there was no effect on the extent of sulfur removal on changing particle size by a factor of five.

Catalyst Activity

As mentioned in the chapter on Experimental Procedure, several samples were taken each run for the select purpose of establishing the extent of catalyst activity decay over the period of the entire sequence of runs. Samples 155, 156, 185 and 186 from the series on particle size are excellent examples and Table XIV shows the results of these samples taken at the same operating conditions but markedly different number of hours of oil on catalyst. Samples 212, 221, 226 and 227 show the effects of reactor start up on catalyst activity. A very slight increase in catalyst activity can be detected up to about 36 hours of operation at a fixed set of conditions, but activity is stable beyond that point as shown at 61 hours.

Pressure Effects

In addition to determining operating parameters such as catalyst activity, particle size, space velocity, non-catalysed reaction, etc.,

TABLE XIII

EXPERIMENTAL RUN #4, NALCOMO 474
40-48 MESH

Sample No.	Nominal Temperature	Nominal Pressure	LVHST	Wt. % S Oil Product
PF 155	700	1000	.375	.067
PF 156	700	1000	.375	.060
PF 167	650	1000	1.5	.041
PF 168	650	1000	1.5	.046
PF 169	650	1000	.75	.073
PF 170	650	1000	.75	.077
PF 171	650	1000	.375	.103
PF 172	650	1000	.375	.104
PF 173	650	1000	1.5	.038
PF 174	650	1000	1.5	.037
PF 175	600	1000	1.5	.084
PF 176	600	1000	1.5	.074
PF 177	600	1000	.75	.118
PF 178	600	1000	.75	.114
PF 179	600	1000	.375	.145
PF 180	600	1000	.375	.147
PF 181	600	1000	1.5	.085
PF 182	600	1000	1.5	.084
PF 185	700	1000	.375	.065
PF 186	700	1000	.375	.072

TABLE XIV

SAMPLING TO DETERMINE CATALYST ACTIVITY

Sample No.	% S Remaining	Hours of Oil	Temperature	Time
155	.067	61	700°F	.375 hr.
156	.060	63	↓	↓
185	.065	186		
186	.072	187		
212	.155	11	600°F	1.5 hr
213	.149	15	↓	↓
214	.167	20		
215	.154	24		
216	.154	28		
217	.146	32		
218	.151	36		
219	.146	40		
221	.142	48		
226	.143	59		
227	.150	61		

pressure effects were also investigated. Runs were made at 650°F, for total reaction pressures of 500, 1000 and 1500 psig. The results of these runs are presented in Table IX. Runs were also made at 700°F for pressures of 500 and 1000 psig. The results of the 700°F runs are also shown in Table IX. Table IX indicates a definite increase in desulfurization with increase in total reactor pressure from 500 to 1000 psig. However, there was no significant increase in desulfurization with a pressure increase from 1000 to 1500 psig. A similar run at 700°F was not made.

Temperature, Space Time and Rate Equations

Experiments conducted to determine temperature and space time effects are the same as those used to check precision, Runs 2, 3 and 10. As can be seen from any run, the effects of temperature are quite dramatic. Desulfurization increases with increasing temperature from 600°F to 700°F. Increasing space time is also important. However, the effect of increasing space time can be seen to have a greater effect in the region from 0 to .75 hr. than from .75 to 1.5 hours. A natural extention of determining space time and temperature effects is to fit data to kinetic models. In as much as most desulfurization has been modeled as first or second order reactions those were the first models tried. For comparison, third and fourth order models were also tried. For clarification, the model studied was:

$$\frac{-dC_s}{dt} = k\, C_s^{\,n}$$

where C_s = sulfur concentration, t = time, k = rate constant, and n (reaction order) was taken as 1 through 4. A least squares curve

fit was made for each order of reaction and a standard deviation was calculated for each isotherm. A sum of standard deviations was calculated for all of the runs to ascertain the suitability of the particular model for all the data. The standard deviation for each run is presented in Table XV and a sum of the deviations presented at the end of each order reaction tried.

A fourth order model fit the data equally as well as second and third order models. The first order model was noticeably worse than the other models, however. The second and higher order models are not intended to describe or represent any sort of mechanism at all, but rather demonstrate that in all probability a complex series of reactions are occurring which can be described on a total basis by the mathematical model.

Catalyst Pore Size Distribution

The extensive investigation of all factors which influence the performance of the reactor and reaction kinetics was conducted to assure an accurate assessment of the effects of changing pore size of the catalyst. Two catalysts were investigated which had changes in the pore size distribution relative to the regular Nalcomo 474. These two catalysts, labeled 72-A and 72-B were of the same chemical composition as Nalcomo 474. Run conditions and pre-run preparations were identical with those conducted on Nalcomo 474. Both catalysts, 72-A and 72-B, had surface areas slightly larger than the area of Nalcomo 474. The major change was that the pore size distribution was much more narrow and with the larger pores eliminated. Figures 12, 13 and 14 show the results of mercury penetration porosimetry performed by the

TABLE XV

RESULTS OF N^{TH} ORDER FIT OF DATA

Run No.	Reaction Order	Cat. Type	Temp.	Press.	Std. Dvn.	Cat. Size	Bed Length
			1st Order Fit of Data				
2	1st	474-Reg	700	1000	.02146	8-10	20 in.
2	1st		650	1000	.0287		
2	1st		600	1000	.0259		
3	1st		700	1000	.0130		
3	1st		700	500	.0262		
3	1st		650	1000	.0263		
3	1st		650	1500	.0263		
3	1st		650	500	.0241		
3	1st		600	1000	.0256		
5	1st		650	1000	.0229	40-48	
5	1st		600	1000	.0261	40-48	
4	1st		650	1000	.0194	8-10	10 in.
4	1st		700	1000	.0274	8-10	10 in.
6	1st	72-B	600	1000	.0231	8-10	20 in.
6	1st	72-B	650	1000	.0258		
6	1st	72-B	700	1000	.0325		
7	1st	72-A	600	1000	.0219		
7	1st	72-A	650	1000	.0278		
9	1st	474-Reg	600	1000	.0234		
9	1st	474-Reg	650	1000	.0248		
9	1st	474-Reg	700	1000	.0248		
Σ Std. Dvn.					.518		

TABLE XV (Continued)

Run No.	Reaction Order	Cat. Type	Temp.	Press.	Std. Dvn.	Cat. Size	Bed Length
			2nd Order Fit of Data				
2	2nd	474-Reg	700	1000	.0193	8-10	20 in.
2	2nd		650	1000	.0116		
2	2nd		600	1000	.0093		
3	2nd		700	1000	.015		
3	2nd		700	500	.0029		
3	2nd		650	1000	.011		
3	2nd		650	1500	.0065		
3	2nd		650	500	.0082		
3	2nd		600	1000	.0099		
5	2nd		650	1000	.0073	40-48	
5	2nd		600	1000	.0113	40-48	
4	2nd		650	1000	.0066	8-10	10 in.
4	2nd		700	1000	.0093	8-10	10 in.
6	2nd	72-B	600	1000	.0123		20 in.
6	2nd		650	1000	.0112		
6	2nd		700	1000	.0123		
7	2nd	72-A	600	1000	.0092		
7	2nd	72-A	650	1000	.0133		
9	2nd	474-Reg	600	1000	.0103		
9	2nd		650	1000	.0007		
9	2nd		700	1000	.0028		
Σ Std. Dvn.					.192		

TABLE XV (Continued)

Run No.	Reaction Order	Cat. Type	Temp.	Press.	Std. Dvn.	Cat. Size	Bed Length
			3rd Order Fit of Data				
2	3rd	474-Reg	700	1000	.0019	8-10	20 in.
2	3rd		650	1000	.0116		
2	3rd		600	1000	.0093		
3	3rd		700	1000	.0151		
3	3rd		700	500	.0029		
3	3rd		650	1000	.0111		
3	3rd		650	1500	.0065		
3	3rd		650	500	.0082		
3	3rd		600	1000	.0092		
5	3rd		650	1000	.0074	40-48	
5	3rd		600	1000	.0113	40-48	
4	3rd		650	1000	.0066	8-10	10 in.
4	3rd		700	1000	.0093		10 in.
6	3rd	72-B	600	1000	.0123		20 in.
6	3rd		650	1000	.0112		
6	3rd		700	1000	.0123		
7	3rd	72-A	600	1000	.0092		
7	3rd	72-A	650	1000	.0134		
9	3rd	474-Reg	600	1000	.0104		
9	3rd		650	1000	.0088		
9	3rd		700	1000	.0028		
Σ Std. Dvn.					.192		

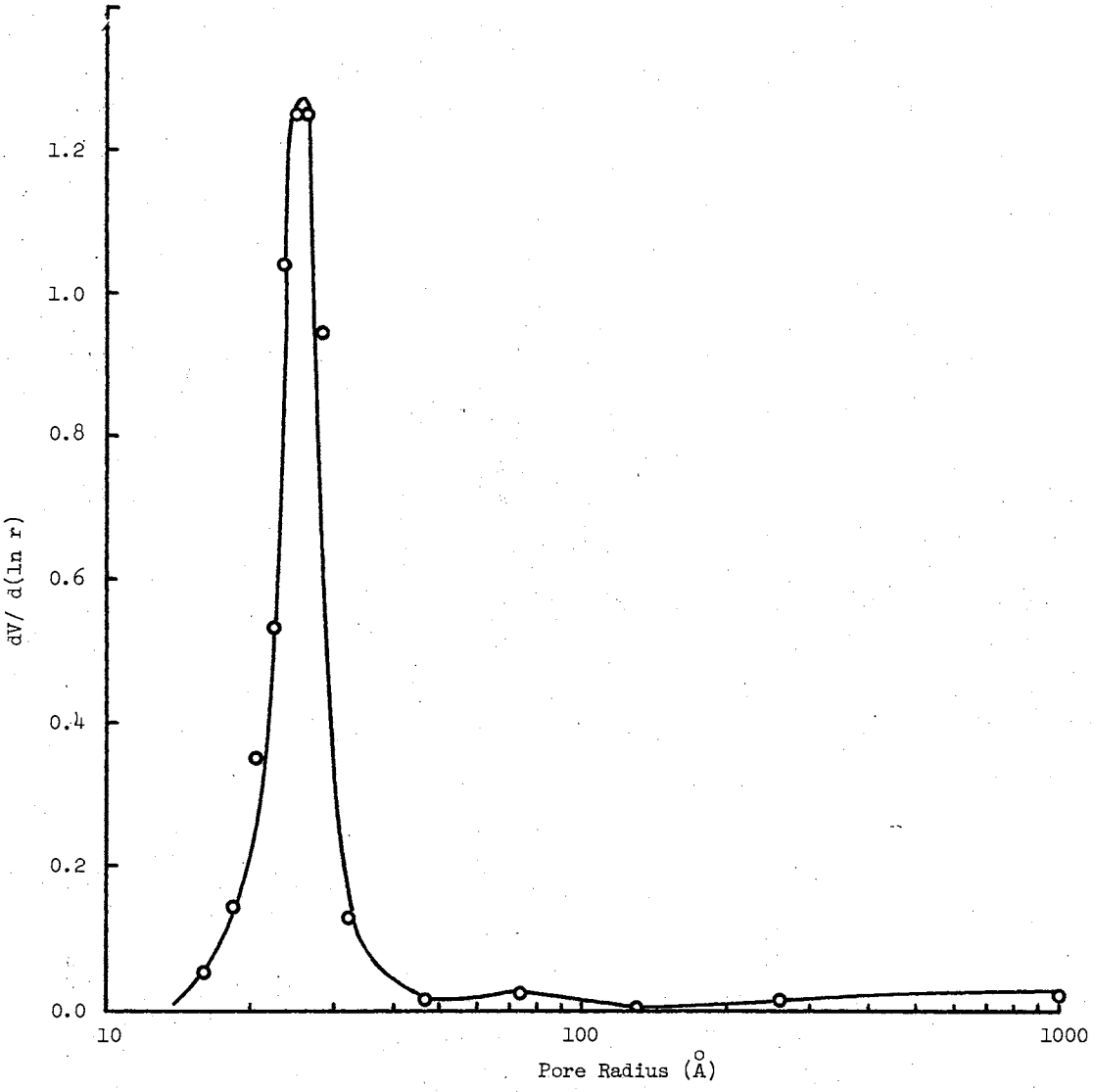

Figure 12. Catalyst 72-A, Pore Distribution from Mercury Porosimetry

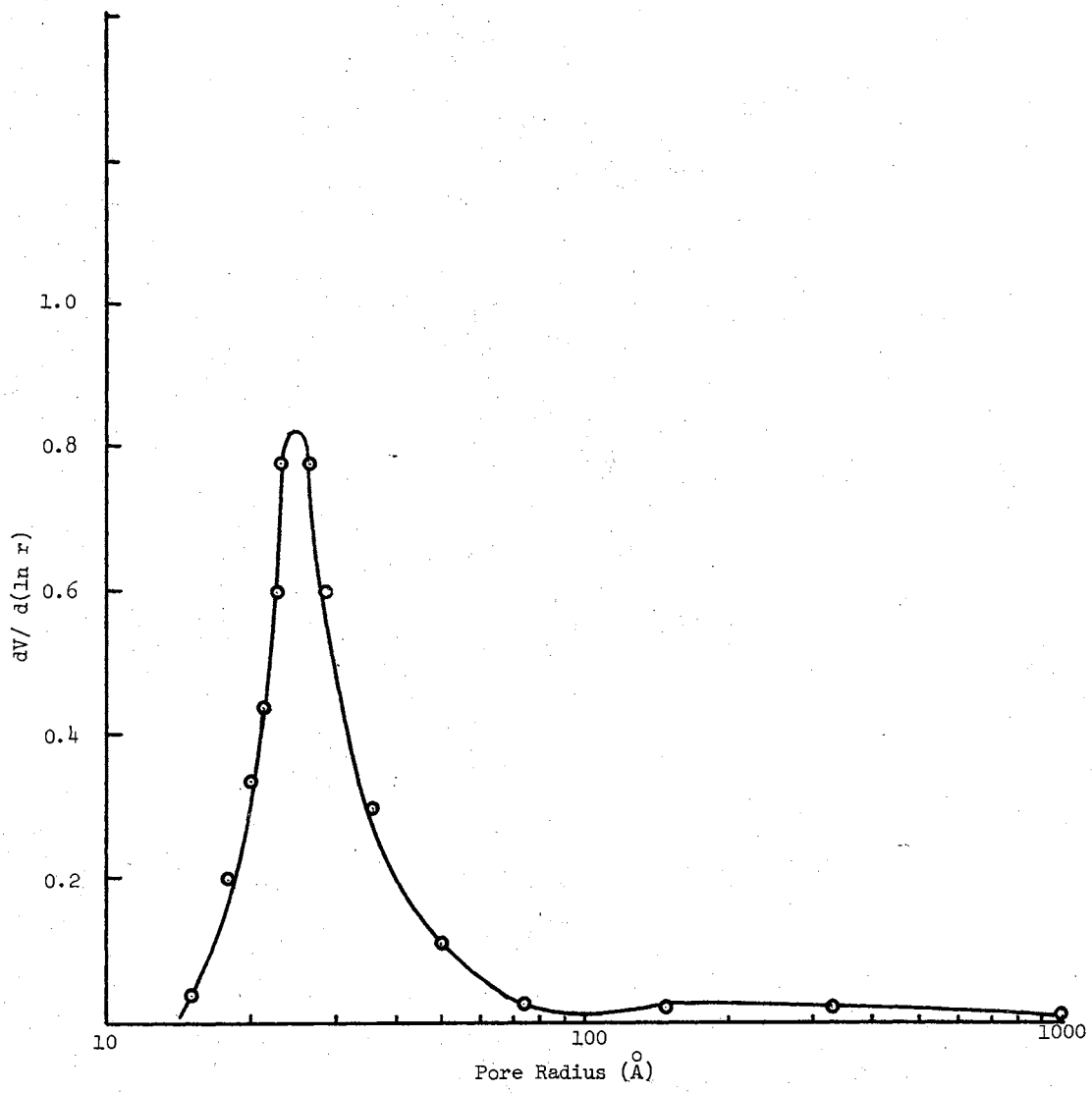

Figure 13. Catalyst 72-B, Pore Distribution from Mercury Porosimetry

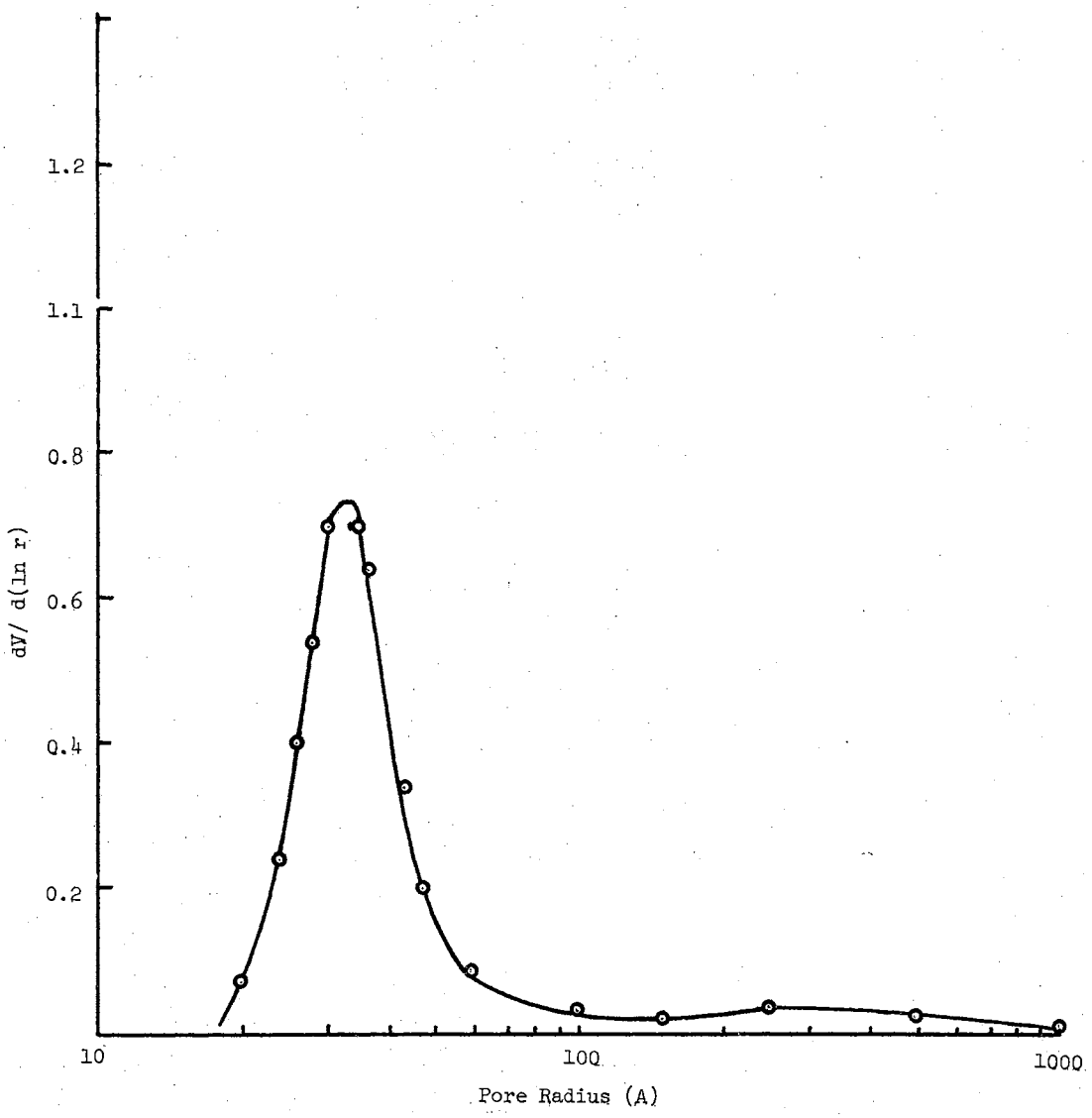

Figure 14. Catalyst Nalcomo 474, Pore Distribution from Mercury Porosimetry

American Instrument Co., Inc. on the catalysts 72-A, 72-B and Nalcomo 474 respectively. The curves presented in Figures 12, 13 and 14 were developed from volume of mercury penetrated into the catalyst for a given pressure and are plots of dV /d (ln r) vs. r. Where the term dV/ d (ln r) is the differential change in volume of mercury penetrated by a change in pressure divided by the natural log of the average pore radius corresponding to the pores filled with mercury at a given level of pressure. Thus, plots such as those in Figures 12, 13 and 14 are a measure of pore frequency as a function of pore size. The actual calculation for these curves as well as catalyst properties and raw mercury penetration data are presented in Appendix I. The surface areas of the catalysts are given in Table XVI and show the differences for the three catalysts.

TABLE XVI

COMPARISON OF CATALYST SURFACE AREAS

Nalcomo 474	240.3 m^2/ gm
72-A	297.7 m^2/ gm
72-B	302.7 m^2/ gm

Results from experimental runs performed with catalysts 72-A and 72-B are shown in Tables XVII and XVIII respectively. Figure 15 is a

TABLE XVII

EXPERIMENTAL RUN #7, 72-A
8-10 MESH

Sample No.	Nominal Temperature	Nominal Pressure	LVHST	Wt. % S Oil Product
PF 252	600	1000	1.5	.131
PF 253	600	1000	1.5	.127
PF 254	600	1000	1.5	.132
PF 255	600	1000	1.5	.120
PF 256	600	1000	1.5	.113
PF 257	600	1000	1.5	.121
PF 258	600	1000	1.5	.117
PF 259	600	1000	1.5	.131
PF 260	600	1000	1.5	.118
PF 261	600	1000	1.5	.120
PF 262	600	1000	1.5	.118
PF 263	600	1000	.75	.159
PF 264	600	1000	.75	.164
PF 265	600	1000	.375	.228
PF 266	600	1000	.375	.225
PF 267	600	1000	1.5	.127
PF 268	600	1000	1.5	.119
PF 269	650	1000	1.5	.075
PF 270	650	1000	1.5	.091
PF 271	650	1000	.75	.110
PF 272	650	1000	.75	.107
PF 273	650	1000	.375	.125
PF 274	650	1000	.375	.148
PF 275	650	1000	1.5	.086
PF 276	650	1000	1.5	.080

TABLE XVIII

EXPERIMENTAL RUN #6, 72-B
8-10 MESH

Sample No.	Nominal Temperature	Nominal Pressure	LVHST	Wt. % S Oil Product
PF 212	600	1000	1.5	.155
PF 213	600	1000	1.5	.149
PF 214	600	1000	1.5	.167
PF 215	600	1000	1.5	.154
PF 216	600	1000	1.5	.154
PF 217	600	1000	1.5	.146
PF 218	600	1000	1.5	.151
PF 219	600	1000	1.5	.146
PF 220	600	1000	1.5	.206
PF 221	600	1000	1.5	.142
PF 222	600	1000	.75	.173
PF 223	600	1000	.75	.184
PF 224	600	1000	.375	.245
PF 225	600	1000	.375	.245
PF 226	600	1000	1.5	.143
PF 227	600	1000	1.5	.150
PF 228	650	1000	1.5	.087
PF 229	650	1000	1.5	.094
PF 230	650	1000	.75	.102
PF 231	650	1000	.75	.113
PF 232	650	1000	.375	.153
PF 233	650	1000	.375	.162
PF 234	650	1000	1.5	.076
PF 235	650	1000	1.5	.076
PF 238	700	1000	.75	.070
PF 239	700	1000	.75	.051
PF 240	700	1000	.375	.078
PF 241	700	1000	.375	.076

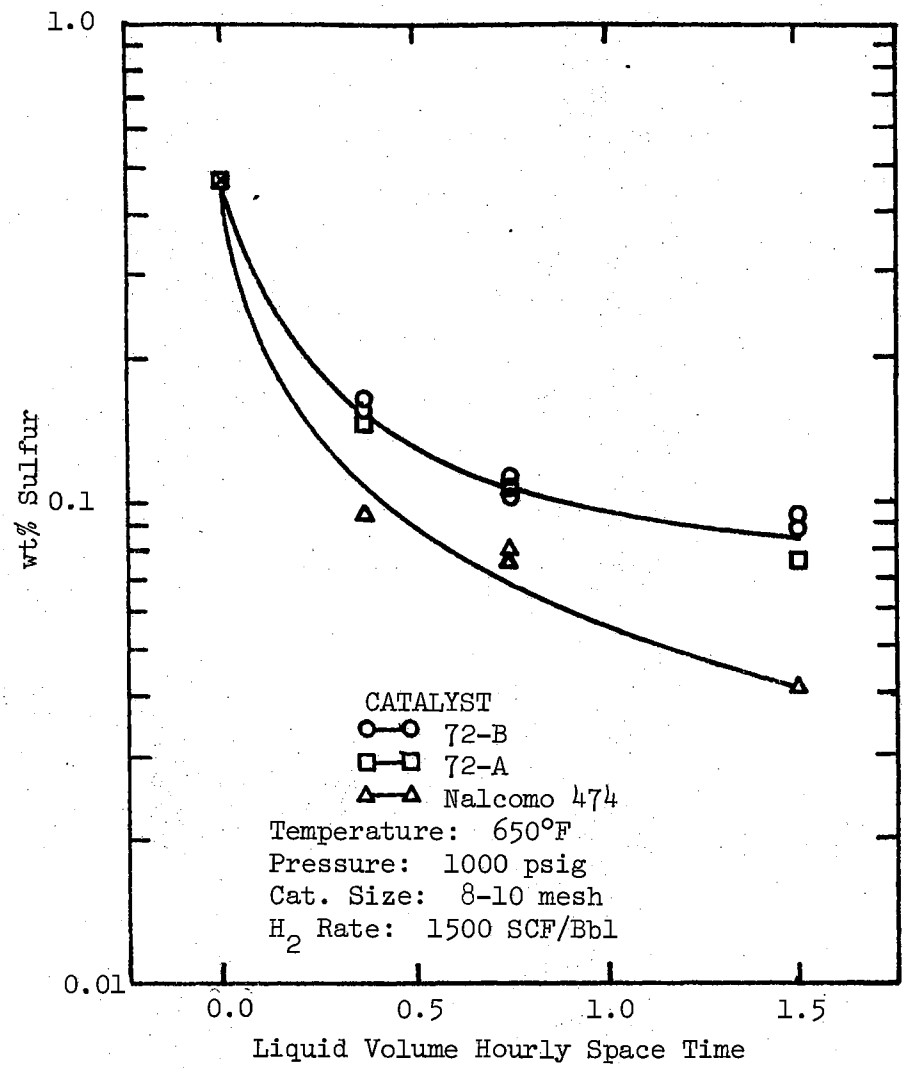

Figure 15. Comparison of Results for Catalysts 72-A, 72-B and Nalcomo 474

plot of 72-A, 72-B, and a Nalcomb 474 data for identical conditions. Figure 15 shows that the narrow distribution catalysts had noticeably poorer sulfur removal than the Nalcomo 474.

Determination of Sulfur in Selected Boiling Fractions

Data on the effect of pore size distribution should be supplemented with additional clarifying information on what is actually happening with the sulfur molecules. The feed oil and products from selected runs were distilled into eight boiling fractions according to a technique developed by Satchell (49), see Appendix J for a brief explanation of technique. These eight fractions were then analyzed for their sulfur content, and the weight percent sulfur plotted against the boiling point of the corresponding fraction. For a temperature of 650°F, a pressure of 1000 psig and a LVHST of 1.5 hours, products were analyzed for both Nalcomo 474 and 72-B. Analysis of the same fractions of the feed oil were also made. Figure 16 is a plot of these results. Comparison of the results of Nalcomo 474 and 72-B shows that the 72-B had poorer desulfurization than the Nalcomo 474 for every fraction. A noticeable decrease in desulfurization is reflected in the 450-475°F boiling range for the 72-B. For further comparison a fractionation and analysis was performed on the product oils obtained from a run made with the reactor packed with inerts and operated at 800°F, 1000 psig, and a LVHST of 1.5 hours. Figure 17 is a plot of these results compared to the unreacted feed oil. The lower boiling fractions are shown to be, by far, the easiest to remove with a fraction boiling in the range of 450-475°F @ 50 mm Hg, being the most difficult to remove. Table XIX is a comparison of the weight fraction

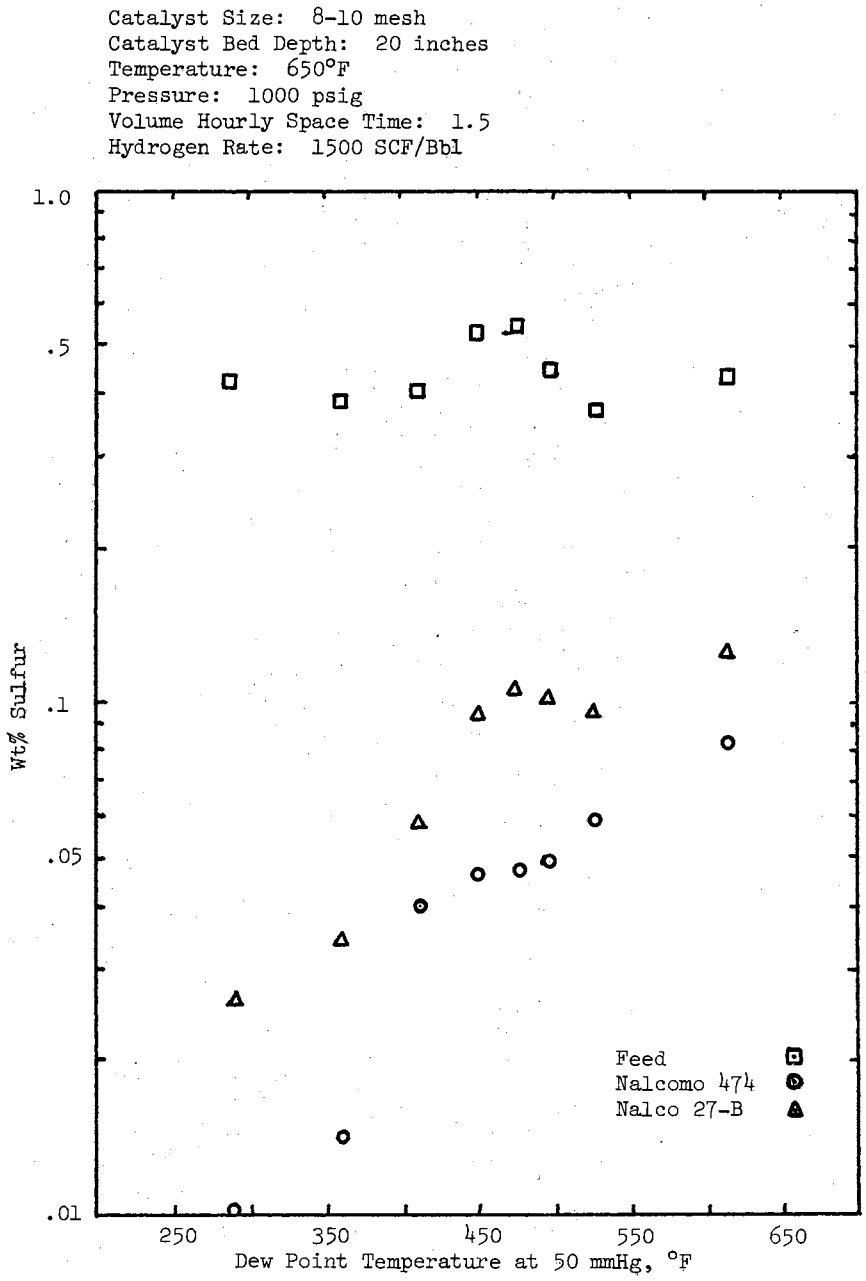

Figure 16. Comparison of Sulfur in Fractions for Feed Material, Nalcomo 474 Product, and 72-B Product

Catalyst Size: 8-10 mesh
Catalyst Bed Depth: 20 inches
Temperature: 800°F
Pressure: 1000 psig
Volume Hourly Space Time: 1.5
Hydrogen Rate: 1500 SCF/Bbl

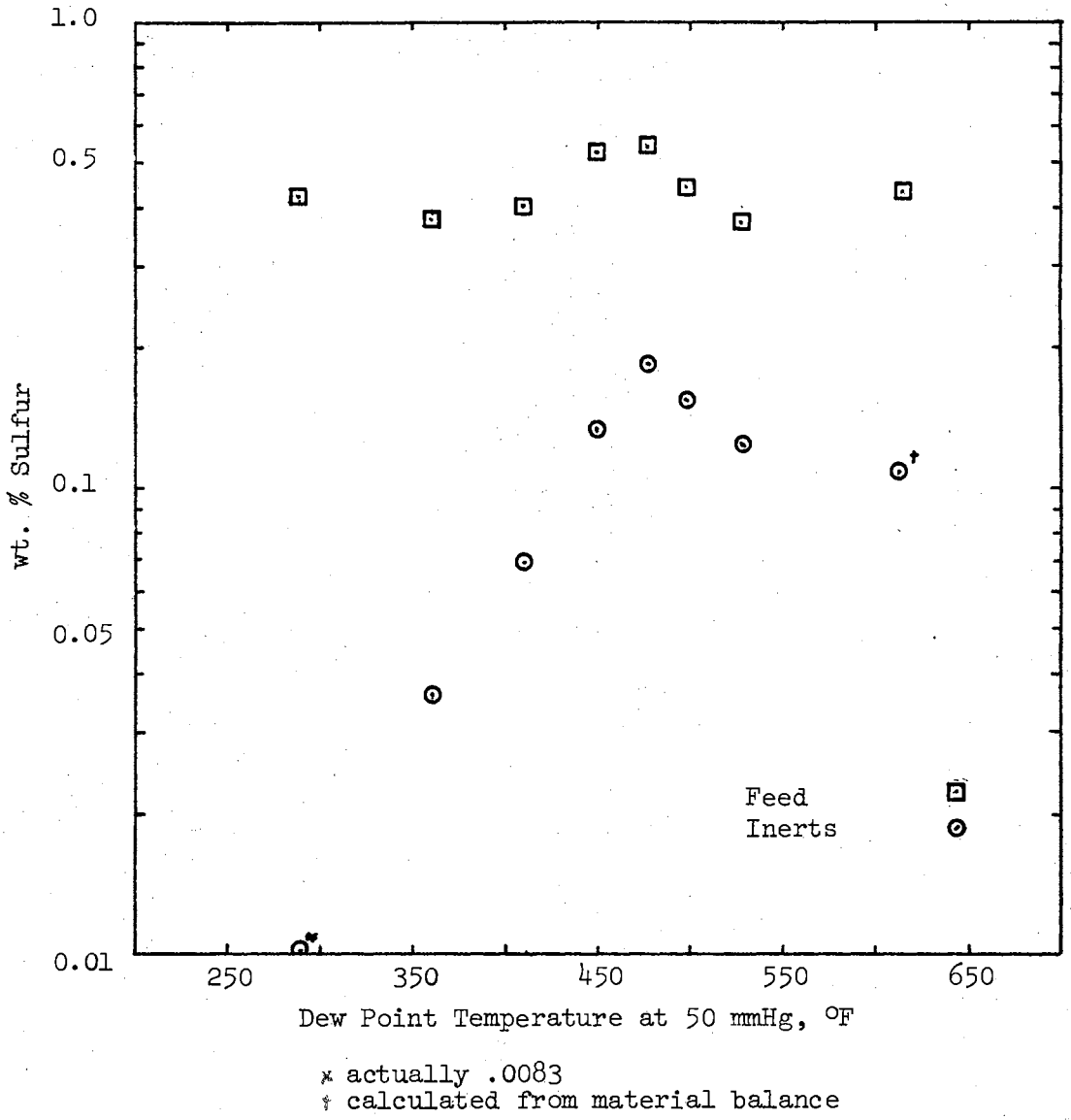

* actually .0083
† calculated from material balance

Figure 17. Comparison of Sulfur in Fractions for Feed Material and Inerts Products

of each cut for feed and product. The major gains from cracking were fractions 1, 2, and 4. Fractions 1 and 2 show the best removal, however. Fraction 4 is one of the higher concentration fractions, but the product shows above average removal from that fraction also. The fractions with heavy losses, 5 through 8, appear to be the most difficult to desulfurize.

TABLE XIX

COMPARISON OF WT OF DISTILLATION FRACTION FOR FEED AND PRODUCT

Fraction	Feed	Product	Δ%
1	10.75 wt.%	14.87 wt.%	+38%
2	11.58	17.28	+49%
3	12.55	11.94	- 5%
4	10.62	12.93	+22%
5	18.05	15.24	-15%
6	8.39	7.35	-12%
7	13.21	9.40	-29%
8	14.85	10.99	-26%

Physical Properties of Feed and Product

Many chemical engineering calculations require additional knowledge of the physical properties of the materials being dealt with. To

provide information for calculations as well as convenience for other experimenters, kinematic viscosity of fractions, density of fractions and feed and TPB data (Tables XX and XXI) are presented here. Explanations of the methods used to obtain the fractions, kinematic viscosity data, and density are given in Appendices J and K respectively.

TABLE XX

DENSITY AND KINEMATIC VISCOSITY OF FRACTIONS

Fraction	Density @ 77°F gm/cc	Kinematic Viscosity (centistokes) @ 100°F	Kinematic Viscosity (centistokes) @ 187.7°F
1	.959	1.71	.813
2	1.020	3.48	1.293
3	1.060	6.22	1.833
4	1.075	10.57	2.37
5	1.092	18.04	3.06
6	1.107	31.10	4.025
7	1.122	65.93	5.48
8	1.137		
Toluene	.871		

TABLE XXI

FEED OIL PROPERTIES

Carbon, wt%	90.65
Hydrogen	5.76
Sulfur	.48
Nitrogen	.91
Oxygen	2.2 (Diff)
Ash	Nil
API Gravity @ 60°F	-7
*Distillation	
Initial	380°F
10 Vol %	450°F
30	570°F
50	650°F
70	700°F
90	815°F

* Normal boiling data were estimated from ASTM D1160 data taken at 50 mm Hg absolute.

Summary

The experimental results have been presented in this section with only a brief identification of conditions and results and some explanation of why the experiments were conducted. No attempt was made to thoroughly explain the results or discuss them. The primary purpose of this section was to relieve the discussion of some data and provide a survey of all results before a detailed discussion was embarked upon.

CHAPTER VI

DISCUSSION

To be able to fully understand and evaluate the results of desulfurization in a particular reactor system, that system itself must be understood and the precision of the data must be determined. It was with these thoughts in mind that the structuring of this section was made. The precision of both analytical and reaction equipment is established first. Next the results of some non-catalyzed runs are discussed. Liquid velocity and catalyst particle size will be discussed to establish their effects on the system. Temperature, pressure, and hydrogen rate are discussed along with various models for the kinetics investigated. Lastly, the effects of changes in catalyst pore size distribution are described and information pertaining to the molecular size of the sulfur containing molecules is brought to bear on the subject. Some discussion may seem repetitive of the results section, however, the repetition often emphasizes a point or gives much more detail than given in the results section.

Standard Deviation of Data

Proper evaluation of the data can only be accomplished when the experimental precision is known. To obtain a measure of the precision of the data, three separate runs were made at identical conditions, using three separate catalyst loadings of Nalcomo 474. The data are

presented in Tables VIII, IX and X of the previous section and Figure 18 of this section. A standard deviation was calculated at each space time for the three isotherms. The standard deviation for each space time and temperature is presented in Table VII, of the previous section. The standard deviations presented in Table VII will be taken as a measure of the reproducibility of the other runs. These direct measurements of standard deviations for the reactor include all variations in the total process (temperature, pressure, flow rates, catalyst activation, catalyst loading, and analysis) and our ability to reproduce them. Examination of Table VII shows that with the exception of the 600°F and 650°F, .75 liquid volume hourly space time (LVHST) points, the lowest space time (higher reaction rate) has in fact the highest error associated with it. The maximum deviation occurs at a liquid hourly space time of .375 hours and a temperature of 700°F. As can be seen in Table VII a deviation of $\pm$ .01% S is much more significant to a temperature of 700°F than one of 600°F. At 600°F and .375 LVHST, .01% S deviation is approximately a 5% error, while at 700°F and .375 LVHST a .01% S deviation is a 20% error. Observation of Table VII then shows that the maximum error is associated with the 700°F isotherms with decreasing error for the 650°F and 600°F isotherms. Some of the increased error for the 700°F isotherm can be attributed to increased analytical error as will be seen in the next paragraph.

From calibration of the sulfur analysis equipment, standard deviations for the sulfur analysis are presented in Table IV, of Chapter V, and calculational details are given in Appendix F. Table IV shows that typically the higher sulfur levels have the

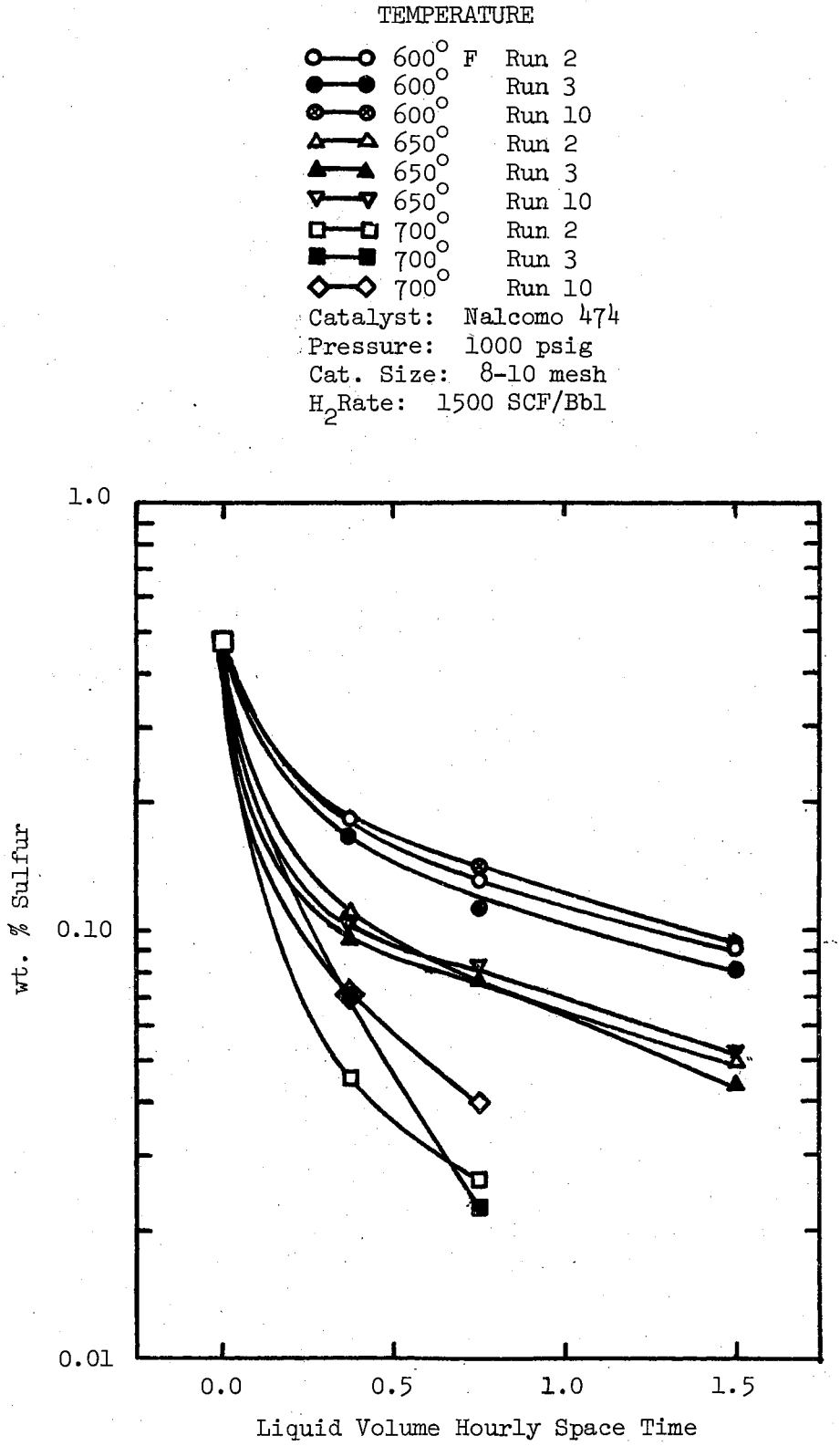

Figure 18. Comparison of Results from Three Identical Runs

smallest amount of error in determination and the lower levels have an error increasing as the sulfur level goes down. The loss of sulfur from the analytical apparatus during the combustion of the sample to SO_2 could be a constant amount which would be reflected in an increasing percentage as the total sulfur level is decreased. The "furnace factor" associated with the analytical equipment is designed to compensate for a constant loss, however, the Leco sulfur analysis equipment manual states that the technique is reliable down to only .06% or 600 ppm. The calibration reveals that serious deviation does not occur until 200 ppm under the conditions of this study.

A brief review of the standard deviations associated with each data point shows that in general, the higher the temperature, the higher the error associated with the data. The error of analysis goes up with decreasing sulfur content which also corresponds to higher temperature operation. In summary of the data on precision, we see that the uncertainty of the data increases with increasing space time and temperature and most of the uncertainty can be attributed to poor analytical precision. The overall deviations of Table VII are made up of all variables as indicated earlier. These overall deviations are approximately fifty percent due to analytical deviation and the percentage remains relatively constant throughout the data. The limiting factor cannot therefore be attributed wholly to analytical imprecision. Half of the imprecision must be attributed to the irreproducibility of the experimental operation. Temperature was reproducible to within .4% at the worst variance of $\pm$ 2°F at 600°F nominal. Pressure was reproducible to within 2.5% at 1000 psi. and was shown to have a minor effect on reaction rate at 1000 psi. Errors in the oil flow

rate and thus in the LVHST were not detectable. The major portion of the innate error must therefore be in catalyst loading, flow rate, activation, etc.

Non-Catalyzed Runs

As shown in the results section, data were taken with a bed of inerts replacing the catalyst bed. Figure 11 is a semi-logarithmic plot of the data and shows that 700°F and higher isotherms do not follow a first order relationship. Some insight must be obtained about the reaction however. A second order plot of the data, Figure 19, shows that there is some need for a better model, but in this case, the second order fit was made to gain further information. Slopes were taken from the straight lines of Figure 19 and plotted on a semi-log plot against reciprocal temperature, Figure 20. Figure 20 is a typical Arrhenius plot of the rate constants for the reaction. Recall that rate constant

$$k = k_o \, e^{-E/RT} \text{ and}$$

$$\ln k = \ln k_o - E/RT \quad \text{where}$$

E = activation energy, R = gas constant, T = temperature, and k_o = frequency factor. From Figure 20 an activation energy of 25 kcal was calculated. See Appendix L for details of the calculations. If the reactions occurring are assumed to be chemical rate controlled thermal decompositions, we might easily expect the activation energy to fall in the range of a chemical rate controlled reaction as it does. Berg (6) indicates that the activation energy needed for decomposition of

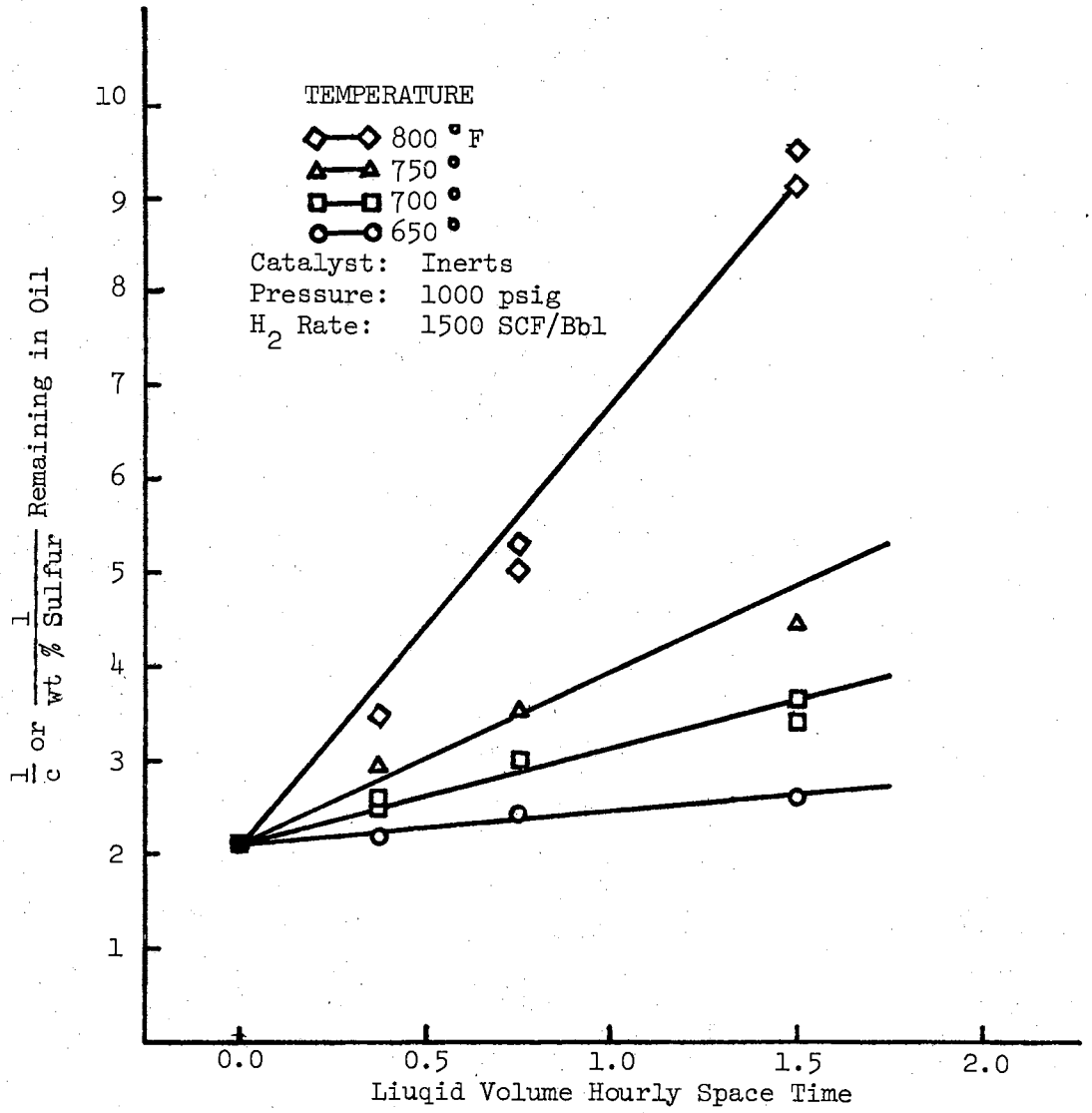

Figure 19. Second Order Plot of Inerts Data

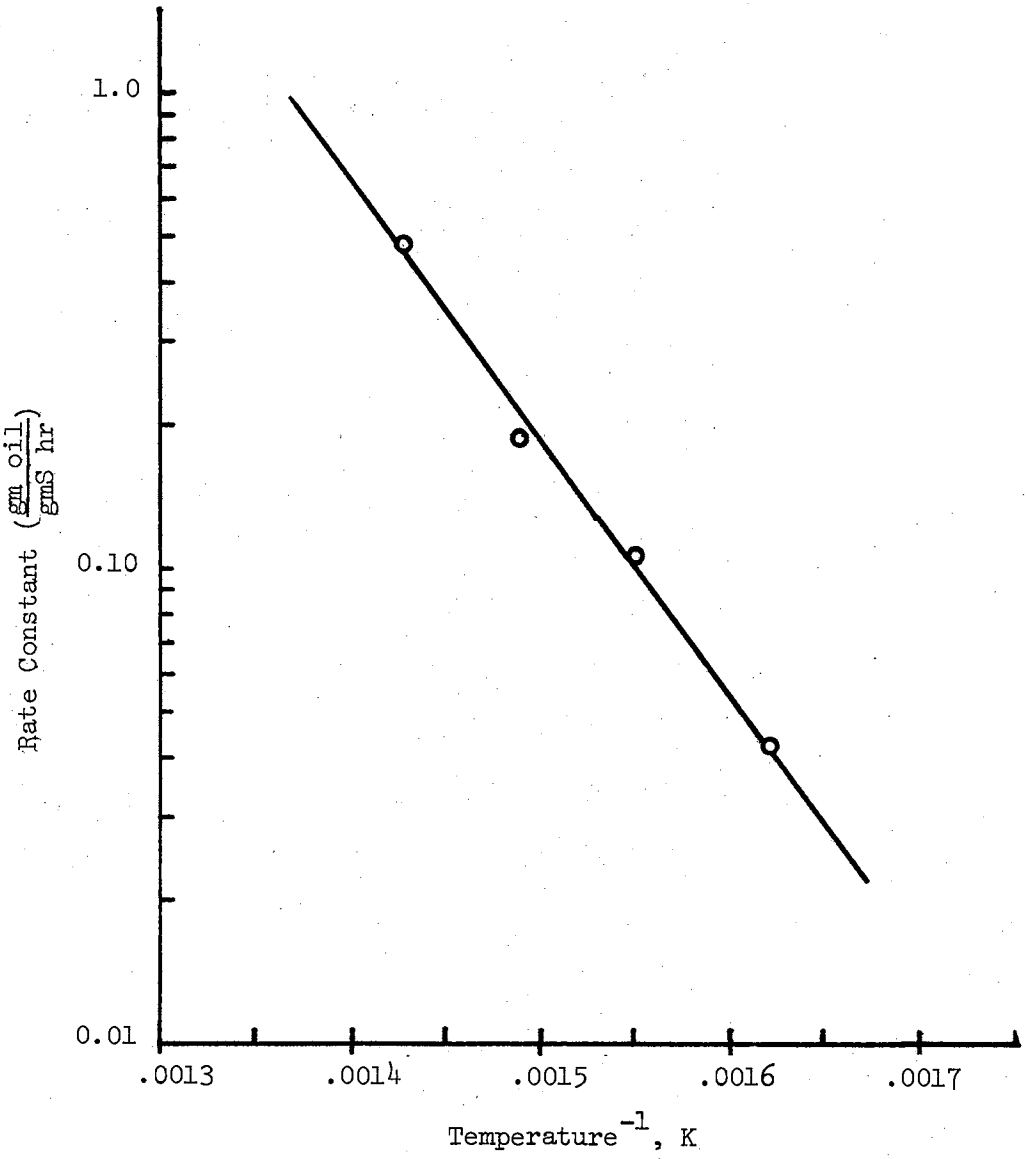

Figure 20. Plot of ln % Rate Constants for Inerts Data

mercaptains is some 19.5 kcal, sulfides require some 36.5 kcal, and thiophenes 73 kcal. The lack of fit of both the first and second order curve fits seem to point out that a complex series of reactions is acutally occurring and the fact that they can be described by a single rate constant is merely expedience for ease of use. Some actual experimental work by the U. S. Bureau of Mines (45) on the thermal decomposition of sulfur compounds found in crude oil shows quite clearly that various sulfur compounds thermally decompose at different rates and that different temperatures are required to decompose different sulfur species. These present thesis data on non-catalyzed desulfurization could easily become the subject of an entire study, particularly since there seems to be little definitive work in thermal decomposition of sulfur containing compounds. Non-catalyzed desulfurization is significant also if kinetic modeling is attempted for desulfurization. One way to incorporate the non-catalyzed data into catalytic desulfurization would be to recognize that the total rate was due to both a non-catalytic decomposition and a catalytic decomposition. Strictly from an overall standpoint, the rate of desulfurization could be represented by:

$$-\frac{dC_s}{dt} = k_c C_s^2 + k_t C_s^2$$

assuming of course that both reactions could be described by simple second order rate expressions with no volumetric expansions. Rate constants are k_c for catalytic removal and k_t for thermal removal. The model would assume, as is obvious, that the reactions occur in parallel. The thermal decomposition is actually occurring in addition to the catalytic desulfurization of the anthracene oil. In fact,

effect of the non-catalyzed reaction is rather minor since the majority of the data were taken at 600° and 650°F where a maximum of some 17% S removal might occur due to non-catalyzed reaction. The extent of non-catalyzed reaction is probably much less since in the presence of a catalyst since some of the bonds which thermally decompose could be removed more quickly catalytically, and therefore, not have the opportunity to thermally decompose. The main point to be made is that the non-catalyzed data will serve to alert the reader to the fact that non-catalyzed reactions can and do occur and that representation of the catalytic data by a single rate constant would be fortuitous. The reaction system is indeed quite complex.

Liquid Distribution and Backmixing

Perhaps one of the more difficult effects to properly assess is that of liquid distribution within the catalyst bed. As shown in the results section, some runs were conducted on a bed of catalyst 10 inches in length as opposed to the normal 20 inch bed of catalyst. By changing the catalyst bed height and holding the LVHST constant, liquid velocity must change for the two beds. If liquid velocity changes then liquid distribution could change and/or a film mass transfer coefficient could change. The results of the run on the shorter 10 inch bed of catalyst was that desulfurization decreased. At first glance, the decrease in desulfurization might be attributed to poor liquid distribution and the data corrected for the poor distribution. From literature reference, the work of Mears (38) may be able to provide some guidance. First, consider the effects of axial dispersion or backmixing for the normal bed of catalyst i.e.

20 inches. Note that $\frac{L}{d_s} > \frac{20n}{B_o} \ln \frac{C_o}{C_f}$ is the criteria to be met. L/d_s is easily calculated to be 231.9 for the 8-10 mesh Nalcomo catalyst particles which were used in the present study. The more difficult part is establishing what the other side of the inequality is. With $B_o = u\, d_s / D_a$, u is calculated to be 339.8 cm/hr for a LVHST of .375 hours and d_s is known to be .219 cm for 8-10 mesh catalyst. The number which is difficult to assess is D_a. However, this problem can be alleviated by calculating B_o directly. From the work of Hockman (25) with N_2 and MeOH on trickle flow reactor systems, we find for a liquid Peclet number of 20 (the case in question here) a Bronstein No. of .25 applies. Using this number (there is no point in calculating D_a now) at 650°F the quantity on the right of the inequality is 229. If the Bronstein No. is higher, perhaps 0.5 as Mears indicates it could be, the required L/d_s would be even smaller. The important point however is that the criteria for absence of axial dispersion is met, at least according to Mears' study. Consult Appendix M for the details of the calculations. Reiterating then, under normal operating conditions, i.e. a 20" bed of catalyst, the reactor is probably free from axial dispersion effects. Now, the comparison must be made with the shorter bed. A check of possible axial dispersion effect would be to reduce L/d_s by a factor of 2. In so doing, we find $L/d_s = 116$, far short of the needed 229. In fact, the problem is worse than the difference in these two numbers suggest. For the shorter bed, a Liquid Peclet number of 9 is achieved and a B_o No. of 0.14 results from Hockman's (25) graph. The resulting number to be free from axial dispersion effects is 315.1. Axial dispersion must therefore be concluded to be at least partly responsible for the

loss in desulfurization for the short bed of catalyst. Data that at first glance might have erroneously been attributed entirely to poor liquid distribution has now been exposed as possible axial dispersion effects.

The possibility for liquid distribution problems could still exist. As a further test of liquid distribution (and diffusion effects) the catalyst particle diameter was reduced by a factor of almost five to 40-48 mesh. The quantity, L/d_s becomes 1451 and the right side of the inequality becomes 635. Axial dispersion effects should definitely not be present. Any possible channeling close to the walls should be reduced since the amount of catalyst contact with the walls would be greatly increased by the smaller particles. As indicated by the results (Table XIII) of the experiments, however no increase in desulfurization was obtained. In summary, the length of catalyst bed chosen (20") is very likely to be free from axial dispersion effects, but axial dispersion effects were probably existent for a shorter bed of catalyst. Smaller particles also show no significant improvement in desulfurization and we must conclude that liquid flow problems are not significant for the system under study here.

Particle Size and Effectiveness Factor

Changing particle size has more than one benefit. In addition to showing that liquid distribution problems do not exist, some significant facts concerning catalyst pore diffusion control can be elucidated. As was mentioned in the literature survey, changes in particle size of a catalyst can be used to calculate an effectiveness factor. Also, as stated earlier, a good approach to determining an effectiveness

factor is through a parameter known as the Thiele modulus. Plots of Thiele modulus vs. effectiveness factor have been worked out for isothermal, and non-isothermal reactions for various order reactions and for various particle shapes. A good place to start in this case would be by a priori prediction of an effectiveness factor and the significance of the experimental work will become apparent as the effectiveness factor is predicted. Satterfield (50) presents a graph similar to Figure 21 where Φ is the Thiele modulus and η is the effectiveness factor. Φ is defined as

$$\Phi = R \sqrt{\frac{k_v c_s^{m-1}}{D_{eff}}}$$

where R is the catalyst radius, k_v is the intrinsic reaction rate constant per unit of gross volume of catalyst pellets and D_{eff} is the effective diffusion coefficient. In the case at hand, some data are available on the rate constant from the curve fit work presented previously in the results section. Without going into rate modeling work in detail, assume the data presented in Table VIII can be described by first order rate equations. A rate constant of 3.11×10^{-4} sec^{-1} can be predicted by fitting the data rather grossly by a first order equation, see Appendix N. The difficult part becomes prediction of a diffusion coefficient. Satterfield suggests a value of 5.2×10^{-5} cm^2/ sec for hydrogenation of 2-methyl styrene (50). Bird, Stewart, and Lightfoot (7) suggest 1.38×10^{-5} cm^2 /sec for TNT in benzene. Using estimated liquid properties and the correlation of Wilke and Chang (65), calculated for diffusion of thiophene in the oil used in this study. Using the calculated diffusion coefficient and a catalyst particle diameter of .219 cm (8-10 mesh) a Φ of .87 was

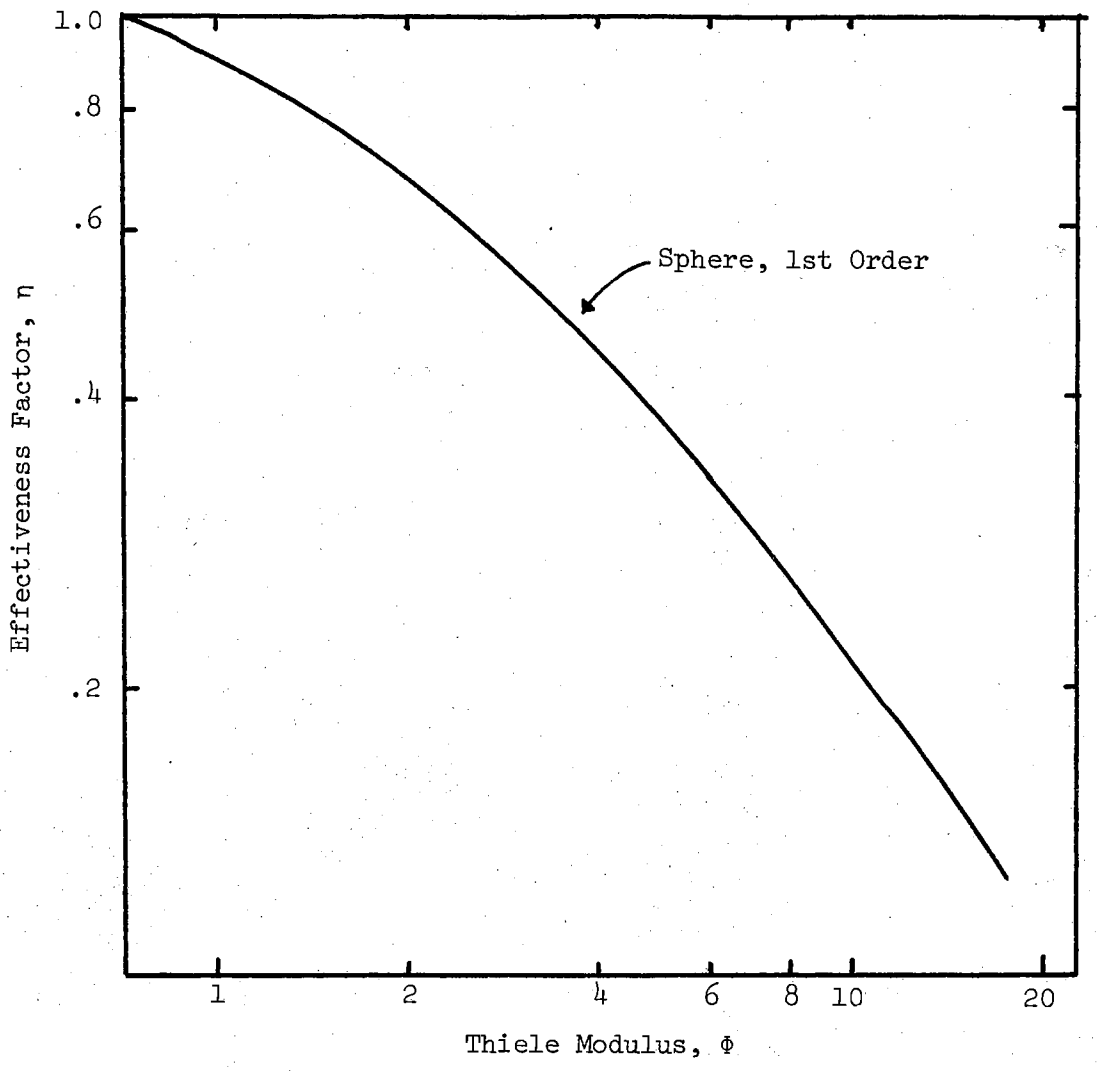

Figure 21. Thiele Modulus vs. Effectiveness Factor

calculated. From the graph of Satterfield, an effectiveness factor between .8 and 1 is predicted. The effect of changing particle size to .035 cm diameter (40-48 mesh) as was done in our case would be to reduce the modulus to .114. Interestingly enough both of these calculations would predict little or no diffusion in the case at hand. The calculation of Φ was also carried out assuming the data presented in Table VIII fit a second order reaction. For the second order case Φ was calculated to be 1.2 and again an effectiveness factor of between .8 and 1 is predicted by Satterfield's graph. An important point to be brought out is that had the modulus turned out high, possibly 20, the reduction in particle size would have reduced the modulus to 3.5 and a significant increase in rate would have been noted. The increased rate can be demonstrated by remembering our rate equation as:

$$-\frac{dc}{dt} = kc\eta$$

That is, the smaller the modulus, Φ, the larger the η, hence a rate increase. In the hypothetical case suggested, a decrease in modulus from 20 to 3.5 would increase the effectiveness factor, η, from 0.15 to 0.7. The experimental work carried out here should have easily shown any diffusional limitations had they existed. Figure 22 is a graphical comparison of the small particle data with large particle data for identical reactor conditions. No significant difference can be detected between the two sets of data and they fall within the reproducibility of the experiment. One other possible explanation of the high effectiveness factor exists, that of a non-isothermal catalyst

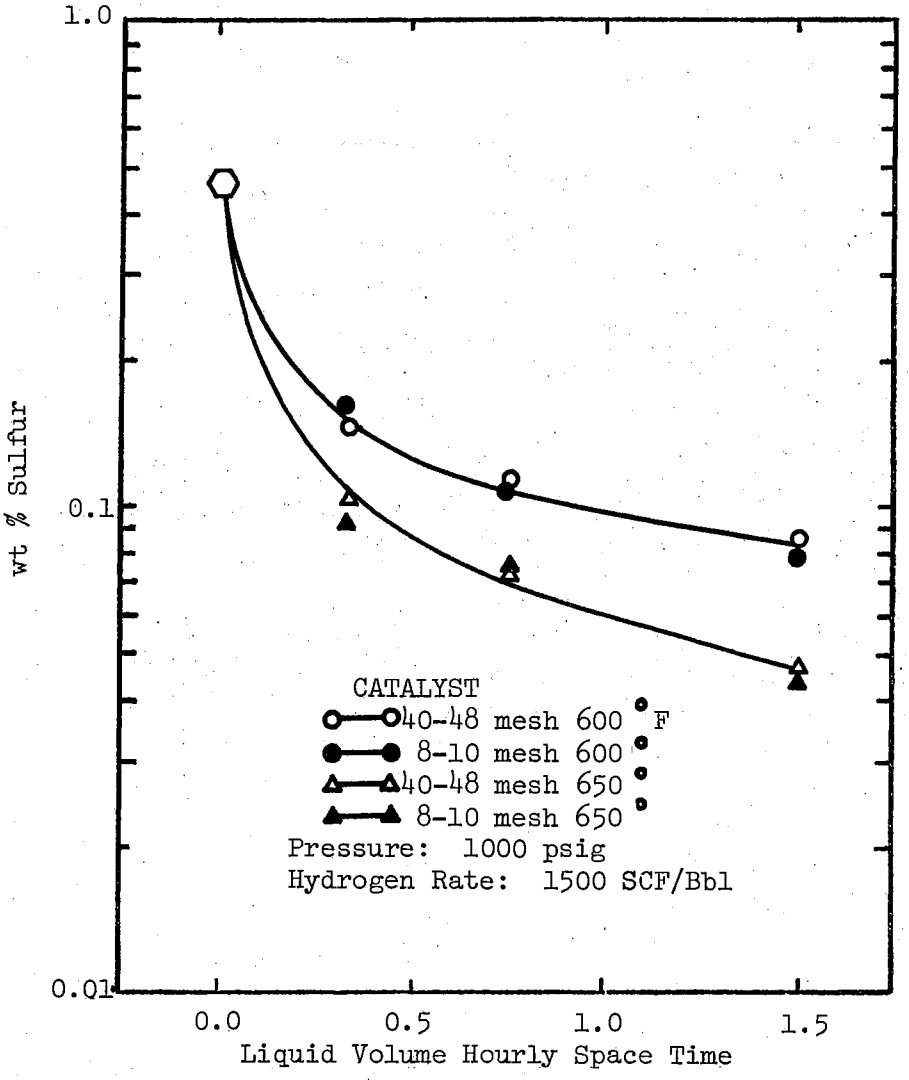

Figure 22. Comparison of Results of 40-48 Mesh Catalyst with Results of 8-10 Mesh Catalyst

pellet due to the large heat of reaction. From a second order fit of the data presented in Figure 22, a heat of reaction was determined and using a method presented by Satterfield (50) a temperature difference of 0.163°C between catalyst surface and center was calculated. (Details of calculations are given in Appendix U). Therefore the higher effectiveness factor was concluded to in no part be due to non-isothermal effects.

Changing catalyst particle size could cause a change in void catalyst bed. Possibilities of a change in bed void fraction (void volume) must therefore be determined for the experimental system of this thesis work. Experimental evidence shows that the void fraction of the catalyst bed does not change on changing catalyst particle size. For a catalyst particle size of 8-10 mesh the weight of catalyst per cubic centimeter of reactor volume was .81 gm/cc as measured in the reactor. The same weight to volume ratio for the 40-48 mesh particles was .82 gm/cc. To further investigate the possibilities of bed void fraction changes on changes in catalyst particle size some experiments were carried out by pouring catalyst into a 50 ml. graduated cylinder. The catalyst was poured into the cylinder in a manner intended to simulate reactor loading. The amount of catalyst in the cylinder was then poured into a cup and weighed. Table XXII shows the results of the experiments. The 8-10 mesh size was checked twice to obtain some measure of the reproducibility of the experiment. As can be seen, the bulk density of the catalyst bed was constant, for all practical purposes. The fact that these bulk bed densities do not correspond to the bulk bed density as measured by the weight of catalyst in the reactor volume is probably indicative of this author's reluctance to rap a glass cylinder as hard as a stainless tube. These

rather simple experiments do show that the loadings were reasonably constant and the bed void fraction was constant. No effects of reactor bed void fraction change should, therefore, be evident in the data on changing particle size.

TABLE XXII

BULK BED DENSITY TESTS FOR CATALYSTS OF VARYING SIZE

Size-mesh	Density gm/cc
1/8" pellets	.72
8-10	.71 .72
10-20	.71
28-35	.72
48-65	.69

In addition to estimating an effectiveness factor of from .8 to 1 for desulfurization from an estimate of the rate of reaction, an effectiveness factor can be estimated directly from the experimental data. Figure 22 is a plot of the data points from the 40-48 mesh catalyst desulfurization and the data from Run 2 on 8-10 mesh catalyst. Although no rates have been calculated one can visually see that within experimental precision of $\pm$ .0085 wt. % S for the 600°F isotherm and $\pm$ .007 for the 650°F isotherm the data are identical. For sake of

argument, however, the ratio of reaction rates was assumed to be .965 by comparing slopes of Figure 22 between 0.0 and .375 LVHST. Appendix R shows the details of the calculations which indicate an effectiveness factor of .96 or greater. Calculation of an effectiveness factor was accomplished by knowing that the ratio of the rates is

$$\frac{-\frac{dc}{dt}}{-\frac{dc}{dt}} = \frac{k\,c\,\eta_1}{k\,c\,\eta_2} = \frac{\eta_1}{\eta_2} = .965$$

and that the ratio of particle radii $R_1/R_2 = d_1/d_2 = 6.25$. By assuming the particles to be spheres, a mathematical relationship between η and Φ is obtained which can be solved by trial and error for the unknowns η and Φ.

To summarize this section, calculation of an effectiveness factor of .8 to 1.0 from a rate constant and Satterfield's (50) graph indicate little diffusion effects were present. Data on bed bulk density indicate that no changes in void fraction occurred in changing particle size and that according to Mears the possibility of bed by-pass effects should have been lessened. Calculation of an effectiveness factor assuming that the ratio of reaction rates was .965 gave an effectiveness factor of .96 or greater, again indicating that no diffusion effects were present in the system. As indicated in the literature survey, experimental work carried out at low temperatures (600-700°F) seems to be characterized by chemical reaction rate controlled steps. The evidence of this work with various particle sizes at principally 600° and 650°F substantiates the evidence of the literature and indicates that diffusion is definitely not a controlling step for the conditions studied here.

Catalyst Activity

Rate of catalyst activity loss is an important variable which must be established for the effect on experimental data, and it is a factor which greatly concerns industrial interests. As indicated in the presentation of experimental results, samples were taken at identical operating conditions at the beginning and at the end of each run. Samples were also taken at the beginning and at the end of each isotherm within a run. For example, for investigation of an isotherm, space times of 1.5, .75, and .375 hours were used and after the last sample was taken at .375 hour, the equipment was then returned to operation at 1.5 hr. to verify that the catalyst activity had not changed during the course of the experimentation on the isotherm. No evidence of catalyst activity change was detected. Additional evidence that the catalyst activity was stable was indicated by the results presented on the continuous sampling at a constant space time and temperature indicated in Table XIV. Figure 23 shows a plot of desulfurization vs. time on oil for the data of Table XIV. The data indicated a slight improvement in sulfur removal up to about 40 hours. The fact that catalyst activity has about stabilized prior to 10 hours on oil is substantiated by Figure 10, of the results section. Inspection of the data in Appendix H shows that 48 hours of oil contacting the catalyst were concluded before sampling was begun on each run. The data in the Appendix H also show that for each activity check per isotherm there was no detectable activity decline. A point worth noting is that the activity of the catalyst appears to increase during the early portion of the sampling period indicating that better methods of sulfiding the catalyst might be possible. Summarizing, no catalyst

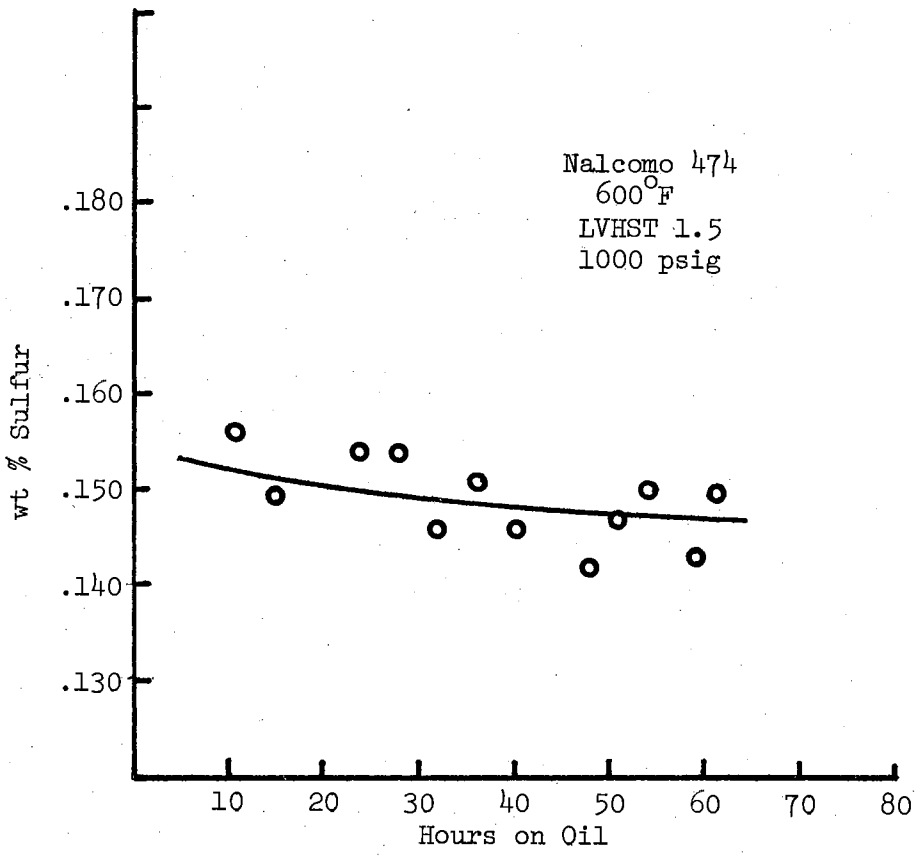

Figure 23. Sulfur Remaining vs. Hours on Oil

deactivation with respect to desulfurization was experimentally detected over the course of an entire run. Catalyst activity can be assumed constant prior to the beginning of all experimental work and during the work. A constant catalyst activity over the period of an experimental run was the main point of concern for this experimental work. Activity checks separated by 187 hours of oil contacting catalyst was sufficient to establish constant catalyst activity for the experimental work of this thesis.

Hydrogen Rate

Changes in hydrogen flow rate can have two effects on overall, observed reaction rate; an effect due to concentration of hydrogen and an effect due to an increased turbulence in the reactor which can affect liquid film thickness and consequently diffusion rates. Hydrogen concentration effects will be covered primarily in the following section on pressure effect. Hydrogen flow rate effects are discussed below.

The flow rate of hydrogen was measured as reactor exit gas flow rate in the case of the experimental work of this thesis. The flow rate was therefore, a combination of excess hydrogen and those gases formed in the reactor. Hoog (26) conducting experimental work on a gas oil found that some 5% of the feed was gasified. Work reported by Chem Systems (14) on the PAMCO process for coal extraction, suggests only some 5% of a coal oil slurry being gasified, at much more severe conditions of 800°F and 2000-3000 psia. Using 5% as a maximum and assuming the molecular weight (MW) of the gas formed to be 28 (MW also from Chem Systems work), an outlet gas of a maximum of 237 SCF was calculated to be non-hydrogen, see Appendix Q for calculations.

Therefore, for a total outlet gas flow rate of 1500 SCF/Bbl, a minimum of 1263 SCF was hydrogen, probably, in fact, more. If an average hydrogen consumption of 453 SCF/Bbl is assumed, see literature survey (17), then the inlet flow would always have been greater than 1500 SCF/Bbl and hydrogen rate effects would not be important. A hydrogen consumption of some 493 SCF/Bbl was calculated from known hetero-atom conversions, off gas made and cracking consumption, see Appendix P. In addition to being relatively close to the hydrogen consumption value expected from the literature, again the hydrogen inlet flow would have been greater than 1500 SCF/Bbl. A check of the effect of hydrogen flow rate was made at 20,000 SCF/Bbl and the results showed that there was no significant difference in the extent of sulfur removal. Comparison of samples 71 and 72 with 73 and 74, shows no significant effect of hydrogen flow rate. Summarizing, adequate hydrogen was provided to the system to prevent the effect of hydrogen flow rate from being significant. Absence of hydrogen effects has been verified from both calculations and experimental evidence.

Pressure Effect

From the literature survey we are led to expect a stronger effect of pressure in the range from 0 to 1000 psig but a decreasing effect some where beyond 1000 psig. Figure 24 is a plot of points for 500, 1000, and 1500 psig for a temperature of 650°F. One can verify the effect of pressure from 500 to 1000 psig. The effect in raising the pressure from 1000 to 1500 psig is quite minimal, and within experimental precision of $\pm$ .0065 wt % S does not exist. Figure 25 is a plot of points for 700°F and 500 and 1000 psig and again the pressure

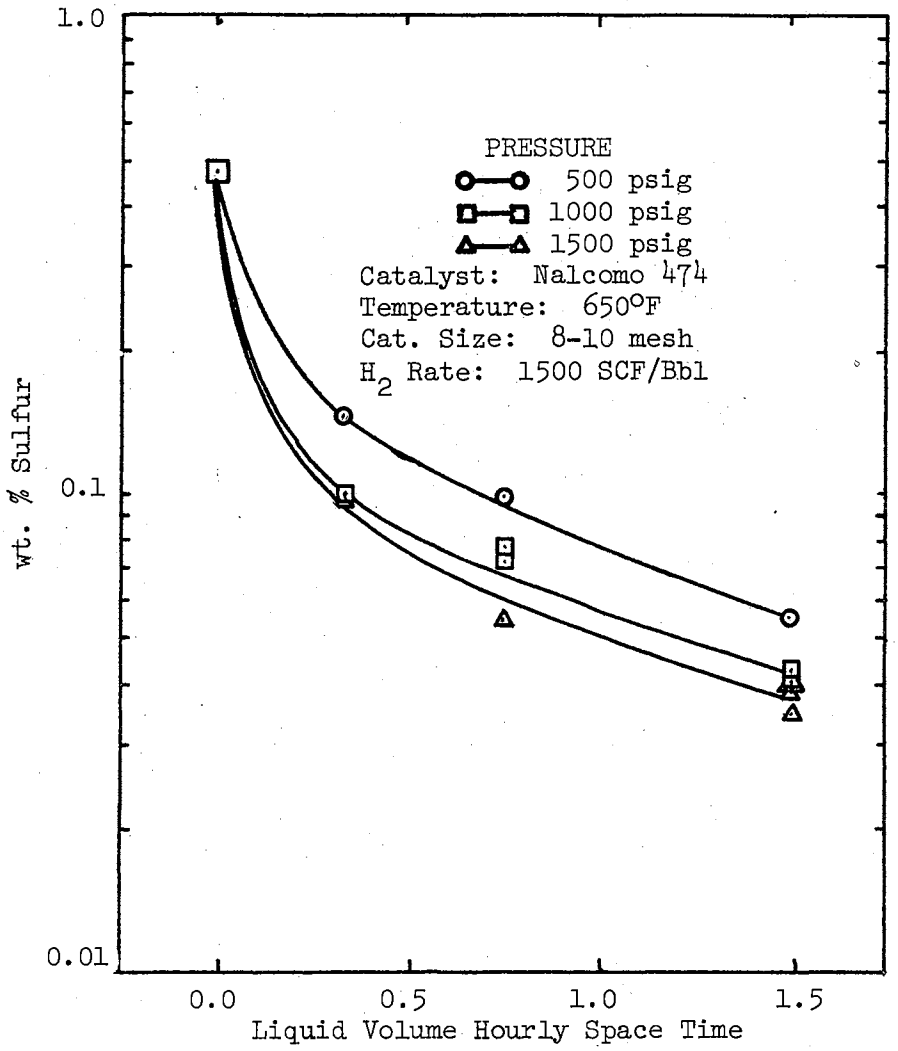

Figure 24. Effect of Pressure on Sulfur Removal, 650°F

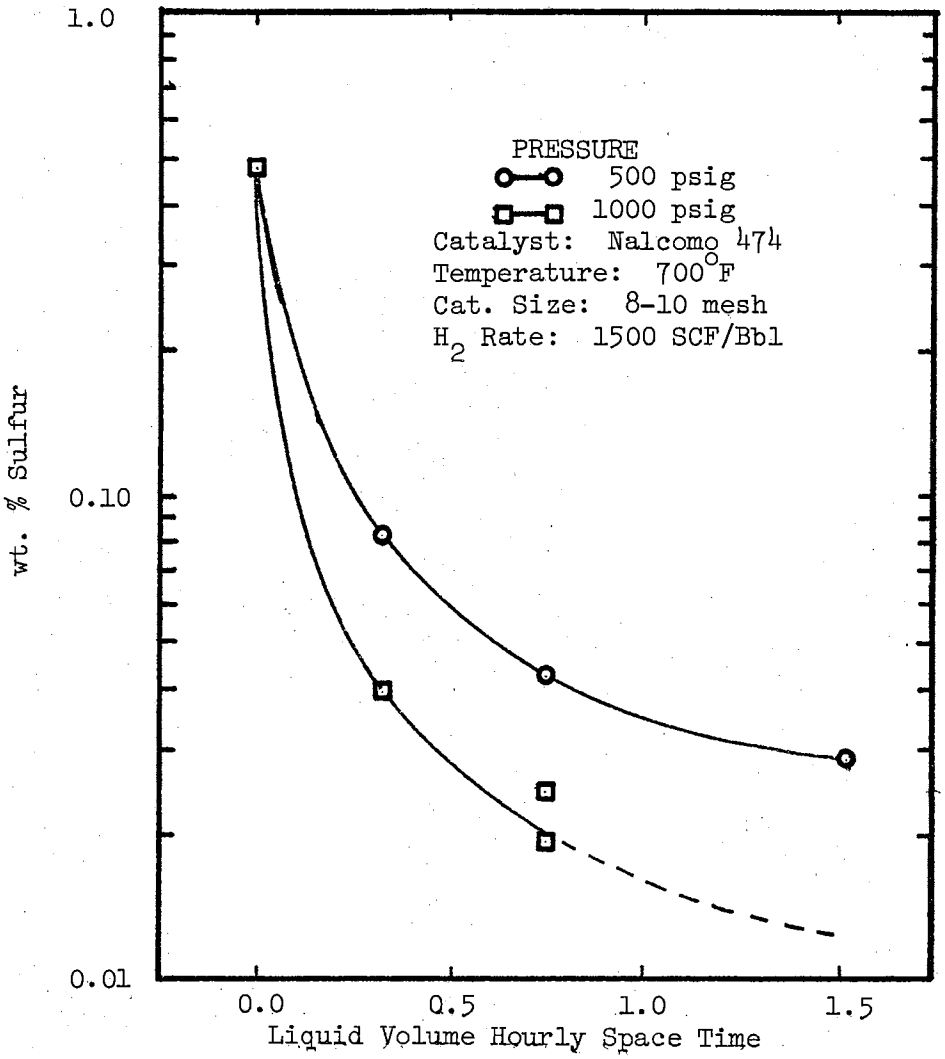

Figure 25. Effect of Pressure on Sulfur Removal, 700°F

effect is easily seen. It is most interesting to note that Wan (61) showed a similar effect of pressure using the same catalyst and feed stock. The increase in desulfurization due to the increased pressure from 500 to 1000 psig indicated that the oil was probably not saturated with hydrogen at the lower pressure. At lower total pressures and consequently lower hydrogen partial pressures the concentration of hydrogen in the liquid phase would be limited. Desulfurization reactions as well as other hetero-atom reactions which rely on hydrogen could be limited by the speed with which hydrogen could diffuse through the liquid and to the catalyst surface. At higher pressures, the concentration of hydrogen in the liquid phase becomes sufficient that the reactions will not deplete the liquid concentration enough to cause diffusion into the liquid to be important. If indeed hydrogen diffusion were limiting at the lower pressure and one assumes the equation of Wilke and Chang (65) to apply then the rate of desulfurization would be expected to increase with the .6 power of pressure. Digressing briefly, the empirical equation of Wilke and Chang is for dilute solution of the diffusing solute and predicts a diffusion coefficient for the dilute solute which is inversely proportional to the molar volume of the solute to the .6 power. As an approximation to the rate of desulfurization at 650°F, a straight line between the feed point and the .375 LVHST point of Figure 24 was drawn and the slope taken as the corresponding rate of reaction. At 500 psia, a slope of 3.05 was calculated. At 1000 psig a slope of 4.13 (Figure 25). For a doubling of pressure and using the 0.6 power, one would predict an increase from 3.05 to 4.6 using Wilke and Chang's equation. Using the Stokes-Einstein equation (7) which predicts pressure

effects to the 1/3 power, a new rate of 3.84 would have been predicted. The Stokes-Einstein equation is a semi-theoretical equation for diffusion coefficients which is inversely proportional to the molar volume of the diffusing specie to the 1/3 power. The Stokes-Einstein is however considered to be the best for large diffusing species. Compromising a little at the .45 power, a new rate of 4.16 is predicted which corresponds quite favorably with that of 4.13 measured. See Appendix S for calculations. To conclude that hydrogen diffusion into the pores is limiting is somewhat questionable and the effect of pressure is quite likely attributable to the effect of increase in concentration as well as a decrease in the amount of the oil vaporized. Compounds vaporized at 500 psig would in effect have a very low residence time in the reactor and would therefore not be properly desulfurized. To summarize this section on pressure effects, from the literature one might expect to see a decrease in pressure effects beyond 1000 psig and indeed there is a significant decrease in the effect of pressure on going from 1000 to 1500 psig. If hydrogen diffusion is controlling, then an increase in rate corresponding to the .45 power of the pressure increase would be reasonable according to theory. The experimental increase in rate corresponds quite well with the .45 power increase. Experimental work carried out at 1000 pounds or greater is therefore, substantially free from hydrogen diffusion limitations.

Temperature and Space Time Effects

From information presented in the results section, the reactor can be considered isothermal along its axial length, and radial

temperature gradients are also minor. As alluded to in both the results and literature sections, temperature effects are generally described by determining activation energies and assuming that the overall reaction rate constants follow an Arrhenius type relationship. Most desulfurization reactions have been described by first or second order kinetics, as mentioned in the literature survey; therefore, an attempt to fit the data by these models was made. Most plots of data in this thesis are first order, semi-log plots and the data can in no way be mistaken for first order. Comparison of the sum of the standard deviations for first and second order fits of the data in the results section shows a marked improvement for the second order fit. Third and fourth order fits of the data, however, did as well as the second order fit. The fact that the third and fourth order models fit the data as well as the second order model suggest that the reactions occurring are of a complex nature. From the section of non-catalyzed reaction, we know there are at least two types of reactions occurring, a homogeneous reaction and a catalyzed reaction. Evidence presented by Hoog (26) indicates that pure sulfur compounds catalytically desulfurize according to a first order relationship. Schmid (56) suggests that what is occurring is a large number of simultaneous reactions of various sulfur compounds. According to Hoog, the different compounds all follow first order relationships but differing rate constants govern the reactions.

If the foregoing evidence and postulations are valid, then the concentration of sulfur remaining should be described by the equation

$$C_s = \sum_i C_{si}\, e^{-K_i t}$$

where C_s = concentration or fraction remaining

C_{si} = initial fraction of sulfur compounds that can be represented by a particular rate constant, K_i

K_i = the first order rate constant which describe the kinetics of the i^{th} portion of the molecules

t = space time

The equation for sulfur remaining in the oil can be developed by considering desulfurization as many simultaneous first order reactions. The working form of the equation presented below is derived in Appendix T. There should be as many rate constants as there are different sulfur species present in the oil. Similar to work done by Gorin (21), there is some evidence that the sulfur reactions can be classified into two broad groups, those which react quickly and those that are slow. Inspection of the data on the distillation fractions shows that the sulfur compounds in the lower boiling fractions are quite readily removed while those of the higher boiling fractions are removed with much more difficulty. If the above model is broken down into only two general fractions, it can be rewritten as

$$C_s / C_{s_o} = \alpha e^{-K_1 t} + (1 - \alpha) e^{-K_2 t} \qquad \text{Eq. 1}$$

where α represents the fraction of initial sulfur compounds reacting fastest, C_{s_o} is the initial weight fraction of sulfur in the oil, and other symbols are as before. Curve fitting the above model to the data of Runs No. 2, 3 and 10, Table XXIII shows the constants for the two reactions. Regression analysis was done by a non-linear regression

analysis program written by Erbar (15). The fact that α was calculated to be high should not be surprising after having viewed the non-catalyzed desulfurization data. At 800°F and 1.5 (Figure 11) hr. space time some 75% was removed. Those molecules which can be thermally decomposed would in all likelihood be a good measure of the "fast" rate.

TABLE XXIII

CONSTANTS FOR EQUATION 1

	600°	650°	700°
α	.63	.717	.81
K_1	5.97 hr^{-1}	227.0 hr^{-1}	3110.0 hr^{-1}
K_2	.425 hr^{-1}	.669 hr^{-1}	1.1 hr^{-1}

The rate constants were assumed to follow an Arrhenius relationship and a plot of ln K vs. 1/T, see Figure 26, shows the straight line relationships. From the slopes of the lines in Figure 26 activation energies were calculated to be 44.65 and 5.4 kcal/mole for K_1 and K_2 respectively. The fast reaction has an activation energy which corresponds to a chemical rate control and the slow reaction has an activation energy the same order of magnitude as energies associated with diffusion control. Examination of the "fractions" data indicates that the two controlling situations could occur in a

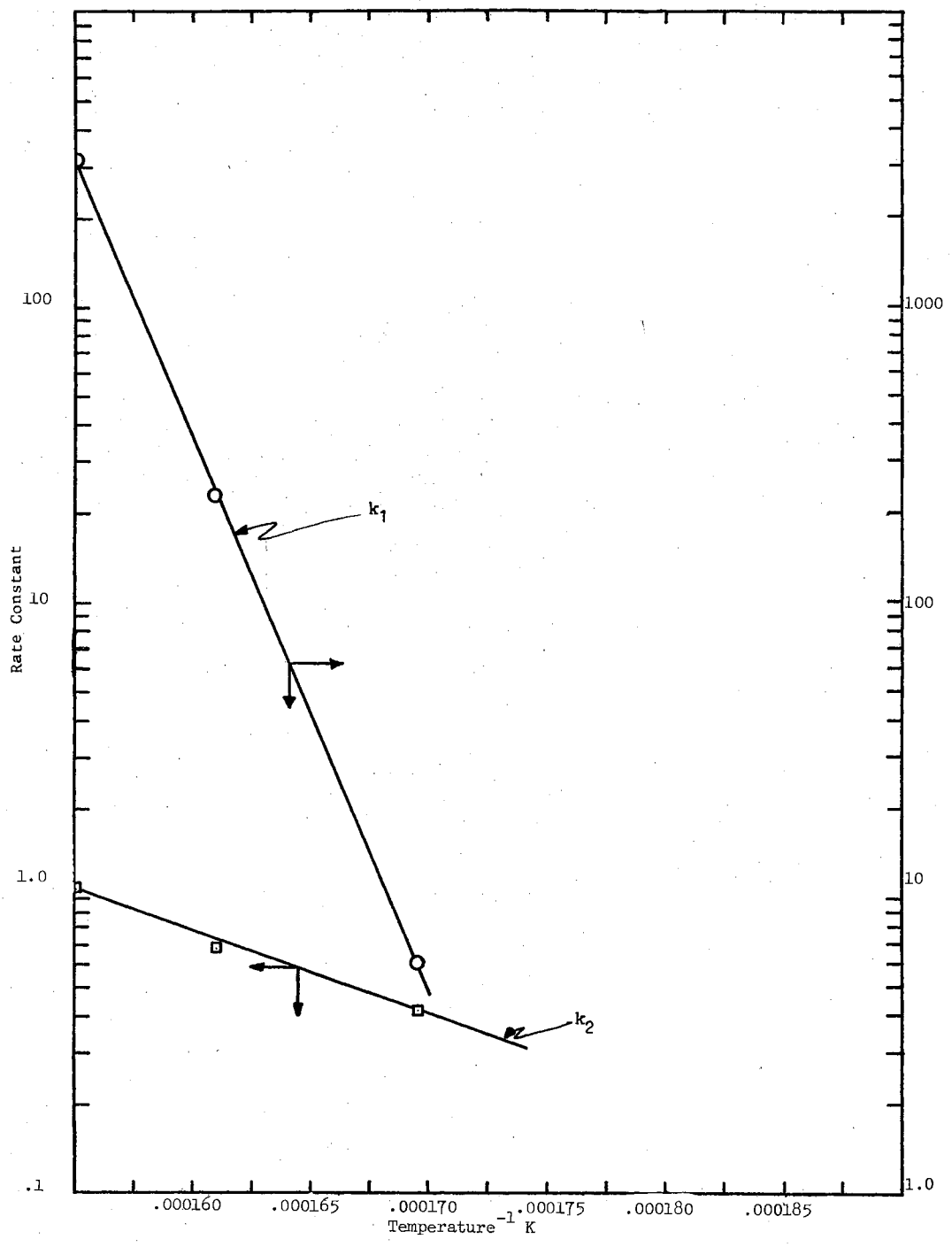

Figure 26. Arrhenius Plot of Rate Constants for Proposed Model

parallel fashion. The very heavy fraction could be responsible for the slower reacting molecules while the lighter fractions are responsible for the faster rate controlled molecules. Figure 27 shows a comparison of a second order fit of the data and the parallel first order model. The parallel first order model is clearly the better of the two models. At least for the 8-10 mesh Nalco 474 data to which it was fit. (Tables VIII, IX, and X.)

In conclusion of this portion of the discussion, the following points seem to stand out. First, the axial temperature profiles are outstanding when compared to the work of others (13) on trickle flow reactors and no significant radial profiles exist. Second, the data do not fit a simple first order relationship, and second order through fourth order fits of the data are better than first order. No reason however, other than simplicity, can be used to select from among the three. A number of parallel first order reactions are suggested as a model to fit the data. Evidence has been presented that the first order reactions can be grouped into two groups, one of fast reactions and another of slow reactions. Fitting the proposed model to the data shows promise for the model as an improvement over a simple second order fit, and holds promise for doing pure component studies with the intention of describing the desulfurization of a coal derived liquid or other wide range hydrocarbon oil.

Catalyst Pore Size

The discussion thus far in this study has been to establish a good knowledge of reactor operation and reaction rate. Guided by this important background, an interpretation of the effects of changing

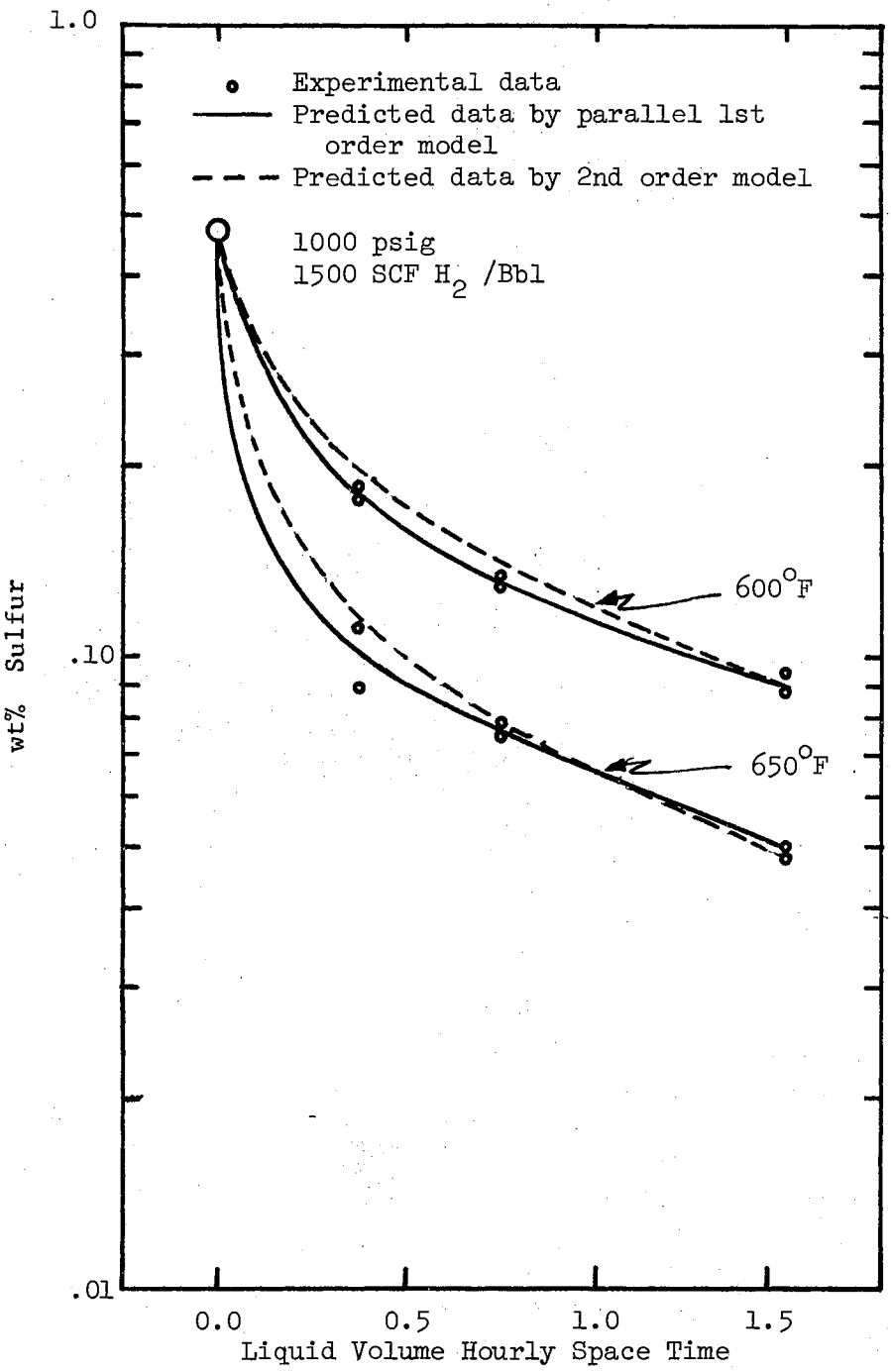

Figure 27. Comparison of Models for Data Prediction

pore size distribution can be made. First, the possibilities for changing the catalyst pore size distribution must be examined. A general broadening of the pore size distribution could result in a change in both the number of large pores available and the surface area available for reaction. Referring to Figure 28a on the next page, a broader pore size distribution would be one with a much wider base on the peak. The top of the peak however, could remain at the same point if the average pore size or pore radius remains constant. A point which immediately stands out is that there are many ways a pore size distribution could be broadened. Figure 28b shows broadening on both sides of the average, Figure 28c shows broadening in the direction of smaller pores, Figure 28d shows broadening in the direction of larger pores and Figure 28e shows a broadening by a bimodel type distribution. Catalyst pore surface area also varies with changes in pore size distribution, however. The smaller pores have the most surface area available for reaction. Sorting pore size effects from surface area effects would be difficult if not impossible. Broadening the distribution on the large pore side would cause a possible loss in surface area per cc pore volume, although the effect would be minimized. In almost all changes in pore size distribution, a change in surface area available for reaction accompanies the pore size change. A shift to a more narrow distribution with a smaller average pore radius would eliminate larger pores and increase surface area per unit of pore volume. For this last case, a chemical rate control situation would tend to increase in rate due to increased surface area if no pore size effects are present. As can be seen from the results of the mercury penetration tests presented earlier,

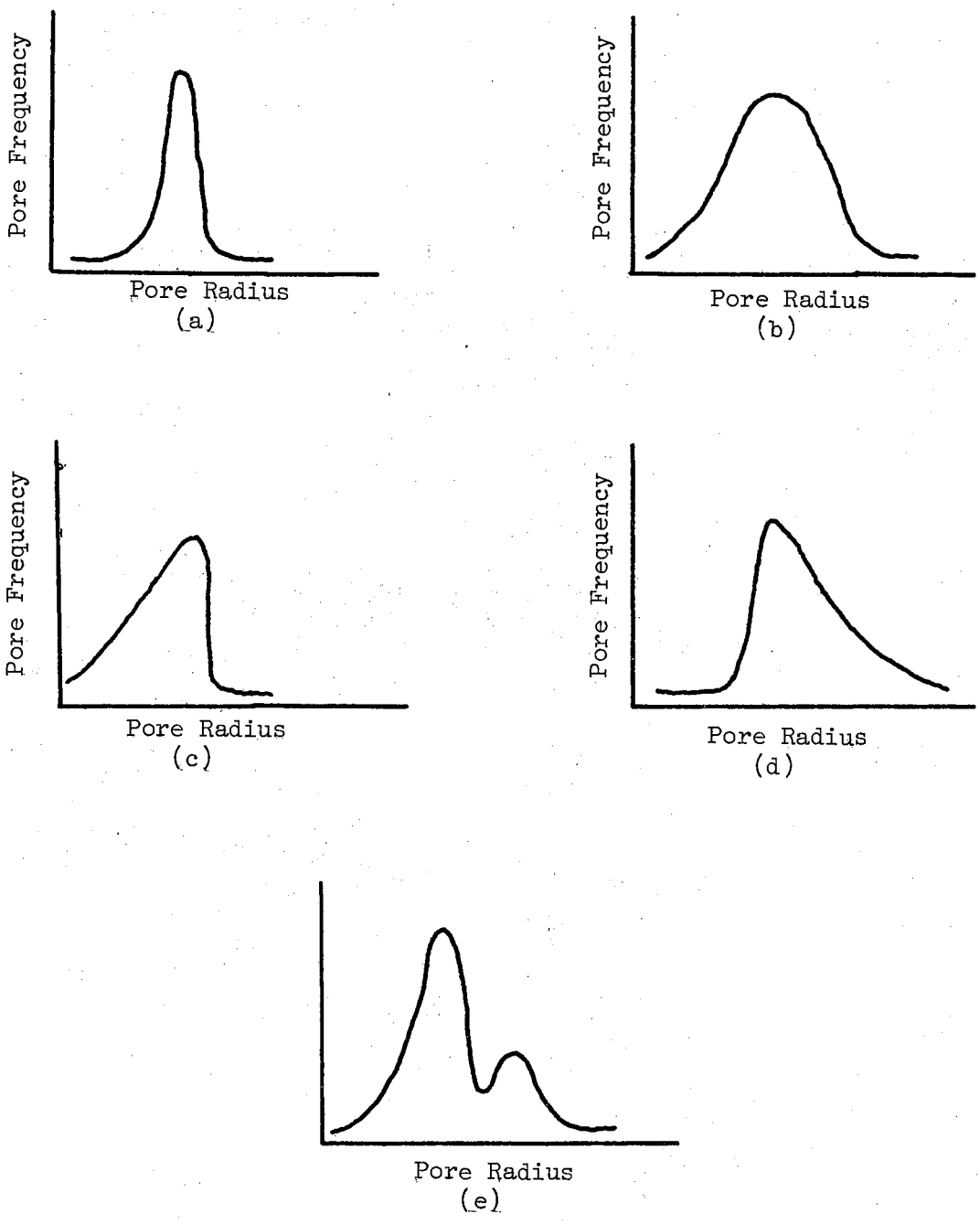

Figure 28. Examples of Various Pore Size Distributions

other catalysts obtained from Nalco, i.e. 72-A and 72-B, have more narrow pore size distributions and smaller average pore radii than the Nalcomo 474. Obtaining catalysts with identical metals content but with specified size distributions from commercial vendors is not an easy task.

Perhaps one of the most important points to remember is that Van Zoonen and Douwes (60) were able to demonstrate that the large pores of a catalyst pellet play a most significant role in desulfurization of a gas oil. Based on our knowledge that we are dealing with a mostly chemical rate controlled situation, a logical expectation would be for both of the narrow distribution catalysts to have an increase in rate (somewhat greater surface areas, see Table XVI). On the contrary, sulfur removal decreased for equivalent LVHST's. A closer look at the pore size distribution curves shows that the mean pore size has been decreased by some 25% from 33 Å to 25 Å for both the new catalysts. A reduction in pore size by 25% can by no means be called insignificant. A comparison of the desulfurization results of the catalysts 72-A and 72-B with those of Nalcomo 474, see Figure 14, indicates that an increase in the amount of sulfur remaining in the product oil of some 50% results for 72-A and 72-B. The reduction in the amount of large pores and the shift in average pore radius appears responsible for the change in desulfurization. This thesis information therefore substantiates the conclusion of Van Zoonen and Douwes that larger pores are necessary to promote desulfurization.

To say that the smaller radius pores are actually preventing entry into the pores is to suppose that the size of the reactant molecule is approaching that of the pore. Calculation of a molecular

size of an anthracene molecule from bond lengths and angles and assuming a planar conformation shows a size of 7.1 Å which is still some 7 times smaller than the 50 Å pore diameter available. Molecular diameters may not necessarily be a good way of characterizing molecules however. Information supplied by Davidson Chemical Division (39) shows that benzene, a molecule of approximately 2.5 A°, has a critical diameter for a mole sieve of 6.7 Å. A sulfur containing molecule in the anthracene oil might therefore have a critical diameter of 20 Å. A thiophene has a critical diameter of 5.3 Å, larger than a mercaptians critical diameter of 4.5 to 5.1 Å. Molecular conformation seems to play an important role in a molecule's diffusion ability and to say which of the molecules would be excluded by a given size pore is, therefore somewhat difficult. In this respect, inspection of Figure 16 on the fractions data may be of help. The 72-B curve compared to the Nalcomo 474 shows a general loss of sulfur removal ability in all fractions. The most dramatic decrease in sulfur removal occurs for those fractions with dew points between 450° and 475° @ 50 mm Hg. One could therefore conclude that those sulfur molecules of the particular type in the indicated fractions are the most difficult to remove and molecular conformation would seem to be the cause. Although entry into the pores would not seem to be a problem, the smaller pores could easily restrict rotation of a molecule for proper surface absorption. One additional possibility must be reckoned with as an explanation of the loss in desulfurization, a general loss in catalyst activity. First, the possibility that two catalysts, such as 72-A and 72-B, from separate batches would have an almost identical decrease in activity seems highly unlikely.

The fact that both have an almost identical average pore radius seems to correspond much more easily with the identical loss in desulfurization. Secondly, if a general loss in activity were affected one would expect an identical fractional increase in sulfur remaining for each fraction of oil, certainly not the case involved here.

Additional evidence that the change in pore size distribution caused the decrease in desulfurization is available from the patent literature. Recommended in patent data (3) was a most frequent pore diameter (defined on page 25) of at least 60 Å. The Nalcomo 474 had a most frequent diameter (D_f) of 66 Å, while catalysts 72-A and 72-B had D_f's of 50 Å. A spread in the range of the more frequent pore diameters (ΔD_r) of at least 10 Å is also recommended by patent literature (2). Nalcomo 474 had a ΔD_r of 18.5 Å, 72-B a ΔD_r of 10.8 Å and 72-A a ΔD_r of 6.5 Å. The catalysts 72-A and 72-B were again marginal or short of the necessary minimum described in the patent literature. As a further check to be free from catalyst pore size problems, the same patent recommends a pore distribution factor of 5.0. Recall from the literature section that

$$PD = \frac{(D_f)^2 \times \Delta D_r}{10^4}$$

For Nalcomo 474 the PD = 6.66. For 72-A, PD = 1.62 and for 72-B, PD = 2.7. By all of the above standards, the catalysts 72-A and 72-B should exhibit a loss in desulfurization compared to Nalcomo 474. With the rather fortuitous choice of catalysts which qualify as being free from pore problems (Nalcomo 474) and those which should exhibit pore distribution problems (72-A and 72-B), the importance of most frequent

pore diameter D_f and range of more frequent pore diameters ΔD_r has been dramatized. Summarizing, a decrease in most frequent pore diameter from 66 Å to 50 Å has a hindering effect on the removal of sulfur. The decrease in desulfurization sustantiated the work of Schmid (56), Van Zonnen and Douwes (60) and patent literature data (9). Molecular weight may be a poor way of characterizing molecules and molecular conformation was indicated as a possible significant consideration. Imposement of a steric hindrance or surface adsorption situation would seem to be responsible for the loss in desulfurization and molecular conformation offers a good explanation for the selectivity in desulfurization as shown from the fractions data.

The fractions data must be examined with a bit more detail. The feed was cut into eight fractions in an attempt to determine where the major portion of the sulfur compounds were located. As can be seen from Figure 16, all eight fractions for the feed have almost equal sulfur concentrations of between .4 and .5%. By comparing the curve for the product from a run on Nalcomo 474 with that of the feed, a determination can be made as to which fractions are the most difficult to remove. The heavier fractions can easily be singled out as those most difficult to desulfurize. Most theories for prediction of diffusion in liquids provide a ready explanation for the observed phenomena. The higher the molecular weight, the smaller the diffusion coefficient. The later stages of reaction might therefore be expected to be limited by a diffusion controlling situation. Evidence presented earlier however clearly show that diffusion is not controlling. Fortunately, there is a logical explanation which is compatible with both the theory and observed phenomena. For large molecules, the

possibility exists that although the molecule is absorbed on the catalyst surface, the proper orientation of the molecule would not be achieved to provide immediate desulfurization. Surface adsorption would become the rate limiting step. Hoog (26) also suggested such a possibility of adsorption difficulties.

In summary, the heavier fractions of the oil are the most difficult to desulfurize. Diffusion has been shown not to be the rate limiting step for these reactions however. Correct adsorption of the large molecules on the surface of the catalyst seems to be the controlling factor. The low rate constant for the slow fraction would be representative of the adsorption controlled situation. Molecular conformation of the molecules seems to be an important facet of desulfurization and offers an explanation of the selective reduction in sulfur removal with the 72-A and 72-B catalysts as well as explaining the difficulty for removal of the heavier fractions. The catalyst pore size and distribution appears to have an important role in not only the effective diffusivity but also in the intrinsic rate of the surface.

CHAPTER VII

CONCLUSIONS AND RECOMMENDATIONS

A trickle flow reactor was constructed with operational capabilities of 77°F to 850°F and 14.7 psia to 1800 psig. Conclusions reached about the reactor system are as follows:

1) Temperature control along the axial length was excellent, approaching an isothermal reactor. Radial temperature gradients were also minimal, again helping the approach to isothermal operation. The specially designed heating blocks gave excellent heat control.
2) Pressure control was adequate, holding pressure constant to within levels which would not cause experimental difficulty.
3) Liquid distribution and axial mixing problems can be avoided with longer beds of catalyst and need not be a detrimental factor for using the trickle flow system in hydrodesulfurization studies.
4) Flow control was adequate and remained constant over a run as long as pressure remained constant.
5) Automation of temperature control decreases temperature deviations and decreases the amount of time required to reach steady state after changing operating temperature.

Concerning the experimental apparatus which was constructed for this work, the following recommendations are offered:

1) A greater number of smaller aluminum blocks and corresponding controllers should be added to improve temperature control at higher temperatures.

2) An external loaded mity-mite pressure controller should be installed for more precise pressure control and safety in changing system pressures. To change system pressure under present conditions requires venting of a small amount of hydrogen to the room. Setting the pressure in the dome of the regulator is very difficult under such conditions.

3) Capillary tubing should be installed in the hydrogen inlet line to provide a means of measuring hydrogen inlet rate. By calibrating pressure drop with flow rate, the hydrogen flow rate can be measured during operation by monitoring the pressure drop across a length of capillary tubing.

4) Other methods of determining sulfur at concentrations below 200 parts per million should be investigated. X-ray florescence and bomb techniques are recommended.

Data were taken on the hydrodesulfurization of a coal derived raw anthracene oil. Concerning the data the following conclusions were reached.

1) Reproducibility of results was good from a total equipment stand point.

2) Non-catalyzed desulfurization does not occur to an appreciable extent for the conditions of this study. Non-catalyzed

desulfurization can, however, become very significant at higher temperatures approaching 800°F.

3) Catalyst beds of 20" or longer are free from axial liquid mixing problems and radial liquid distribution problems. A ten inch bed does have axial mixing problems however.

4) Desulfurization does not follow a first order relationship. Choice of second, third, or fourth order fit for the data must be made on the basis of simplicity of use and indicates that the true mechanism of reaction is likely none of the above models.

5) A parallel first order reaction model was demonstrated to achieve the best fit of the data and can be derived from pure component studies based on the theory of Hoog (26).

6) Reducing the average pore radius from 33 Å to 25 Å has a detrimental effect on desulfurization and the 33 Å radius must be taken as an improvement over the smaller pore catalyst.

7) Low removal of the higher boiling fraction sulfur compounds limits the desulfurization process. Surface adsorption of large molecules is a reasonable explanation of the controlling step which prevents faster removal of sulfur attached to heavier molecules.

8) Pressure was shown to have an effect on desulfurization in the range of 500 to 1000 psig. Beyond 1000 psig improvement in desulfurization is small.

9) Increase in hydrogen flow rate of from 1500 to 20,000 SCF/Bbl does not improve desulfurization.

10) Reducing particle size from 8-10 mesh to 40-48 mesh does not increase reaction rate. An effectiveness factor of very near one was calculated.

11) These results were obtained on raw, solids-free anthracene oil and should be verified on additional coal derived oils before they are generalized.

From the conclusions drawn on the experimental data of this thesis, several important and interesting recommendations can be made for additional experimental programs.

1) Non-catalyzed desulfurization should be investigated by conducting experiments at higher temperatures to examine the possibilities of non-catalyzed desulfurization being the most economical alternative to catalytic desulfurization. By fractionating the feed into two fractions, one fraction could be thermally desulfurized while the other would be most economically removed catalytically. Also a more precise knowledge of non-catalyzed desulfurization must be obtained before a good model for catalytic desulfurization can be formulated.

2) The feed oil should be broken into the separate fractions and a concerted effort made to identify the majority of the sulfur compounds contained in each fraction. This recommendation is recognized as a rather lengthy and time consuming one.

3) Having completed or parallel to identification of the sulfur compounds in the oil, pure component desulfurization studies should be made to determine the rate of reaction and order of reaction for the pure sulfur compounds in a trickle flow reactor.

4) Parallel to the pure component work, the feed oil should be broken into the eight fractions in sufficient quantity to perform desulfurization studies on each fraction. The rate constants and reaction orders should be determined to provide information for formulation of a model for desulfurization of the whole feed similar to the parallel path model presented in this thesis.

5) Further catalyst studies would be made to determine whether or not increases in average pore diameter without loss of surface area would be an improvement in removal of the heavier sulfur bearing molecules. Changes in ratios of metals impregnated in the support should also be investigated as a possibility for improvement of desulfurization. To fully understand and improve desulfurization of large molecules a more detailed knowledge of adsorption, activation, and desulfurization must be made.

6) The desulfurization of other coal derived liquids should be studied to obtain data on their dependency on catalyst pore support properties. This last recommendation will have increasing significance as natural coal liquids become available from present developing coal liquefaction processes.

In summary, the trickle flow reactor has been shown to be an excellent tool for study of desulfurization reactions. Further research programs should follow this study and can be conducted on this system.

BIBLIOGRAPHY

1. Ahuja, S. P., M. L. Derrien, and J. F. le Page. Ind. Engr. Chem. Prod. Res. Develop. 9, 272 (1970).

2. Anderson, James A., et.al. U. S. 2,890, 192 (1960).

3. Anderson, James A., et.al. U. S. 2,924,568 (1961).

4. Baker, T., T. H. Chilton, and H. C. Vernon. Trans. Am. Inst. Chem. Engr. 31, 296 (1934).

5. Beers, Yardly. "Theory of Error." Addison-Wesley Publishing Co., Inc., Reading, Mass., (1962).

6. Berg, C., W. E. Bradley, R. I. Stirton, R. G. Fairfield, C. B. Leflert, and J. H. Ballard. Trans. Am. Inst. Chem. Engr. 43, 1 (1947).

7. Bird, B. R., W. E. Stewart, and E. N. Lightfoot. "Transport Phenomena." John Wiley & Sons, Inc., New York, (1960).

8. Brown, C. L., A. Vooshiers, Jr., and W. M. Smith. Ind. Engr. Chem. 38, 136 (1946).

9. Beuther, H. and B. K. Schmid. U. S. 3,383,301 (1967).

10. Byrns, H. C., W. E. Bradley and M. W. Lee. Ind. Engr. Chem. 35, 1160 (1943).

11. Chervenak, M. C., E. S. Johnson, C. A. Johnson, S. C. Schuman, and M. Sze. Oil and Gas J. 58, 80 (1960).

12. Cole, R. M. and D. D. Davidson. Ind. Eng. Chem. 41, 2711 (1949).

13. Cottingham, P. L., E. R. White, and C. M. Frost. Ind. Engr. Chem. 49, 679 (1957).

14. _____, "Development of a Process for Producing an Ashless, Low-Sulfur Fuel from Coal." Interim Report No. 3, R&D Report No. 53, U. S. Department of the Interior, Office of Coal Research (1971).

15. Erbar, J. H. Personal Communication, School of Chemical Engineering, Oklahoma State University, Stillwater, Oklahoma, (1972).

16. Finar, I. L. "Organic Chemistry." John Wiley and Sons, Inc., New York, New York, (1963).

17. Frost, C. M. and P. L. Cottingham. U. S. Bureau of Mines Rept. of Investigations 7418, (1970).

18. Frost, C. M. and P. L. Cottingham. U. S. Bureau of Mines Rept. of Investigations 7464, (1971).

19. Frye, C. G. and J. F. Mosby. Chem. Engr. Prog. 63, 66 (1967).

20. Glaser, M. B. and I. Lichtenstein. Am. Inst. Chem. Engr. J. 9, 30 (1963).

21. Gorin, E., R. T. Struck, and G. D. Curran. Ind. Eng. Chem. Process Des. Develop. 6, 166 (1967).

22. Gwin, G. T., R. L. Heinrich, E. J. Hoffmann, R. S. Manne, H. W. H. Meyer, J. R. Miller, and C. L. Thorpe. Ind. Eng. Chem. 49, 668 (1957).

23. Hammar, C. G. B. Third World Petroleum Congress. Section IV, 295 (1951).

24. Hill, G. R., D. J. Johnson, L. Miller, and J. L. Dougan. Ind. Eng. Chem. Prod. Res. Develop. 6, 52 (1957).

25. Hockman, J. M. and E. Effron. Ind. Eng. Chem. Fund. 8, 63 (1969).

26. Hoog, H. J. Inst. Petrol., 36, 738 (1950).

27. Hoog, H. Recueil. 69, 1289 (1950).

28. Hoog, H., H. G. Klinkert, and A. Schaafsma. Petrol. Refiner. 32, 137 (1953).

29. Hoog, H., J. Koome, and K. A. Weeds. Proceedings of the Second Oil Shale and Channel Coal Conference. July, 562 (1950).

30. Hoog, H., G. H. Reman, and W. C. B. Smithuysen. Third World Petroleum Congress. Section IV, 282 (1951).

31. Huntington, M. G. U. S. 3244615 (1966).

32. Jones, J. and Friedman. "Char Oil Energy Development Final Report." R&D Report No. 56, U. S. Department of the Interior, Office of Coal Research, (1972).

33. LeNoble, J. W. and J. H. Choufoer. Fifth World Petroleum Congress. Section III, paper 18 (1959).

34. Levenspiel, O. "Chemical Reaction Engineering." John Wiley and Sons, Inc., New York, New York, (1962).

35. Likins, M. L. Unpublished paper, School of Chemical Engineering, Oklahoma State University, (1972).

36. Lowry, H. H., Ed. "Chemistry of Coal Utilization," John Wiley and Sons, Inc., New York, New York (1945).

37. Massagutov, R. M., G. A. Berg, G. M. Kulinich, and T. S. Kirillov. Proc. 7th World Petrol. Congr., 4, 177 (1967).

38. Mears, D. E. Chem. Engr. Sci. 26, 1361 (1971).

39. _____. "Molecular Sieves." Davidson Chemical Division of W. R. Grace and Co., 5 (1969).

40. Partington, J. and F. Parker. J.S.C.I., 75 (1919).

41. Quader, S. A. and G. R. Hill. Ind. Eng. Chem. Process Des. Develop. 8, 450 (1969).

42. Quader, S. A. and G. R. Hill. Ind. Eng. Chem. Process Des. Develop. 8, 456 (1969).

43. Quader, S. A., W. H. Wiser, and G. R. Hill. Ind. Eng. Chem. Process Des. Develop. 7, 390 (1968).

44. Raines, G. E. and T. E. Corrigan. "The Use of the Axial Dispersion Model to Predict Conversions of First- and Second-Order Reactions." Symposium on Recent Advances in Kinetics, Fifty-ninth Annual Meeting of A.I.Ch.E., December 4-8 (1966).

45. Rall, H. T., C. J. Thompson, H. J. Coleman and R. L. Hopkins. U. S. Bureau of Mines, Separation and Identification Section RP48A (1970).

46. Richardson, J. T. Ind. Eng. Chem. Process Des. Develop., 11, 8 (1972).

47. Richardson, J. T. Ind. Eng. Chem. Process Des. Develop. 11, 12 (1972).

48. Ross, L. D. Chem. Eng. Prog., 61, 77 (1965).

49. Satchell, D. P. Ph.D. Thesis, Oklahoma State University, Stillwater, Oklahoma, (In Preparation).

50. Satterfield, C. N. "Mass Transfer in Heterogeneous Catalysis." M.I.T. Press, Cambridge, Mass. (1970).

51. Satterfield, C. N., A. A. Pelossof, and T. K. Sherwood. Am. Inst. Chem. Eng. J. 15, 227 (1969).

52. Schiesser, W. E. and L. Lapidus. Am. Inst. Chem. Engr. J. 7, 163 (1961).

53. Schuman, S. C. Chem. Engr. Prog. 57, 49 (1961).

54. Schwartz, C. E. and J. M. Smith. Ind. Engr. Chem., 45, 1209 (1953).

55. Schwartz, J. G. and G. W. Roberts. "Analysis of Trickle Bed Reactors: Liquid Backmixing and Liquid-Solid Contacting." 74th National Meeting of A.I.Ch.E., New Orleans, Louisiana, March 11-15 (1973).

56. Schmid, B. K. and H. Beuther. Sixth World Petroleum Congress, Section VII, 233 (1963).

57. Scott, A. H., Trans. Inst. Chem. Engr. 13, 211 (1935).

58. Smith, J. M. "Chemical Engineering Kinetics," McGraw-Hill Book Co., New York, New York (1970).

59. Stevenson, D. H. and H. Heinemann. Ind. Engr. Chem. 49, 664 (1957).

60. Van Zoonen, D. and C. Th. Douwes. J. Inst. Petrol. 49, 383 (1963).

61. Wan, K. T. M.S. Thesis, Oklahoma State University, Stillwater Oklahoma (1971).

62. Wakau, N. and J. M. Smith. Ind. Engr. Chem. Fund., 3, 123, (1964).

63. White, P. J., J. P. Jones, and R. T. Eddinger. Hydrocarbon Processing. 47, 97 (1968).

64. Wilhelm, R. H. Pure and Appl. Chem. 5, 403 (1962).

65. Wilke, C. R. and P. Chang. Am. Inst. Chem. Engr. J., 1, 264 (1955).

66. Wilson, W. A., W. E. Voreck, and R. V. Malo. Ind. Engr. Chem. 49, 657 (1957).

APPENDIX A

DESCRIPTION OF BACKMIX REACTOR SYSTEM

The following is a brief description of some of the problems encountered with operation of the backmix reactor and system. This initial system was built around a one liter Parr reactor as seen in Figure 29. The oil was fed into the system by a Ruska metering pump. Maintaining a constant liquid level and thus a constant space time in the reactor was dependent on controlled removal of liquid from the system. Withdrawal of liquid in a satisfactory manner however, became a severe problem. Separate liquid and vapor withdrawals were tried initially; however, the high pressure drop across a pressure let-down valve on the liquid stream resulted in flashing. The hot liquid caused the internals of the valve to swell to the extent that the valve would shut off until cooled down. Cooling the liquid and heating the valve externals did not alleviate the problems. A two-phase flow from a single dip tube was the next attempt. The two-phase flow was taken to a high pressure liquid-vapor separator where the flow was controlled by gas flow rate. Liquid withdrawal from the separation tank was intermittent but seemed successful in controlling liquid withdrawal. Some problems were still experienced by liquid sloshing in the reactor due to stirrer blades and by possible foaming. The reactor did not permit placement of the withdrawal tube near the center stirring shaft in a quiecent spot. No further attempts were made at liquid level control.

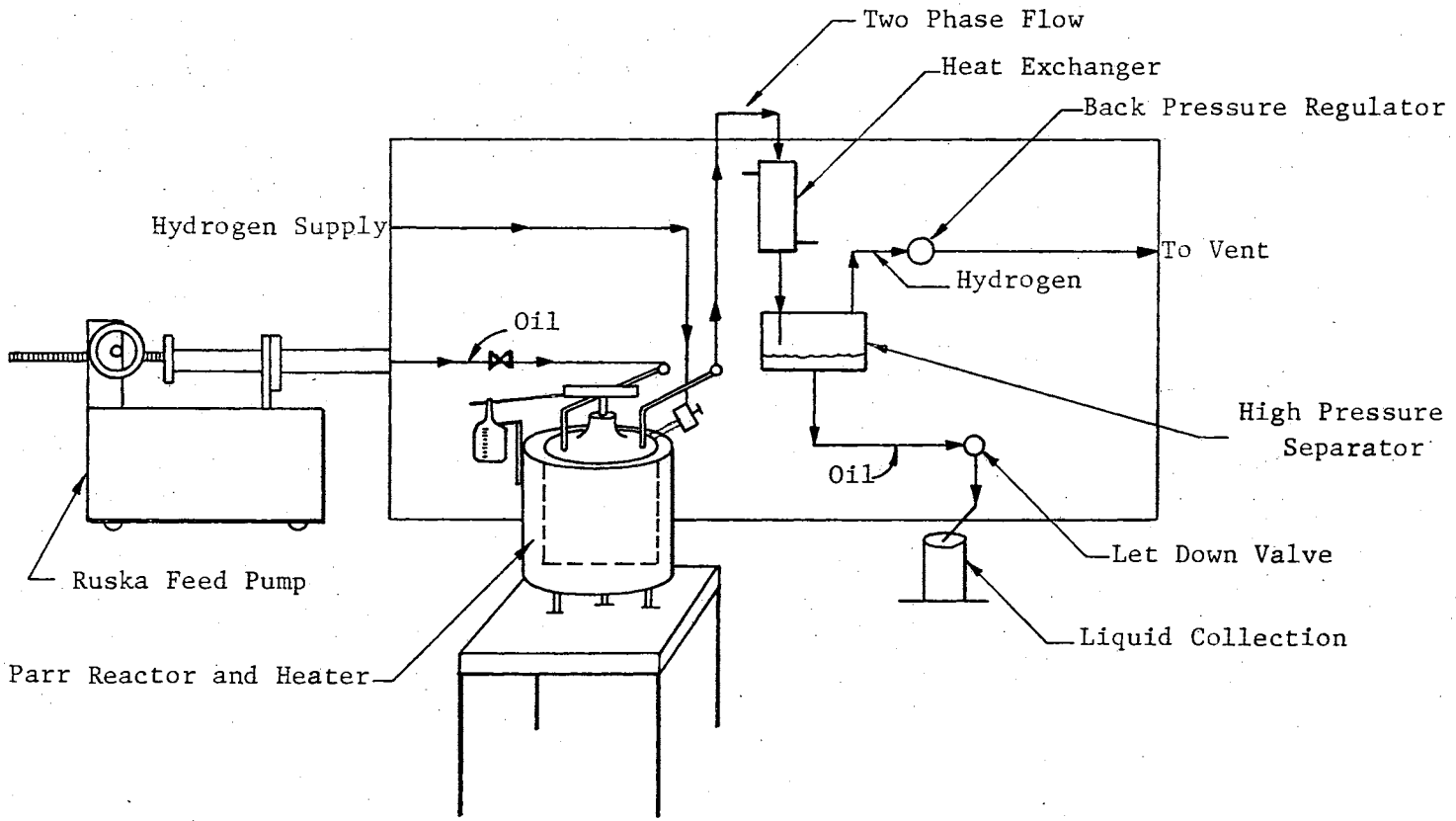

Figure 29. Initial Reaction System

The second and more serious problem, was that of high catalyst attrition. Successively smaller screens were constructed to fit on the liquid withdrawal tube to prevent withdrawal of catalyst in the liquid exit stream. The screen also provided some protection against liquid sloshing. With a 90 mesh screen, catalyst loss rates were still very high, far too high to ignore. Since the catalyst support properties were fixed by a commercial catalyst vendor, no possibilities existed in our laboratories for strengthening them. At this time, other systems for processing the oil were considered.

APPENDIX B

THERMOCOUPLE CALIBRATION

Thermocouples designated as 1 and 2 were calibrated using a platinum resistance thermometer. The platinum thermometer was calibrated by the U. S. Bureau of Standards. A copy of the calibration letter is shown as Table XXIV of this Appendix. The equation given is used to calculate the actual temperature read by the thermometer for a given temperature. The calibration procedure for thermocouples is described in the Leeds and Northrup manual No. 77-14-0-12 "Thermocouple Checking Furnaces." The general procedure was to tie the tips of the thermocouples to be calibrated very close to, but not touching, the tip of the platinum resistance thermometer. The thermometer and thermocouples were connected to Leeds and Northrup model 8686-3 potentiometers and the platinum resistance thermometer to a Muller Bridge and Leeds and Northrup model 2239 galvanometer. Reference junctions were constructed using copper wire and the junctions were placed in test tubes of glycerol. The glycerol test tubes were immersed in a bath of ice and distilled water. The furnace was turned on at a rate that would allow a temperature rise of $0.5^{\circ}F$ per min. The temperature of the thermocouples and the thermometer were read at various intervals in the desired temperature range. Results of calibration of thermocouples 1 and 2 are presented in Figure 30. Thermocouples 3 and 4 were claibrated using a platinum vs. platinum

TABLE XXIV

CALIBRATION CERTIFICATE FOR PLATINUM RESISTANCE THERMOMETER

NBS406B

UNITED STATES DEPARTMENT OF COMMERCE
WASHINGTON

National Bureau of Standards

Certificate

Platinum Resistance Thermometer

Leeds and Northrup Company; Serial Number 1613906

Submitted by

Oklahoma State University
Stillwater, Oklahoma

The following values were found for the constants in the formula,

$$t=\frac{R_t-R_0}{\alpha R_0}+\delta\left(\frac{t}{100}-1\right)\frac{t}{100}+\beta\left(\frac{t}{100}-1\right)\left(\frac{t}{100}\right)^3,$$

in which t is the temperature, at the outside surface of the tube protecting the platinum resistor, in °C on the International Temperature Scale of 1948 (J. Research NBS 42, 209 (1949) RP1962) and R_t and R_0 are the resistances of the platinum resistor at $t°$ and 0°C, respectively, measured with a continuous current of 2.0 milliamperes.

Constant	Value
α	0.0039268_{98}
δ	1.491_{90}
β	0.110_{15} (t below 0°C) 0 (t above 0°C)
R_0	25.548 Abs. Ohms

For the Director
National Bureau of Standards

John L. Riddle, Physicist
Temperature Measurements Section
Heat and Power Division

Test No. G 32392
Date May 17, 1963
JLR/nem

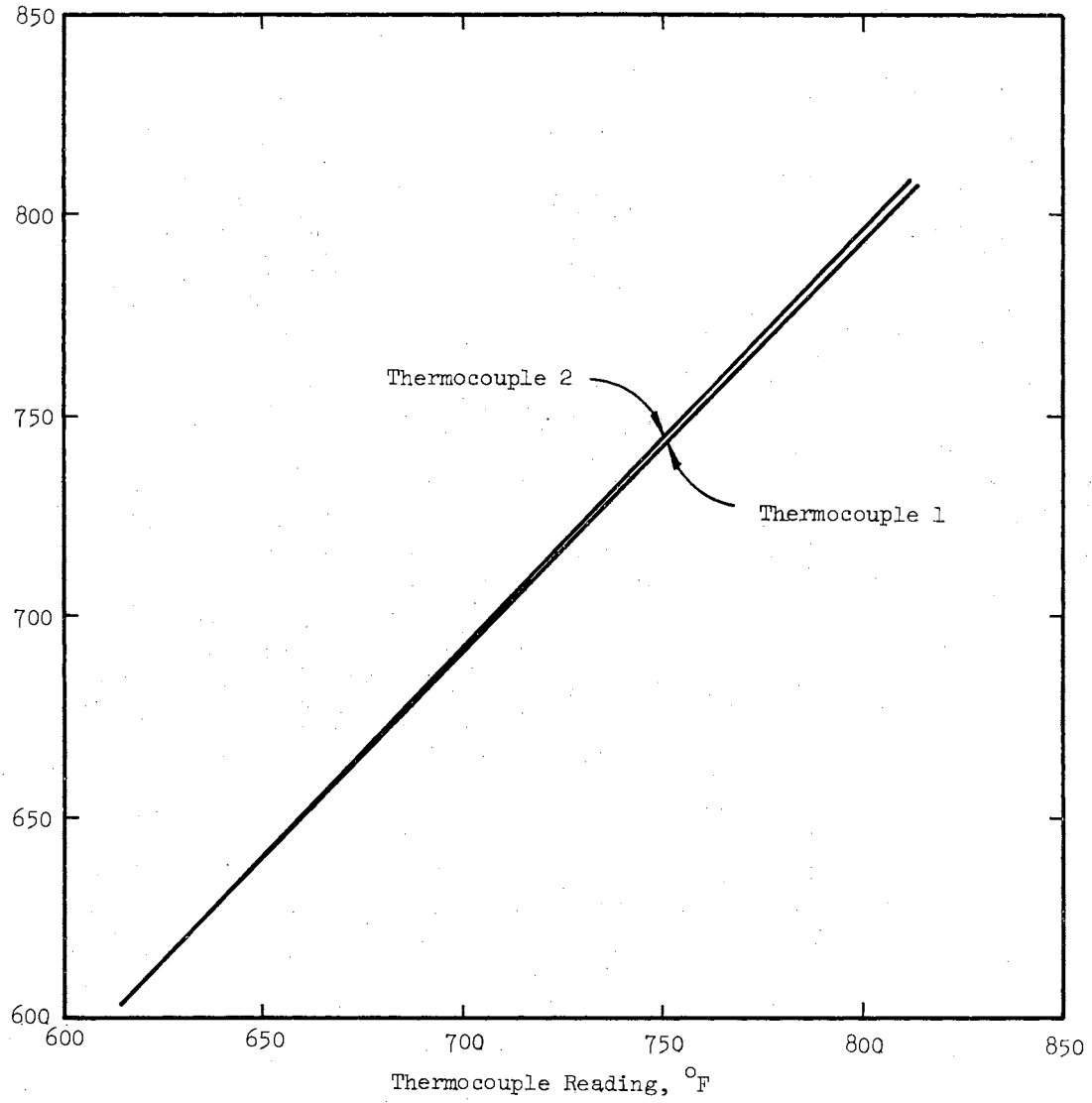

Figure 30. Temperature Calibration for Platinum Resistance Thermometer vs. Thermocouples 1 & 2

(+) 10% rhodium thermocouple. The rhodium-platinum thermocouple was calibrated by Leeds and Northrup Co. in the range of 0 to 1400°C. A copy of the calibration letter is shown as Table XXV this Appendix. Calibration proceeded using the same procedure and equipment as with the platinum resistance thermometer. Results of the calibrations are presented in Figure 31.

TABLE XXV

CALIBRATION CERTIFICATE FOR PLATINUM VS. RHODIUM THERMOCOUPLE

Pioneers in Precision

LEEDS & NORTHRUP COMPANY 4901 STENTON AVE · PHILADELPHIA 44, PA · 215 DA9-4900

L & N Order No. 37563-3

CERTIFICATE

FOR

PLATINUM VS. PLATINUM +10% RHODIUM THERMOCOUPLE

TEST NO. 175190-K-35

-oOo-

The following values of electromotive force and corresponding temperatures of the measuring junction apply when the reference junctions are maintained at 0° C:

Absolute Millivolts	International 1948 Deg. C	Deg. F	Absolute Millivolts	International 1948 Deg. C	Deg. F
0.000	0.0	32.0	7.000	768.4	1415.1
0.143	25.0	77.0	8.000	859.8	1579.6
0.299	50.0	122.0	9.000	949.0	1740.2
1.000	146.5	295.7	10.000	1035.9	1896.6
2.000	264.6	508.3	11.000	1120.9	2049.6
3.000	373.0	703.4	12.00	1205.	2201.
4.000	476.9	890.4	13.00	1288.	2350.
5.000	577.2	1071.0	14.00	1371.	2500.
6.000	674.2	1245.6	15.00	1455.	2651.

The uncertainties in the above values are not more than 0.75° C in the range 0° to 1100° C and then increase to not more than 3° C at 1400° C.

The thermocouple was made from selected annealed wire, samples of which have been calibrated at 1063° C (gold point), 960.8° C (silver point), 630.5° C and 419.5° C (zinc point) by the National Bureau of Standards. Because of the high accuracy of this type calibration (±2 microvolts at each temperature), and also because of the uniformity in thermoelectric properties of the wire as shown by the samples tested, the above values are at least as accurate as if the thermocouple had been calibrated directly by comparison with a standard thermocouple.

LEEDS & NORTHRUP COMPANY

For the Director of Manufacturing

K. A. Walch

K. A. Walch
Head, Standardizing Laboratory

July 1, 1963

CABLE ADDRESS "LEEDSNORTH"

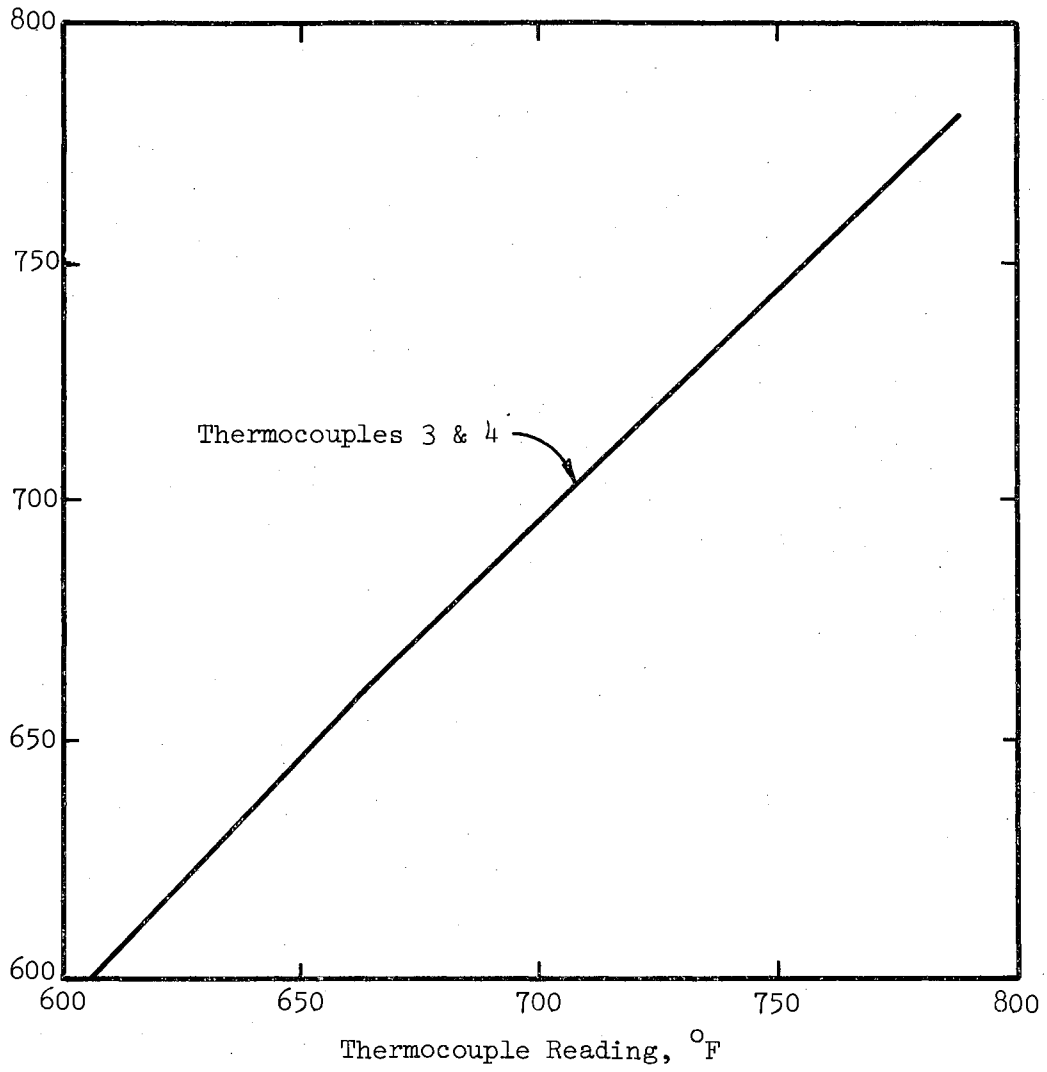

Figure 31. Temperature Calibration for Platinum vs. Rhodium Thermocouple vs. Thermocouples 3 & 4

APPENDIX C

CALIBRATION OF HEISE GAUGE AND DIGITAL READOUT

The Heise gauge used as the pressure indicator for the hydrotreating system was calibrated at the factory. Table XXVI of this Appendix is a copy of the calibration letter. The gauge was calibrated from 250 to 5000 psi and at no point shows a deviation of more than 5 psi.

The Numatron digital temperature readout was calibrated according to the procedure set forth in Leeds and Northrup model 900 digital readout bulletin. After linearization was completed, an input signal was fed to the digital readout from a potentiometer. Correspondence between what the digitial readout should have read and the actual reading is given in Table XXVII. Correspondence between the two was quite good and a deviation of no more than $0.4^{\circ}F$ was detected.

TABLE XXVI

CERTIFICATION REPORT OF HEISE GAUGE NO. 52143

HEISE BOURDON TUBE CO., INC.

Manufacturers of the Heise Gauge ,
Newtown, Conn.

This gauge has been calibrated with a piston gauge which has been compared with master piston gauges whose effective areas were determined with an estimated accuracy of 3 parts in 100,000 by the National Bureau of Standards Reports No. P6744 and No. P6745. The weights for those dead weight piston gauges have also been certified by the Bureau of Standards to have an average accuracy of within one part in 35,000.

READING NUMBER	DEAD WEIGHT OR Hg COL. READING	GAUGE READING (Deviation from Dead Wt. or Hg. Col.)
1	250 psi	--
2	500 psi	--
3	750 psi	--
4	1000 psi	--
5	1250 psi	--
6	1500 psi	--
7	1750 psi	--
8	2000 psi	--
9	2250 psi	--
10	2500 psi	--
11	2750 psi	--
12	3000 psi	--
13	3250 psi	--
14	3500 psi	--
15	3750 psi	--
16	4000 psi	--
17	4250 psi	--
18	4500 psi	--
19	4750 psi	--
20	5000 psi	--

Room Temperature at Test 70°F

Maximum Hysteresis 5 psi

Remarks: Corrections are indicated where error is 5 psi or more.

Date Tested 9-28-67

Signed A. K. Arndt

TABLE XXVII

NUMATRON LINEARIZATION

Temperature, °F	Supply EMF	Numatron Reading, °F
250	7.31	250.1
300	8.83	300.0
350	10.37	349.9
400	11.92	400.2
450	13.46	450.0
500	15.01	500.3
550	16.54	549.9
600	18.07	600.1
650	19.61	650.0
700	21.15	700.4
750	22.68	750.0
800	24.21	800.0
850	25.74	850.1
900	27.29	900.4

APPENDIX D

LIST OF GASES, CHEMICALS, AND CATALYSTS

Gases Used in the Reactor System:

Hydrogen - prepurified (99.95%) 3500 psig - Matheson

Nitrogen - prepurified (99.997%) 3500 psig - Matheson

5% H_2S in Hydrogen - Air Products

Gases Used in Sulfur Analysis:

Oxygen - 99.5% pure - Sooner Supply

Chemicals Used in Reactor System:

Sodium Hydroxide Pellets - Fisher Scientific

"Silver Goop," lubricant - Ben McKalip

Chemicals Used in Sulfur Analysis

MgO, Magnesium Oxide - Curtin Scientific

KIO_3, Potassium Iodate - Curtin Scientific

HCl, Hydrochloric Acid - Fisher Scientific

Arrowroot Starch - Curtin Scientific

NaN_3, Sodium Azide - Fisher Scientific

Distilled Water

Iron Chips - Curtin Scientific

Tin Granuales - Curtin Scientific

Crucible and Lid - Curtin Scientific

Catalysts Used in Reactor System:

Nalcomo 474, 72-A, 72-B

*CoO, wt%	3.5
*MoO, wt%	12.5
Support	Alumina
Pellet Density, g/cc	1.31
Packed Bed Density, g/cc	.73

*Nalco Data

APPENDIX E

SAMPLE CALCULATION FOR SULFUR ANALYSIS

A furnace factor is obtained for the system which accounts for vaporization, incomplete combustion or other factors which cause the system to deviate from correct determination. From a sample of known sulfur concentration, the furnace factor (ff) is calcualted according to the formula:

$$ff = \frac{(\text{wt \% S})(\text{wt of sample})}{(\text{volume titrated} - \text{blank})}$$

Using the calculated furnace factor, a volume titrated on the titrator is turned into a wt % S by using the formula:

$$\text{wt \% S} = \frac{(ff)(\text{volume titrated} - \text{blank})}{(\text{wt of sample})}$$

Which is just a rearrangement of the first equation.

Sample:

ff = 2.78

blank = .011

volume titrated = .053

$$\text{wt \% S} = \frac{(2.78)(.053 - .011)}{100.00} = .116 \text{ \% S}$$

APPENDIX F

CALCULATION OF STANDARD DEVIATION FOR ANALYTICAL EQUIPMENT

Following the realtionship presented by Beers (5) the standard deviation of sulfur analysis was calculated for seven concentrations of sulfur.

$$S = \sqrt{\frac{\sum_{n=1}^{k} (\delta X_n)^2}{k-1}}$$

Where S = standard deviation

k = number of data points

δX = known sulfur concentration - determined sulfur concentration

A sample calculation is as follows:

Known Sulfur Level - .06%

Known	Determined	δX	δX^2
.06	.0569	.0031	.0000096
.06	.0586	.0014	.0000014
.06	.0554	.0046	.0000211
.06	.0531	.0069	.0000476
.06	.0559	.0041	.0000168

$$\Sigma(\delta X_n)^2 = .000047$$

$$k = 4$$

$$S = \frac{.000097}{4} = \pm .00491$$

Standard deviations were calculated for six additional levels similarly and are listed as follows:

Known Level	Std. Dvn.	% Dvn.
.02	± .004	20 %
.04	± .00379	9.5%
.06	± .00491	8.2%
.08	± .00692	8.6%
.10	± .00581	5.8%
.15	± .00525	3.5%
.20	± .00838	4.0%

A % deviation relative to the given sulfur level was also calculated.

Example: $\frac{.004}{.02} = 20\%$

The % deviations are also listed above.

APPENDIX G

CALCULATION OF STANDARD DEVIATION FOR REPRODUCIBILITY RUNS

Again following the relationship presented by Beers (5), the standard deviation of the various data points reproduced in Runs 2, 3, and 9 is calculated.

$$S = \sqrt{\frac{\sum_{n=1}^{k} X_n^2 - k\,\overline{X}^2}{k-1}}$$

where S = standard deviation

X = determined sulfur value

k = number of data points

$$\overline{X} = \frac{\sum_{n=1}^{k} X_n}{k}$$

A sample calculation is as follows:

@ 600 F, .375 LHSV, 1000 psig

Determined Sulfur Concentrations	X^2
.186	.034596
.177	.031329
.170	.0289
.162	.026243
.187	.034469
.190	.036099
$\Sigma X_n = 1.072$	$\Sigma X_n^2 = .192138$

$$\bar{X} = \frac{\Sigma X_n}{k} = 1.7866 \qquad k\bar{X}^2 = .19152$$

$$S = \sqrt{\frac{.192138 - .19152}{5}} = 5.0110$$

Standard deviations were claculated for seven additional points as listed below.

Temp \ LHSV	.375	.75	1.5
600	± .011	.0133	.00895
650	.0119	.0033	.00648
700	.0139	.0102	

APPENDIX H

EXPERIMENTAL RUN DATA

The following table is a list of the reactor conditions for each sample taken. Nominal temperatures and pressures are shown as well as actual reactor pressure. Actual temperatures did not deviate more than $\pm$ 3°F over the profile and all profiles would be much too lengthy to include. Catalyst type, size and volume in the reactor are also shown. Run numbers are included and desulfurization results can be correlated with results tables in the discussion section. Reactor space time "t" (vol catalyst/vol oil/hr) is shown for each run. Hydrogen rate and total hours of catalyst on oil are also listed.

TABLE XXVIII

EXPERIMENTAL RESULTS

Sample No	Nominal Temp	Nominal Press	t	Cat Type	Cat Size (Mesh)	Reactor Volume	Reactor Pressure	Hrs on Oil	H_2 Rate SCF/Bbl	Series Loading
PF35A	700	1000	1.5	474 reg	8-10	37.65	1010	18	1500	1
PF35B	700	1000	1.5	474 reg	8-10	37.65	1010	23	1500	1
PF36	700	1000	1.5	474 reg	8-10	37.65	1010	25	1500	1
PF37	700	1000	1.5	474 reg	8-10	37.65	1010	32	1500	1
PF38	700	1000	1.5	474 reg	8-10	37.65	1010	34	1500	1
PF39	700	1000	1.5	474 reg	8-10	37.65	1010	36	1500	1
PF40	700	1000	1.5	474 reg	8-10	37.65	1010	38	1500	1
PF41	700	1000	1.5	474 reg	8-10	37.65	1010	40	1500	1
PF42	700	1000	1.5	474 reg	8010	37.65	1010	42	1500	1
PF43	700	1000	.75	474 reg	8-10	37.65	1008	50	1500	1
PF44	700	1000	.75	474 reg	8-10	37.65	1008	51	1500	1
PF45	700	1000	.375	474 reg	8-10	37.65	1012	57	1500	1
PF46	700	1000	.375	474 reg	8-10	37.65	1012	58	1500	1
PF47	750	1000	1.5	474 reg	8-10	37.65	1012	71	1500	1
PF48	750	1000	1.5	474 reg	8-10	37.65	1012	73	1500	1
PF49	750	1000	.75	474 reg	8-10	37.65	1020	80	1500	1
PF50	750	1000	.75	474 reg	8-10	37.65	1020	82	1500	1
PF51	750	1000	.375	474 reg	8-10	37.65	1010	89	1500	1
PF52	750	1000	.375	474 reg	8-10	37.65	1010	90	1500	1
PF53	750	1000	1.5	474 reg	8-10	37.65	1020	97	1500	1
PF54	800	1000	1.5	474 reg	8-10	37.65	1020	105	1500	1
PF55	800	1000	1.5	474 reg	8-10	37.65	1020	107	1500	1
PF56	800	1000	.75	474 reg	8-10	37.65	1025	116	1500	1

TABLE XXVIII (Continued)

Sample No	Nominal Temp	Nominal Press	t	Cat Type	Cat Size (Mesh)	Reactor Volume	Reactor Pressure	Hrs on Oil	H_2 Rate SCF/Bbl	Series Loading
PF57	800	1000	.75	474 reg	8-10	37.65	1008	120	1500	1
PF58	800	1000	.375	474 reg	8-10	37.65	1030	122	1500	1
PF59	800	1000	.375	474 reg	8-10	37.65	1030	123	1500	1
PF60	800	1000	1.5	474 reg	8-10	37.65	990	139	1500	1
PF61	700	1000	1.5	474 reg	8-10	37.65	995	147	1500	1
PF62	700	1000	1.5	474 reg	8-10	37.65	995	151	1500	1
PF63	700	1000	1.5	474 reg	8-10	37.65	995	156	20000	1
PF64	700	1000	1.5	474 reg	8-10	37.65	995	158	20000	1
PF65	650	1000	1.5	474 reg	8-10	37.65	1004	172	1500	1
PF66	650	1000	1.5	474 reg	8-10	37.65	1004	173	1500	1
PF67	650	1000	.75	474 reg	8-10	37.65	1005	179	1500	1
PF68	650	1000	.75	474 reg	8-10	37.65	1000	180	1500	1
PF69	650	1000	.375	474 reg	8-10	37.65	1000	182	1500	1
PF70	650	1000	.375	474 reg	8-10	37.65	1000	183	1500	1
PF71	650	1000	1.5	474 reg	8-10	37.65	1000	188	1500	1
PF72	650	1000	1.5	474 reg	8-10	37.65	1000	189	1500	1
PF73	650	1000	1.5	474 reg	8-10	37.65	1000	193	20000	1
PF74	650	1000	1.5	474 reg	8-10	37.65	1000	195	20000	1
PF75	600	1000	1.5	474 reg	8-10	37.65	1000	199	1500	1
PF76	600	1000	1.5	474 reg	8-10	37.65	1005	201	1500	1
PF77	600	1000	.75	474 reg	8-10	37.65	1000	205	1500	1
PF78	600	1000	.75	474 reg	8-10	37.65	1000	207	1500	1
PF79	600	1000	.375	474 reg	8-10	37.65	1000	210	1500	1
PF80	600	1000	.375	474 reg	8-10	37.65	1000	211	1500	1
PF81	700	1000	1.5	474 reg	8-10	37.65	1010	12	1500	2
PF82	700	1000	1.5	474 reg	8-10	37.65	1010	16	1500	2

TABLE XXVIII (Continued)

Sample No	Nominal Temp	Nominal Press	t	Cat Type	Cat Size (Mesh)	Reactor Volume	Reactor Pressure	Hrs on Oil	H_2 Rate SCF/Bbl	Series Loading
PF83	700	1000	1.5	474 reg	8-10	37.65	1000	20	1500	2
PF84	700	1000	1.5	474 reg	8-10	37.65	1015	24	1500	2
PF85	700	1000	1.5	474 reg	8-10	37.65	1015	28	1500	2
PF86	700	1000	1.5	474 reg	8-10	37.65	1014	32	1500	2
PF87	700	1000	1.5	474 reg	8-10	37.65	1012	35	1500	2
PF88	700	1000	1.5	474 reg	8-10	37.65	1015	40	1500	2
PF89	700	1000	1.5	474 reg	8-10	37.65	1015	44	1500	2
PF90	700	1000	1.5	474 reg	8-10	37.65	1015	48	1500	2
PF91	700	1000	.75	474 reg	8-10	37.65	1021	55	1500	2
PF92	700	1000	.75	474 reg	8-10	37.65	1020	58	1500	2
PF93	700	1000	.375	474 reg	8-10	37.65	1020	61	1500	2
PF94	700	1000	.375	474 reg	8-10	37.65	1020	62	1500	2
PF95	700	1000	1.5	474 reg	8-10	37.65	1020	66	1500	2
PF96	700	1000	1.5	474 reg	8-10	37.65	1020	68	1500	2
PF97	700	1000	.375	474 reg	8-10	37.65	1015	74	1500	2
PF98	700	1000	.375	474 reg	8-10	37.65	1005	75	1500	2
PF99	700	1500	1.5	474 reg	8-10	37.65	1480	83	1500	2
PF100	700	1500	1.5	474 reg	8-10	37.65	1480	85	1500	2
PF101	700	1500	.75	474 reg	8-10	37.65	1480	91	1500	2
PF102	700	1500	.75	474 reg	8-10	37.65	1480	92	1500	2
PF103	700	1500	.375	474 reg	8-10	37.65	1480	98	1500	2
PF104	700	1580	.375	474 reg	8-10	37.65	1480	100	1500	2
PF105	700	1500	1.5	474 reg	8-10	37.65	1480	105	1500	2
PF106	700	1500	1.5	474 reg	8-10	37.65	1480	107	1500	2
PF107	700	500	1.5	474 reg	8-10	37.65	505	115	1500	2
PF108	700	500	1.5	474 reg	8-10	37.65	508	116	1500	2

TABLE XXVIII (Continued)

Sample No	Nominal Temp	Nominal Press	t	Cat Type	Cat Size (Mesh)	Reactor Volume	Reactor Pressure	Hrs on Oil	H_2 Rate SCF/Bbl	Series Loading
PF109	700	500	.75	474 reg	8-10	37.65	507	120	1500	2
PF110	700	500	.75	474 reg	8-10	37.65	507	121	1500	2
PF111	700	500	.375	474 reg	8-10	37.65	507	125	1500	2
PF112	700	500	.375	474 reg	8-10	37.65	507	126	1500	2
PF113	650	1000	1.5	474 reg	8-10	37.65	1000	135	1500	2
PF114	650	1000	1.5	474 reg	8-10	37.65	995	138	1500	2
PF115	650	1000	.75	474 reg	8-10	37.65	997	142	1500	2
PF116	650	1000	.75	474 reg	8-10	37.65	997	143	1500	2
PF117	650	1000	.375	474 reg	8-10	37.65	996	146	1500	2
PF118	650	1000	.375	474 reg	8-10	37.65	996	147	1500	2
PF119	650	1000	1.5	474 reg	8-10	37.65	995	151	1500	2
PF120	650	1000	1.5	474 reg	8-10	37.65	995	153	1500	2
PF121	650	1500	1.5	474 reg	8-10	37.65	1505	161	1500	2
PF122	650	1500	1.5	474 reg	8-10	37.65	1505	162	1500	2
PF123	650	1500	.75	474 reg	8-10	37.65	1510	167	1500	2
PF124	650	1500	.75	474 reg	8-10	37.65	1510	168	1500	2
PF125	650	1500	.375	474 reg	8-10	37.65	1510	173	1500	2
PF126	650	1500	.375	474 reg	8-10	37.65	1510	174	1500	2
PF127	650	1500	1.5	474 reg	8-10	37.65	1510	178	1500	2
PF128	650	1500	1.5	474 reg	8-10	37.65	1510	180	1500	2
PF129	650	500	1.5	474 reg	8-10	37.65	520	192	1500	2
PF130	650	500	1.5	474 reg	8-10	37.65	526	194	1500	2
PF131	650	500	.75	474 reg	8-10	37.65	520	196	1500	2
PF132	650	500	.75	474 reg	8-10	37.65	520	197	1500	2
PF133	650	500	.375	474 reg	8-10	37.65	520	200	1500	2
PF134	650	500	.375	474 reg	8-10	37.65	520	201	1500	2

TABLE XXVIII (Continued)

Sample No	Nominal Temp	Nominal Press	t	Cat Type	Cat Size (Mesh)	Reactor Volume	Reactor Pressure	Hrs on Oil	H_2 Rate SCF/Bbl	Series Loading
PF135	650	500	1.5	474 reg	8-10	37.65	520	213	1500	2
PF136	650	500	1.5	474 reg	8-10	37.65	520	215	1500	2
PF137	600	1000	1.5	474 reg	8-10	37.65	1005	222	1500	2
PF138	600	1000	1.5	474 reg	8-10	37.65	1000	224	1500	2
PF139	600	1000	.75	474 reg	8-10	37.65	1010	228	1500	2
PF140	600	1000	.75	474 reg	8-10	37.65	1010	229	1500	2
PF141	600	1000	.375	474 reg	8-10	37.65	1000	236	1500	2
PF142	600	1000	.375	474 reg	8-10	37.65	1000	238	1500	2
PF143	600	1000	1.5	474 reg	8-10	37.65	1000	242	1500	2
PF144	600	1000	1.5	474 reg	8-10	37.65	1000	245	1500	2
PF145	600	1500	1.5	474 reg	8-10	37.65	1510	251	1500	2
PF146	600	1500	1.5	474 reg	8-10	37.65	1510	253	1500	2
PF147	700	1000	1.5	474 reg	40-48	37.65	1015	24	1500	3
PF148	700	1000	1.5	474 reg	40-48	37.65	1010	34	1500	3
PF149	700	1000	1.5	474 reg	40-48	37.65	1010	36	1500	3
PF150	700	1000	1.5	474 reg	40-48	37.65	1010	40	1500	3
PF151	700	1000	1.5	474 reg	40-48	37.65	1010	44	1500	3
PF152	700	1000	1.5	474 reg	40-48	37.65	1010	48	1500	3
PF153	700	1000	.75	474 reg	40-48	37.65	1010	54	1500	3
PF154	700	1000	.75	474 reg	40-48	37.65	1010	55	1500	3
PF155	700	1000	.375	474 reg	40-48	37.65	1015	61	1500	3
PF156	700	1000	.375	474 reg	40-48	37.65	1010	63	1500	3
PF157	700	1000	1.5	474 reg	40-48	37.65	1015	71	1500	3
PF158	700	1000	1.5	474 reg	40-48	37.65	1015	73	1500	3
PF159	750	1000	1.5	474 reg	40-48	37.65	1010	88	1500	3
PF160	750	1000	1.5	474 reg	40-48	37.65	1010	89	1500	3

TABLE XXVIII (Continued)

Sample No	Nominal Temp	Nominal Press	t	Cat Type	Cat Size (Mesh)	Reactor Volume	Reactor Pressure	Hrs on Oil	H_2 Rate SCF/Bbl	Series Loading
PF161	750	1000	.75	474 reg	40-48	37.65	1017	96	1500	3
PF162	750	1000	.75	474 reg	40-48	37.65	1017	97	1500	3
PF163	750	1000	.375	474 reg	40-48	37.65	1015	103	1500	3
PF164	750	1000	.375	474 reg	40-48	37.65	1015	106	1500	3
PF165	750	1000	1.5	474 reg	40-48	37.65	1010	111	1500	3
PF166	750	1000	1.5	474 reg	40-48	37.65	1010	113	1500	3
PF167	650	1000	1.5	474 reg	40-48	37.65	1014	122	1500	3
PF168	650	1000	1.5	474 reg	40-48	37.65	1010	124	1500	3
PF169	650	1000	.75	474 reg	40-48	37.65	1010	129	1500	3
PF170	650	1000	.75	474 reg	40-48	37.65	1010	130	1500	3
PF171	650	1000	.375	474 reg	40-48	37.65	1010	135	1500	3
PF172	650	1000	.375	474 reg	40-48	37.65	1010	136	1500	3
PF173	650	1000	1.5	474 reg	40-48	37.65	1010	139	1500	3
PF174	650	1000	1.5	474 reg	40-48	37.65	1010	141	1500	3
PF175	600	1000	1.5	474 reg	40-48	37.65	1010	150	1500	3
PF176	600	1000	1.5	474 reg	40-48	37.65	1010	152	1500	3
PF177	600	1000	.75	474 reg	40-48	37.65	1010	158	1500	3
PF178	600	1000	.75	474 reg	40-48	37.65	1010	159	1500	3
PF179	600	1000	.375	474 reg	40-48	37.65	1012	163	1500	3
PF180	600	1000	.375	474 reg	40-48	37.65	1012	164	1500	3
PF181	600	1000	1.5	474 reg	40-48	37.65	1012	169	1500	3
PF182	600	1000	1.5	474 reg	40-48	37.65	1010	172	1500	3
PF183	700	1000	1.5	474 reg	40-48	37.65	1010	176	1500	3
PF184	700	1000	1.5	474 reg	40-48	37.65	1010	179	1500	3
PF185	700	1000	.375	474 reg	40-48	37.65	1010	186	1500	3
PF186	700	1000	.375	474 reg	40-48	37.65	1000	187	1500	3
PF187	650	1000	.75	474 reg	8-10	18.82	990	15	1500	4

TABLE XXVIII (Continued)

Sample No	Nominal Temp	Nominal Press	t	Cat Type	Cat Size (Mesh)	Reactor Volume	Reactor Pressure	Hrs on Oil	H_2 Rate SCF/Bbl	Series Loading
PF188	650	1000	.75	474 reg	8-10	18.82	993	19	1500	4
PF189	650	1000	.75	474 reg	8-10	18.82	993	25	1500	4
PF190	650	1000	.75	474 reg	8-10	18.82	995	33	1500	4
PF191	650	1000	.75	474 reg	8-10	18.82	995	38	1500	4
PF192	650	1000	.75	474 reg	8-10	18.82	995	42	1500	4
PF193	650	1000	.75	474 reg	8-10	18.82	996	46	1500	4
PF194	650	1000	1.5	474 reg	8-10	18.82	995	55	1500	4
PF195	650	1000	1.5	474 reg	8-10	18.82	995	58	1500	4
PF196	650	1000	.75	474 reg	8-10	18.82	995	63	1000	4
PF197	650	1000	.75	474 reg	8-10	18.82	995	65	1500	4
PF198	650	1000	.375	474 reg	8-10	18.82	995	69	1500	4
PF199	650	1000	.375	474 reg	8-10	18.82	995	70	1500	4
PF200	650	1000	1.5	474 reg	8-10	18.82	995	79	1500	4
PF201	650	1000	1.5	474 reg	8-10	18.82	995	81	1500	4
PF202	700	1000	1.5	474 reg	8-10	18.82	1005	91	1500	4
PF203	700	1000	1.5	474 reg	8-10	18.82	999	95	1500	4
PF204	700	1000	.75	474 reg	8-10	18.82	998	100	1500	4
PF205	700	1000	.75	474 reg	8-10	18.82	998	102	1500	4
PF206	700	1000	.375	474 reg	8-10	18.82	998	106	1500	4
PF207	700	1000	.375	474 reg	8-10	18.82	995	107	1500	4
PF208	700	1000	1.5	474 reg	8-10	18.82	995	111	1500	4
PF209	700	1000	1.5	474 reg	8-10	18.82	995	114	1500	4
PF210	650	1000	.75	474 reg	8-10	18.82	997	119	1500	4
PF211	650	1000	.75	474 reg	8-10	18.82	997	121	1500	4
PF212	600	1000	1.5	72-B	8-10	18.82	1000	11	1500	5
PF213	600	1000	1.5	72-B	8-10	37.65	1000	15	1500	5

TABLE XXVIII (Continued)

Sample No	Nominal Temp	Nominal Press	t	Cat Type	Cat Size (Mesh)	Reactor Volume	Reactor Pressure	Hrs on Oil	H_2 Rate SCF/Bbl	Series Loading
PF214	600	1000	1.5	72-B	8-10	37.65	1000	20	1500	5
PF215	600	1000	1.5	72-B	8-10	37.65	1000	24	1500	5
PF216	600	1000	1.5	72-B	8-10	37.65	1000	28	1500	5
PF217	600	1000	1.5	27-B	8-10	37.65	1000	32	1500	5
PF218	600	1000	1.5	72-B	8-10	37.65	1500	36	1500	5
PF219	600	1000	1.5	72-B	8-10	37.65	1000	40	1500	5
PF220	600	1000	1.5	72-B	8-10	37.65	1000	44	1500	5
PF221	600	1000	1.5	72-B	8-10	37.65	1000	48	1500	5
PF222	600	1000	.75	72-B	8-10	37.65	1000	50	1500	5
PF223	600	1000	.75	72-B	8-10	37.65	1000	57	1500	5
PF224	600	1000	.375	72-B	8-10	37.65	1010	55	1500	5
PF225	600	1000	.375	72-B	8-10	37.65	1010	57	1500	5
PF226	600	1000	1.5	72-B	8-10	37.65	1005	59	1500	5
PF227	600	1000	1.5	72-B	8-10	37.65	1005	61	1500	5
PF228	650	1000	1.5	72-B	8-10	37.65	1008	74	1500	5
PF229	650	1000	1.5	72-B	8-10	37.65	1008	76	1500	5
PF230	650	1000	.75	72-B	8-10	37.65	1020	80	1500	5
PF231	650	1000	.75	72-B	8-10	37.65	1020	81	1500	5
PF232	650	1000	.375	72-B	8-10	37.65	998	85	1500	5
PF233	650	1000	.375	72-B	8-10	37.65	998	86	1500	5
PF234	650	1000	1.5	72-B	8-10	37.65	995	90	1500	5
PF235	650	1000	1.5	72-B	8-10	37.65	995	92	1500	5
PF236	700	1000	1.5	72-B	8-10	37.65	1002	101	1500	5
PF237	700	1000	1.5	72-B	8-10	37.65	1002	103	1500	5
PF238	700	1000	.75	72-B	8-10	37.65	1002	106	1500	5
PF239	700	1000	.75	72-B	8-10	37.65	1004	107	1500	5

TABLE XXVIII (Continued)

Sample No	Nominal Temp	Nominal Press	t	Cat Type	Cat Size (Mesh)	Reactor Volume	Reactor Pressure	Hrs on Oil	H_2 Rate SCF/Bbl	Series Loading
PF240	700	1000	.375	72-B	8-10	37.65	1005	112	1500	5
PF241	700	1000	.375	72-B	8-10	37.65	1000	113	1500	5
PF242	700	1000	1.5	72-B	8-10	37.65	1000	117	1500	5
PF243	700	1000	1.5	72-B	8-10	37.65	1000	120	1500	5
PF244	750	1000	1.5	72-B	8-10	37.65	1000	130	1500	5
PF245	750	1000	1.5	72-B	8-10	37.65	1000	132	1500	5
PF246	750	1000	.75	72-B	8-10	37.65	1000	138	1500	5
PF247	750	1000	.75	72-B	8-10	37.65	1000	139	1500	5
PF248	750	1000	.375	72-B	8-10	37.65	1006	143	1500	5
PF249	750	1000	.375	72-B	8-10	37.65	1006	145	1500	5
PF250	750	1000	1.5	72-B	8-10	37.65	1005	150	1500	5
PF251	750	1000	1.5	72-B	8-10	37.65	1005	151	1500	5
PF252	600	1000	1.5	72-A	8-10	37.65	1000	4	1500	6
PF253	600	1000	1.5	72-A	8-10	37.65	1000	8	1500	6
PF254	600	1000	1.5	72-A	8-10	37.65	1010	12	1500	6
PF255	600	1000	1.5	72-A	8-10	37.65	995	16	1500	6
PF256	600	1000	1.5	72-A	8-10	37.65	995	20	1500	6
PF257	600	1000	1.5	72-A	8-10	37.65	995	27	1500	6
PF258	600	1000	1.5	72-A	8-10	37.65	997	30	1500	6
PF259	600	1000	1.5	72-A	8-10	37.65	997	34	1500	6
PF260	600	1000	1.5	72-A	8-10	37.65	997	38	1500	6
PF261	600	1000	1.5	72-A	8-10	37.65	995	42	1500	6
PF262	600	1000	1.5	72-A	8-10	37.65	996	46	1500	6
PF263	600	1000	.75	72-A	8-10	37.65	1007	50	1500	6
PF264	600	1000	.75	72-A	8-10	37.65	1007	51	1500	6
PF265	600	1000	.375	72-A	8-10	37.65	1010	56	1500	6

TABLE XXVIII (Continued)

Sample No	Nominal Temp	Nominal Press	t	Cat Type	Cat Size (Mesh)	Reactor Volume	Reactor Pressure	Hrs on Oil	H_2 Rate SCF/Bbl	Series Loading
PF266	600	1000	.375	72-A	8-10	37.65	1010	57	1500	6
PF267	600	1000	1.5	72-A	8-10	37.65	1010	61	1500	6
PF268	600	1000	1.5	72-A	8-10	37.65	1010	63	1500	6
PF269	650	1000	1.5	72-A	8-10	37.65	1010	69	1500	6
PF270	650	1000	1.5	72-A	8-10	37.65	1010	71	1500	6
PF271	650	1000	.75	72-A	8-10	37.65	1010	74	1500	6
PF272	650	1000	.75	72-A	8-10	37.65	1010	75	1500	6
PF273	650	1000	.375	72-A	8-10	37.65	1010	79	1500	6
PF274	650	1000	.375	72-A	8-10	37.65	1010	80	1500	6
PF275	650	1000	1.5	72-A	8-10	37.65	1010	84	1500	6
PF276	650	1000	1.5	72-A	8-10	37.65	1010	86	1500	6
PF277	700	1000	1.5	72-A	8-10	37.65	1010	92	1500	6
PF278	700	1000	1.5	72-A	8-10	37.65	1015	99	1500	6
PF279	700	1000	.75	72-A	8-10	37.65	1015	102	1500	6
PF280	700	1000	.75	72-A	8-10	37.65	1015	103	1500	6
PF281	700	1000	.375	72-A	8-10	37.65	1015	107	1500	6
PF282	700	1000	.375	72-A	8-10	37.65	1015	108	1500	6
PF283	700	1000	1.5	72-A	8-10	37.65	1015	117	1500	6
PF284	700	1000	1.5	72-A	8-10	37.65	1019	119	1500	6
PF285	750	1000	1.5	72-A	8-10	37.65	1019	124	1500	6
PF286	750	1000	1.5	72-A	8-10	37.65	1015	126	1500	6
PF287	750	1000	.75	72-A	8-10	37.65	1010	130	1500	6
PF288	750	1000	.75	72-A	8-10	37.65	1010	131	1500	6
PF289	600	1000	1.5	Inerts	8-10	37.65	1005	6	1500	7
PF290	600	1000	1.5	Inerts	8-10	37.65	1005	8	1500	7
PF291	600	1000	.75	Inerts	8-10	37.65	1005	11	1500	7

TABLE XXVIII (Continued)

Sample No	Nominal Temp	Nominal Press	t	Cat Type	Cat Size (Mesh)	Reactor Volume	Reactor Pressure	Hrs on Oil	H_2 Rate SCF/Bbl	Series Loading
PF292	600	1000	.75	Inerts	8-10	37.65	1005	12	1500	7
PF293	600	1000	.375	Inerts	8-10	37.65	1005	15	1500	7
PF294	600	1000	.375	Inerts	8-10	37.65	1005	16	1500	7
PF295	650	1000	1.5	Inerts	8-10	37.65	1005	22	1500	7
PF296	650	1000	1.5	Inerts	8-10	37.65	1005	24	1500	7
PF297	650	1000	.75	Inerts	8-10	37.65	1005	26	1500	7
PF298	650	1000	.75	Inerts	8-10	37.65	1005	27	1500	7
PF299	650	1000	.375	Inerts	8-10	37.65	1005	30	1500	7
PF300	650	1000	.375	Inerts	8-10	37.65	1005	31	1500	7
PF301	600	1000	1.5	474 reg	8-10	37.65	1002	7	1500	8
PF302	600	1000	1.5	474 reg	8-10	37.65	1001	12	1500	8
PF303	600	1000	1.5	474 reg	8-10	37.65	1000	16	1500	8
PF304	600	1000	1.5	474 reg	8-10	37.65	1003	20	1500	8
PF305	600	1000	1.5	474 reg	8-10	37.65	1003	24	1500	8
PF306	600	1000	1.5	474 reg	8-10	37.65	1002	28	1500	8
PF307	600	1000	1.5	474 reg	8-10	37.65	1002	32	1500	8
PF308	600	1000	1.5	474 reg	8-10	37.65	1002	36	1500	8
PF309	600	1000	1.5	474 reg	8-10	37.65	1000	40	1500	8
PF310	600	1000	1.5	474 reg	8-10	37.65	1006	44	1500	8
PF311	600	1000	1.5	474 reg	8-10	37.65	1006	48	1500	8
PF312	600	1000	.75	474 reg	8-10	37.65	1005	50	1500	8
PF313	600	1000	.75	474 reg	8-10	37.65	1005	52	1500	8
PF314	600	1000	.375	474 reg	8-10	37.65	1007	56	1500	8
PF315	600	1000	.375	474 reg	8-10	37.65	1007	57	1500	8
PF316	600	1000	1.5	474 reg	8-10	37.65	1006	60	1500	8
PF317	600	1000	1.5	474 reg	8-10	37.65	1006	62	1500	8

TABLE XXVIII (Continued)

Sample No	Nominal Temp	Nominal Press	t	Cat Type	Cat Size (Mesh)	Reactor Volume	Reactor Pressure	Hrs on Oil	H_2 Rate SCF/Bbl	Series Loading
PF318	650	1000	1.5	474 reg	8-10	37.65	1014	68	1500	8
PF319	650	1000	1.5	474 reg	8-10	37.65	1012	70	1500	8
PF320	650	1000	.75	474 reg	8-10	37.65	1010	76	1500	8
PF321	650	1000	.75	474 reg	8-10	37.65	1010	77	1500	8
PF322	650	1000	.375	474 reg	8-10	37.65	1010	80	1500	8
PF323	650	1000	.375	474 reg	8-10	37.65	1010	81	1500	8
PF324	650	1000	1.5	474 reg	8-10	37.65	1010	85	1500	8
PF325	650	1000	1.5	474 reg	8-10	37.65	1010	87	1500	8
PF326	700	1000	1.5	474 reg	8-10	37.65	1010	82	1500	8
PF327	700	1000	1.5	474 reg	8-10	37.65	1010	94	1500	8
PF328	700	1000	.75	474 reg	8-10	37.65	1010	100	1500	8
PF329	700	1000	.75	474 reg	8-10	37.65	1010	101	1500	8
PF330	700	1000	.375	474 reg	8-10	37.65	1010	104	1500	8
PF331	700	1000	.375	474 reg	8-10	37.65	1010	105	1500	8
PF332	700	1000	1.5	474 reg	8-10	37.65	1005	109	1500	8
PF333	700	1000	1.5	474 reg	8-10	37.65	1005	111	1500	8
PF334	750	1000	1.5	474 reg	8-10	37.65	1006	118	1500	8
PF335	750	1000	1.5	474 reg	8-10	37.65	1006	120	1500	8
PF336	750	1000	.75	474 reg	8-10	37.65	1005	124	1500	8
PF337	750	1000	.75	474 reg	8-10	37.65	1005	125	1500	8
PF338	750	1000	.375	474 reg	8-10	37.65	1005	128	1500	8
PF339	750	1000	.375	474 reg	8-10	37.65	1005	129	1500	8
PF340	750	1000	1.5	474 reg	8-10	37.65	1005	134	1500	8
PF341	750	1000	1.5	474 reg	8-10	37.65	1005	136	1500	8

APPENDIX I

CALCULATION OF PORE SIZE DISTRIBUTION CURVES

The three curves, Figures 32, 33 and 34, are the experimental results from mercury penetration studies. The curves are plots of the cumulative penetration volume vs. the pressure and/or pore diameter. These curves can be converted to a pore distribution curve by the method shown below.

The curve of 72-B was selected for the example. First, Table XXIX was prepared. By dividing the change in volume by the log of the change in pore size a convenient measure of the number of pores of a given size is obtained. The number of pores of a given size ($\Delta V/\Delta \ln r$) is then plotted vs. ln pore radius and Figure 13 of the results section was generated. Data from Figures 33 and 34 were used in a similar fashion to generate Figures 12 and 14 respectively.

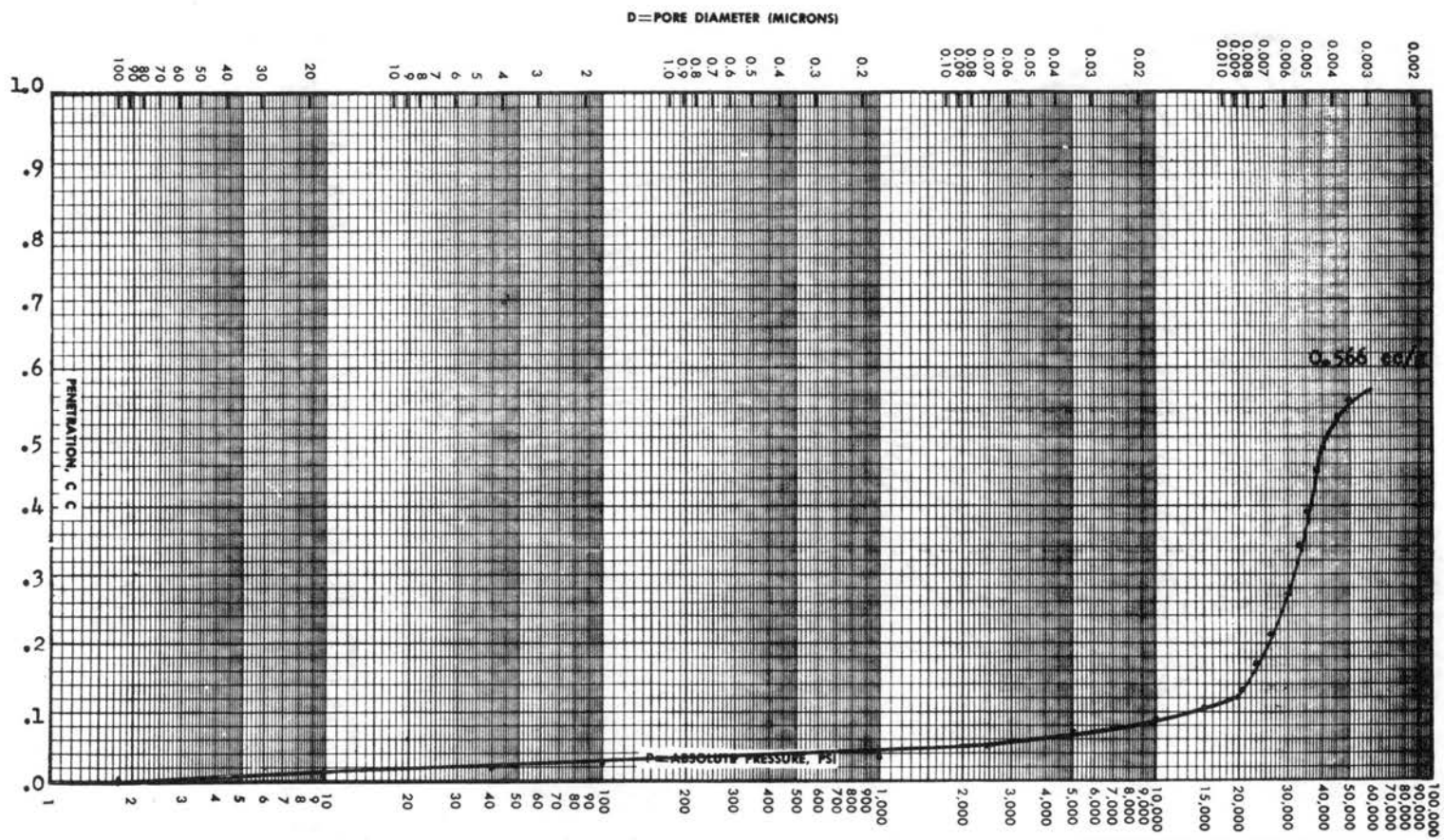

Figure 32. Porosity Determination, Catalyst 72-B

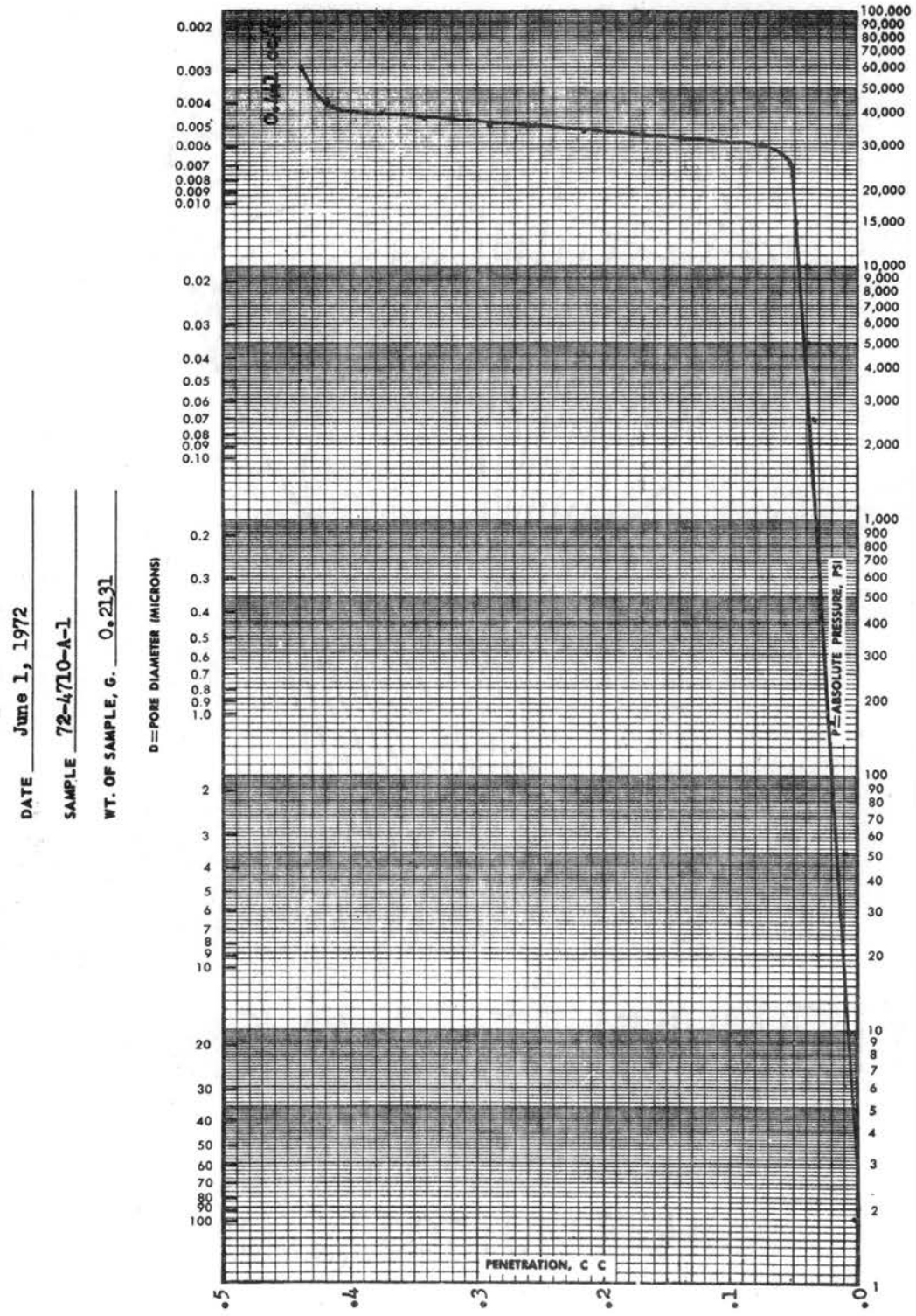

Figure 33. Porosity Determination, Catalyst 72-A

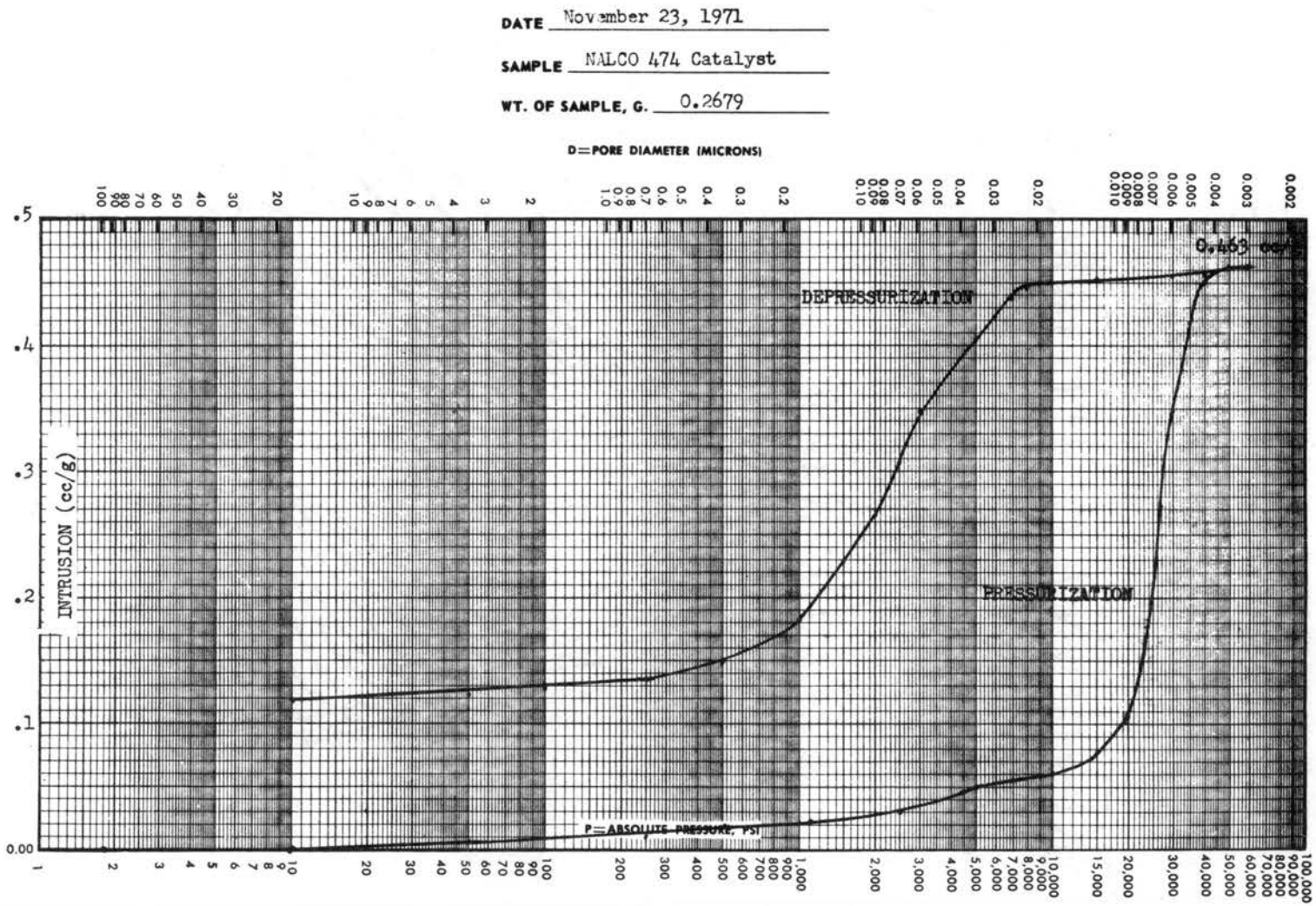

Figure 34. Porosity Determination, Catalyst Nalcomo 474

TABLE XXIX

CALCULATIONS FOR PORE SIZE DISTRIBUTION CURVE

V Cumulative	Δ V	r	ln r	Δ ln r	$\frac{\Delta V}{\Delta \ln r}$
.566		486000	1309		
	.013			1.70	.00764
.553		88400	11.39		
	.007			1.40	.00500
.546		21875	9.99		
	.006			0.91	.00659
.540		8750	9.08		
	.004			1.1	.00363
.536		2917	7.98		
	.003			1.19	.00252
.533		875	6.79		
	.016			0.93	.0172
.517		350	5.86		
	.023			0.69	.0333
.494		175	5.17		
	.020			0.70	.0286
.474		87.5	4.47		
	.013			0.41	.0317
.461		58.3	4.06		
	.017			0.28	.0607
.444		43.7	3.78		

TABLE XXIX (Continued)

V Cumulative	Δ V	r	ln r	Δ ln r	$\frac{\Delta V}{\Delta \ln r}$
	.046			0.14	.329
.398		38.0	3.64		
	.042			0.12	.350
.356		33.7	3.52		
	.060			0.14	.428
.296		29.2	3.38		
	.072			0.10	.720
.224		26.5	3.28		
	.049			0.06	.817
.175		25.0	3.22		
	.063			0.08	.788
.112		23.0	3.14		
	.029			0.06	.483
.083		21.9	3.08		
	.046			0.12	.383
.037		19.4	2.96		
	.023			0.10	.230
.014		17.5	2.86		
	.014			0.18	.0777
0.000		14.6	2.86		

APPENDIX J

BRIEF DESCRIPTION OF OBTAINING FRACTIONS

The general equipment used to take the fractions was an ASTM D-86 distillation apparatus. The vacuum was controlled by a manostat connected to a vacuum pump. Heat was supplied by a heating mantle and temperature monitored by a thermocouple and potentiometer.

To the distillation flask, a handful of Berl saddles was added to act as boiling chips. The flask and saddles were weighed and 100 cc oil added to the flask. The flask was again reweighed. The flask and contents were then attached to the distillation apparatus and the system flushed with CO_2. The system was then evacuated to 50 mm Hg and the heat turned on. The oil was allowed to distill over as long as the temperature was constant within the flask. When the temperature began to rise, indicating the oil boiling in a particular range had been distilled over, the heating mantle was dropped and the system filled to atmospheric pressure with CO_2 the portion of oil distilled over was poured out and weighed. The system was reassembled and the procedure repeated for the remaining seven fractions. For the last fraction, the flask, boiling chips and residue were weighed to determine the weight of the fraction.

Data for the selected samples is presented below.

	Sample PF19	Sample PF 113,114,119,120	Sample PF 228,229,234,235	Feed
Cut 1	9.03 gm	19.06 gm	15.29 gm	11.59 gm
Cut 2	13.34	16.18	17.77	12.48
Cut 3	11.75	10.83	12.28	13.53
Cut 4	10.91	11.96	13.30	11.45
Cut 5	15.37	16.67	15.67	19.46
Cut 6	10.03	6.76	7.56	9.05
Cut 7	12.83	8.77	9.67	14.24
Cut 8	15.63	10.70	11.30	16.01

Results of Sulfur analysis are shown in Figures 16 and 17 of the results section.

APPENDIX K

CHARACTERIZATION OF ANTHRACENE OIL

For the convenience of later experimental work density and kinematic viscosity of the fractions were determined. The results of the experiments are presented in Table XXX. Density was determined at 77°F and kinematic viscosity at two temperatures of 100°F and 187.7°F. Feed oil preperties are listed in the results section.

Density measurements were made using a 5 ml pipette. The pipette was calibrated using distilled water to determine the volume. The pipette was then filled with the oil and weighed. From the known volume and the weight the density was calculated. The procedure was repeated for each fraction of oil. For a comparison point the density of research grade toluene was also determined.

Kinematic viscosity measurements were made using viscometers. The viscometers were first calibrated with ASTM certified calibrating fluid. The fractions were then poured into the viscometer and the time for the fluid to fill the same volume as the calibrating oils was measured. The kinematic viscosity was then calculated using the formula

$$\nu = \frac{\mu}{\rho} = k\ t$$

where: ν = kinematic viscosity, centistokes

μ = viscosity, centipoise

TABLE XXX

DENSITY AND KINEMATIC VISCOSITY OF FRACTIONS

Fraction	Density @ 77°F gm/cc	Kinematic Viscosity (centistokes) @ 100°F)	Kinematic Viscosity (centistokes) @ 187.7°F
1	.959	1.71	.813
2	1.020	3.48	1.293
3	1.060	6.22	1.833
4	1.075	10.57	2.37
5	1.092	18.04	3.06
6	1.107	31.10	4.025
7	1.122	65.93	5.48
8	1.137		
Toluene	.871		

ρ = density, gm/cc

k = calibration constant obtained from oil or known viscosity

t = time, seconds

APPENDIX L

CALCULATION OF ACTIVATION ENERGY FOR 2ND ORDER FIT OF INERTS DATA

For second order reaction

$$-\frac{dc}{dt} = k\, c^2$$

where c = mol sulfur in product oil

k = rate constant, cc^2/mol hr

t = time, hr

integrating

$$\frac{1}{c} = \frac{1}{c_o} + kt$$

Therefore a plot of 1/c vs. t has an intercept of $1/c_o$ and a slope of k. Figure 19 is a plot of 1/c vs. t and slopes of the isotherms are:

Temp.	k
650°F	.0427 cc^2/mol hr
700°F	.107
750°F	.187
800°F	.477

Assuming that the rate constant k can be represented by an Arrhenius expression

$$k = k_o e^{-E/RT}$$

$$\text{or } \ln k = \ln k_o - E/RT$$

a plot of ln k vs. 1/T will give an intercept of $\ln k_o$ and a slope of

-E/R. Figure 20 is a plot of ln k vs. 1/T.

$$\text{slope of Figure 20} = \frac{\ln .0427 - \ln .471}{.01622 - .001428} = \frac{-2.413}{1.94 \times 10^{-4}} = 12440$$

therefore $-12440 = -E/R$

$E = 24{,}700$ cal/mol

APPENDIX M

CALCULATION OF MEAR'S (38) CRITERIA FOR AXIAL DISPERSION EFFECTS

For larger bed, 20"

The inequality to described axial dispersion effects is

$$L/ds > \frac{20n}{B_o} \ln \frac{C_o}{C_f}$$

First L/ds is calculated.

L = 50.79 cm = reactor length

ds = .219 (8-10 mesh) - diameter of spherical particle

L/ds = 231.9

B_o is obtained from Hockman (25) graph which requires calculation of a liquid Peclet No., $\frac{ds\ U}{\mu}$

ds = particle diameter - .219 cm

U = mass/time-area

$$= \frac{100 \text{ cc}}{\text{hr}} \left| \frac{1.02 \text{ gm}}{\text{cc}} \right| \frac{}{.295 \text{ cm}^2} = 345.8 \text{ gm/hr cm}^2$$

μ = liquid viscosity = 3.8 gm/cm hr (Estimated from kinematic viscosity data)

$$\frac{ds\ U}{\mu} = \frac{.219\ (345.8)}{3.8} = 20$$

B_o from Hockman's graph = .25

$$\left(\frac{20\ n}{B_o}\right) \ln \frac{C_o}{C_f} = \frac{40}{.25} \ln \left(\frac{.47}{.112}\right) = 229$$

$$\overset{o}{o\ o} \quad L/ds > \frac{20n}{B_o} \ln \left(\frac{C_o}{C_f}\right)$$

or $231.9 > 229$

For shorter 10" bed

$$L/ds = 115.9$$

$$L_s = 172.9$$

$$\frac{dp\ L_s}{\mu} = 9.9$$

From Hockman's graph $B_o = .14$

$$\frac{20n}{B_o} \ln \frac{C_o}{C_f} = \frac{40}{.14} \ln \frac{.47}{.156} = 315.1$$

$$\overset{o}{o\ o} \quad L/ds > \frac{20n}{B_o} \ln \frac{C_o}{C_f}$$

or $172.9 < 315.1$

APPENDIX N

CALCULATION OF EFFECTIVENESS FACTOR FROM 1ST AND 2ND ORDER RATE CONSTANTS

From 1st order fit of data in Table VIII

at 650°F $\quad k = 3.11 \times 10^{-4}\ \text{sec}^{-1}$

then for a sphere $\quad \phi_s = R\sqrt{\dfrac{kC^{m-1}}{D_{eff}}}$

substituting the necessary constants

$$\phi_s = .219\sqrt{\frac{3.11 \times 10^{-4}}{1.94 \times 10^{-5}}}$$

$$\phi_s = .87$$

From Satterfield (50) graph $\eta = .8$ to 1.0

From 2nd order fit of data in Table VIII

at 650°F $\quad k = 3.01 \times 10^{-3}\ \dfrac{\text{sgm}^2}{(\text{gm oil})\ \text{sec}}$

For a sphere $\quad \phi_s = R\sqrt{\dfrac{k\ C^{m-1}}{D_{eff}}}$

$$\phi_s = .219 \sqrt{\frac{3.01 \times 10^{-3}(.14)}{1.94 \times 10^{-5}}}$$

.14 = avg. conc. of sulfur

$$\phi_s = 1.02$$

From Satterfields graph η = .8 to 1.0

APPENDIX O

CALCULATION OF DIFFUSION COEFFICIENT FOR THIOPHENE IN ANTHRACENE OIL

Using the Wilke and Chang (65) correlation

$$D_{12} = 7.4 \times 10^{-10} \quad \frac{T\,(X M_2)^{\frac{1}{2}}}{\mu V_b^{.6}}$$

For Thiophene in Anthracene Oil

$T = 616^{\circ}K\ (650^{\circ}F)$

$X = 1$

$M_2 = 88.1$

$\mu = 1.6$ cp $= .016$ poise

$V_b = 78.6$ cc/gm-mol

$$D_{12} = 7.4 \times 10^{-10} \quad \frac{(616)((1)\ (88.1))^{\frac{1}{2}}}{(.016)\ (78.6)^{.6}}$$

$$D_{12} = 1.94 \times 10^{-5}\ cm^2/sec$$

APPENDIX P

CALCULATION OF H_2 CONSUMPTION FROM KNOWN CONVERSIONS

Sulfur Removal:

Initial Conc. .47%

Final Conc. .03%

Removal .44% = .0044 gm S/gm oil

$$= \frac{.0001375 \text{ mol S}}{\text{gm oil}}$$

$$= \frac{.0039 \text{ mol S}}{25 \text{ cc oil}} = 1.48 \text{ SCF } H_2 \text{ / 25 cc oil}$$

= .055 mol H_2 / Bbl oil = 20.9 SCF H_2 / Bbl

N_2 Removal:

Removal - .50% = 1.99 # N/Bbl - .142 mol H_2 = 81 SCF H_2 /Bbl

O_2 Removal

Assume (2%) = 7.96 # O_2 = .248 mol H_2 = 94.58 SCF H_2/Bbl

Gas Make

Assume (5%) = 19.9 # gas = .695 mol gas - 264 mol H_2
(MW 28.6) @ 1 mol H_2/ mol gas

Hydrocracking Consumption:

From Wan (61) data 8 vol % conversion of 650 $^+$ boilers

= .04 Bbl involved or 15.98 #

Assume mol wt of 650^{+} boilers = 180

o o .088 moles were converted @ 1 mol H_2 / mol oil = 33 SCF H_2

Total H_2 Consumption = 493 SCF H_2 /Bbl Feed

APPENDIX Q

CALCULATION OF GAS MAKE IN HYDROTREATER

The rate of gas from the reactor was measured on a bubble meter. The inlet flow of hydrogen was however not measured. To obtain a measure of hydrogen flow rate, a gas make as well as the consumption calculated in Appendix P are needed. The 5% gasified is a reasonable assumption based on the literature (14) and the calculations for the gas make as shown below.

Consider

$$\left[\frac{100\ cc}{hr.}\right]\left[\frac{Bbl}{1.59 \times 10^{-5} cc}\right] = 6.289 \times 10^{-4}\ Bbl/hr.$$

$$\frac{100\ cc}{hr.}\left|\frac{102\ gm}{cc}\right. = (102\ gm/hr.)\ .05 = 5.1\ gm/hr.\ \text{gasified}$$

*Assuming MW 28.6

$$\frac{5.1\ gm}{hr.}\left|\frac{mol}{28.6}\right. = .178\ \frac{gm\ mol}{hr} = 3.928 \times 10^{-4}\ \frac{lb\ mole}{1\ hr.} = .1494\ \frac{SCF}{hr}$$

$$\frac{.1494\ SCF}{6.289 \times 10^{-4}} = \underline{237\ SCF/Bbl}\ \text{gasified}$$

*Gas Make (14)

		Contribution to Avg. Molecular Wt.
CO_2	259 TPD	2.47
H_2S	913	6.73
C_2^1	1903	6.60
C_1^2	830	5.39
C_2^3	483	4.60
C_4	224	2.8
	4612	Avg. Mol. Wt. 28.6

APPENDIX R

CALCULATION OF η_1 AND η_2 FROM RATION OF RATES FOR TWO PARTICLE SIZES

Consider the slope of a straight line between a LVHST of 0.0 and .375 as representative of the rate of reaction for both the small catalyst data (40-48 mesh) the large catalyst data (8-10 mesh), on Figure 22.

(40-40 mesh) slope = .9733

(8-10 mesh) slope = 1.008

$$\frac{(dc/dt)_2}{(dc/dt)_1} = \frac{1.008}{.9733} = 1.036 = \eta_2/\eta$$

also

$$\frac{R_1}{R_2} = \frac{\phi_1}{\phi_2} = \frac{.219}{.03504} = 6.25$$

Assuming the catalyst can be considered spherical particles, the relationship

$$\eta = \frac{3}{\phi}\left[\frac{1}{\tanh \phi} - \frac{1}{\phi}\right]$$

has been derived by most kinetics texts (34,58).

Therefore

$$.965\ \eta_2 = \frac{3}{6.25\ \phi_2}\left[\frac{1}{\tanh\ (6.25\ \phi_2} - \frac{1}{6.25\ \phi_2}\right] \qquad (1)$$

also

$$\eta_2 = \frac{3}{\phi_2}\left[\frac{1}{\tanh\ \phi_2} - \frac{1}{\phi_2}\right]$$

By Trial and Error

		η_2 eq. 1	η_2 eq. 2
assume	$\phi_2 = .2$	.87	.997
	$\phi_2 = .05$	.948	.999
	$\phi_2 = .01$	.97	.999

If $\eta_2 = .999$ $\eta_1 = .964$

APPENDIX S

ESTIMATION OF THE EFFECT OF PRESSURE IN THE REGION FROM 500-1000 PSIG

For sake of approximation a straight line was considered to represent the slope from the feed point to .375 hrs. on Figure 24.

The slope then is

$$\underline{\text{for 500 psig}} \quad \frac{\ln .47 - \ln .15}{.375} = \frac{-.755 - 1.897}{.375} = \frac{-1.142}{.375} = 3.0456$$

and

$$\underline{\text{for 1000 psig}} \quad \frac{\ln .47 - \ln .1}{.375} = \frac{-.755 - 2.3025}{.375} = \frac{1.5476}{.375} = 4.126$$

Since the pressure doubled, the rate would be expected to go up by a factor of 1.5 or to 4.616 according to the theory of Wilke and Chang (65). If one chooses the Stokes-Eisenstein equation (50) to represent the rate, the increase should be by a factor of .333 to 3.837.

If the molar volume to the .45 power is considered the correct measure of molar volume effect, the rate (slope) should increase by a factor of 1.36 to 4.16.

Actual increase by above = $\frac{4.126}{3.0456}$ or 1.35.

APPENDIX T

DERIVATION OF DESULFURIZATION MODEL

Consider the desulfurization reactions as represented by the equation

$$\frac{dc}{dt} = \frac{dc_1}{dt} + \frac{dc_2}{dt}$$

Where the rate of removal of c_1 and c_2 both follow 1st order models. Then

$$\frac{dc_1}{dt} = -k_1 c_1 \rightarrow \ln c \Big|_{c_{1o}}^{c_1} = -k_1 t = \ln \frac{c_1}{c_{1o}} = -k_1 t$$

$$\frac{dc_2}{dt} = -k_2 c_2 \rightarrow \ln c \Big|_{c_2}^{c_2} = -k_2 t = \ln \frac{c_2}{c_{2o}} = -k_2 t$$

Solving for c_1 and c_2

$$c_1 = c_{1o} e^{-k_1 t} \qquad c_2 = c_{2o} e^{-k_2 t}$$

Consider the total concentration* c equal to the sum of the independent concentrations

$$c = c_1 + c_2 = c_{1o} e^{-k_1 t} + c_{2o} e^{-k_2 t}$$

Let α represent the fraction of molecules reacting with the slower rate and let the subscript $_o$ indicate initial concentration. Then

$$c_{1o} = \alpha(c_o)$$

$$c_{2o} = (1 - \alpha)(c_o)$$

Substituting,

$$c = \alpha c_o e^{-k_1 t} + (1 - \alpha) c_o e^{-k_2 t}$$

Which is the form of the equation to be used here.

* Concentration is defined here as $\frac{\text{gms in product}}{\text{total gm product}}$

APPENDIX U

CALCULATION OF CATALYST INTERNAL TEMPERATURE

Reduction of catalyst size could possibly ignore a non-isothermal catalyst pellet and lead to the erroneous conclusion that the effectiveness factor was one when indeed it might be greater than one. From heat of reaction effects, it is possible to calculate the internal temperature of the catalyst and determine whether these are enough difference in temperature to cause significant changes in reaction rate.

From Satterfield (50) the expression

$(T_c - T_s) = \frac{(-\Delta H)(D_{eff})}{\lambda} (C_s - C_c)$ is given for the difference in temperature between catalyst particle center and catalyst particle surface.

ΔH = enthalpy change on reaction = cal/mole = -34,000 cal/mol for this case

D_{eff} = effective diffusivity - cm^2/sec - 1.95×10^{-5} cm^2/sec per Appendix O

λ = thermal conductivity of the alumina support cal/sec.cm. $^oC = 6.2 \times 10^{-4}$

C_s = concentration of sulfur at surface = mol/cc_1 = .000153 mol/cc

C_c = concentration of sulfur at catalyst center = 0

Substituting in $T_c - T_s = \frac{-(-(34{,}000))(1.95 \times 10^{-5})(.000153)}{6.2 \times 10^{-4}} = .163^{\circ}C$

The temperature rise due to reaction was therefore concluded to be unimportant for calculation of the effectiveness factor.

VITA

Matthew Colvin Sooter

Candidate for the Degree of

Doctor of Philosophy

Thesis: EFFECT OF CATALYST PORE SIZE ON HYDRODESULFURIZATION OF COAL DERIVED LIQUIDS

Major Field: Chemical Engineering

Biographical:

Personal Data: Born in Shattuck, Oklahoma, July 24, 1946, to Matthew C. and Odessa Sooter.

Education: Attended elementary school in Cheyenne, Oklahoma, graduated in 1964 from Cheyenne High School; received the degree of Bachelor of Science in Chemical Engineering at Oklahoma State University, Stillwater, Oklahoma in 1969; received Master of Science in Chemical Engineering from Oklahoma State University, Stillwater, Oklahoma in 1971; completed requirements for the Doctor of Philosophy degree at Oklahoma State University in May, 1974.

Professional Experience: Employed by The Southwestern Company, Nashville, Tennessee, summers of 1964 and 1966 as salesman; employed by Irby Construction Company, Jackson, Mississippi, summer of 1965 as construction worker; employed by Oklahoma State University, Stillwater, Oklahoma, January to May, 1968 as physics tutor; employed by Monsanto Company, St. Louis, Missouri during summer of 1968; employed by Monsanto Company, Texas City, Texas, as a technical service engineer, May 1969 to January 1970; employed by Catalyst, Inc., Philadelphia, Pennsylvania from January 1973 to present.